POLITECNICO DI TORINO

Department of Mechanical and Aerospace Engineering

Politecnico
di Torino

Master's Thesis

in

Mechanical Engineering

Virtual validation of the head impact on the dashboard of a vehicle

Tutor:
Prof. Alessandro Scattina

Candidate:
Davide Vianello

Academic Year 2021/2022

SUMMARY

List of figures

ACKNOWLEDGEMENTS

Vorrei prima di tutto ringraziare il Professore Alessandro Scattina per la Vostra attenta dedizione e disponibilità mostrata durante questo lavoro di tesi e per aver messo a disposizione tutta la Vostra esperienza per guidarmi durante questo percorso di crescita personale. Vorrei anche ringraziare l'Ingegnere Simone Calcopietro per avermi permesso di conoscere un ambito che non è ancora riuscito ad approfondire durante la mia carriera universitaria e per avermi suggerito un metodo di lavoro che sicuramente mi aiuterà nelle mie future esperienze lavorative.

Un ringraziamento immenso e speciale va a mia madre, a mio padre e a mio fratello che mi hanno sempre sostenuto e incoraggiato nei momenti di difficoltà che ho incontrato in questi cinque anni di studio, permettendomi sempre di trovare una soluzione ad ogni problema che mi trovavo ad affrontare. Un ultimo grazie va infine a tutti gli amici che ho conosciuto in questo ambiente universitario e con i quali ho trascorso momenti che difficilmente dimenticherò.

ABSTRACT

The role played by safety in the design of the vehicle has increased in the last years with the introduction of more active and passive devices for the prevention of accident and minimization of injuries of the occupants. The thesis is based on occupant protection against the interior of the car with the purpose of virtually validating the head impact on the dashboard of the vehicle according to FMVSS 201L regulations, focusing on the interaction between the head impactor and the monitor of the dashboard.

Consequently, the setup of the model for the analysis is focused on the monitor. The first step is the pre-processing phase, starting from the creation of the mesh up to the definition of all the properties that determine the mechanical behaviour of the component.

Once this step is completed, some structural simulations are carried out with the implicit solver OptiStruct. In particular, a modal analysis is conducted to check that the structural modes of the monitor are above the target in terms of frequency required to avoid noise and internal vibrations. Linear static analyses are instead performed, by applying a load on different components of the monitor, to compute its stiffness.

After these structural analyses, the head impact tests on the dashboard are performed with the explicit solver Ls-Dyna. The simulations were performed on two different points of impact, chosen by the car manufacturer as the most representative of the interaction between the monitor and the head impactor.

The results obtained from these simulations are analyzed in the post-processing phase in terms of energy balance, deceleration of the head impactor and contact force between the impactor and the dashboard. Finally, a change of the material of structural elements of the monitor and the lower shell of the instrument panel is considered, in order to understand their influence in the behavior of the dashboard.

INTRODUCTION

Over the last years, safety has played a primary role in the design of a vehicle and more and more systems, adopted both for active and passive safety, are mandatory and required by regulations.
The focus, in this thesis, is on the passive safety of the internal trim and passive devices are adopted in order not to prevent the accident but to minimize possible injuries of the occupants. Their primary purpose is to absorb the kinetic energy of the passengers of the vehicle in order to reduce at minimum the consequences caused by the impact of the occupant against the vehicle's structures.
The main objectives of the thesis are the following:

- to have an idea of the motion and response of the monitor of the dashboard, that is the focus in the first part of the thesis, by performing modal and linear static analysis with implicit solver OptiStruct
- to virtually validate, with the use of the explicit solver Ls-Dyna R12.0, the head impact on the dashboard of a vehicle according to FMVSS 201L regulations, focusing on the interaction between the head impactor and the monitor of the dashboard
- to modify the model of the dashboard with the change of the material of the components that are more subjected to the influence of the impact, to understand the effect that these modifications cause on the global response of the system
- to observe how impact tests are engineered, by performing a comparison of two head impact simulations with different speed of the head impactor.

Even if the final aim of the thesis is the virtual validation of the entire dashboard, at the beginning of the development of this work, the setup for the analysis is focused on the monitor of the dashboard.
In the first chapter is, thus, described the pre-processing phase of the monitor of the dashboard with the use of HyperMesh software and this step is fundamental to achieve accurate and reliable results from the structural analyses and crash test simulations. It starts from the import of the CAD model, with subsequent topology repair and geometry cleanup. Once the geometry of the model is considered appropriate for the discretization using finite element method, it is possible to mesh the different components of the monitor, according to the criteria of the car manufacturer. After this operation not all the elements of the mesh have a good quality and so it is necessary to perform a topology refinement with the modification of the shape of the elements that do not satisfy the requirements. The final step is to define all the features that determines the mechanical behaviour of the component such as the contacts and the connections between the different components, the materials and their properties. In the definition of these features, some assumptions and simplifications are considered to find a trade-off between the accuracy of the results and the computational time requested.
The second chapter is focused on the modal analysis of the monitor of the dashboard, with the use of the implicit solver OptiStruct, in order to have a preliminary view of the behaviour of the component and with

the main purpose of checking that the structural modes of the monitor are above the target in terms of frequency required to avoid noise and internal vibrations. .

In the third chapter there is a brief description of the two linear static analysis that has been performed, by applying a load in the same position but on different components, in order to compute the static stiffness and understand the influence of the force in the different components of the monitor.

In the fourth chapter is, thus, described the setup of the new model of the monitor with the definition of the materials and the properties in the Ls-Dyna interface. After this operation, the monitor is placed in the entire model of the dashboard with the identification of all the different contacts between the monitor and the model of the dashboard.

The fifth chapter is the core of the thesis and is focused on the description and post-processing analysis of the crash test simulations. It is, firstly, identified the area of possible head impact, according to FMVSS 201L regulations and, in this thesis, two points of impact are analyzed. They are chosen by the car manufacturer as the most representative for the simulation of the interaction between the monitor and the head impactor. The results obtained from these simulations with solver Ls-Dyna are then analyzed in terms of energy balance, deceleration of the head impactor and contact force between the head impactor and the dashboard. After the analysis of the simulations obtained from the two points of impact, it is considered a change of the material of the structural components of the monitor and of the lower shell of the instrument panel. The results are then analyzed with a comparison on each impact point, to understand how these modifications influence the general behavior of the entire dashboard.

Finally, it is analyzed the comparison of the head impact simulation between the two different speeds of the head impactor, due to the presence or not of the airbags. This comparison is performed to underline how impact tests are engineered.

1 PRE-PROCESSING PHASE OF THE MONITOR OF THE DASHBOARD

In order to understand the interaction between the head impactor and the monitor, the setup is focused on the monitor of the dashboard. The first step is the pre-processing with the use of Hyper Mesh software and this phase is fundamental to achieve accurate and reliable results. The purpose of the pre-processing is the preparation of the numerical model for the finite element analysis and it consists of a sequence of passages to perform:

- Geometry cleanup of the imported CAD model
- Creation of the mesh
- Definition of the properties
- Definition of the materials
- Assignment of the constraints and loads

The numerical model considers all the different components of the monitor, but some simplifications are applied to the CAD model, in order to better understand and analyze the results of the simulation in the post-processing. These assumptions a tradeoff between the requested computational time and the accuracy of the solution of the analysis.

1.1 DESCRIPTION OF THE MODEL

The monitor is composed by different elements that are listed in *table 1.1* and their balloons are shown in *figure 1.1*, where each component is associated to a different color for a better visualization.

Ballooning	Component of the monitor
1	Rear cover
2	Soft component
3	PCB
4	Front frame
5	Glue
6	Back case
7	Board
8	Front case
9	Front panel

Table 1.1 - Ballooning of the monitor

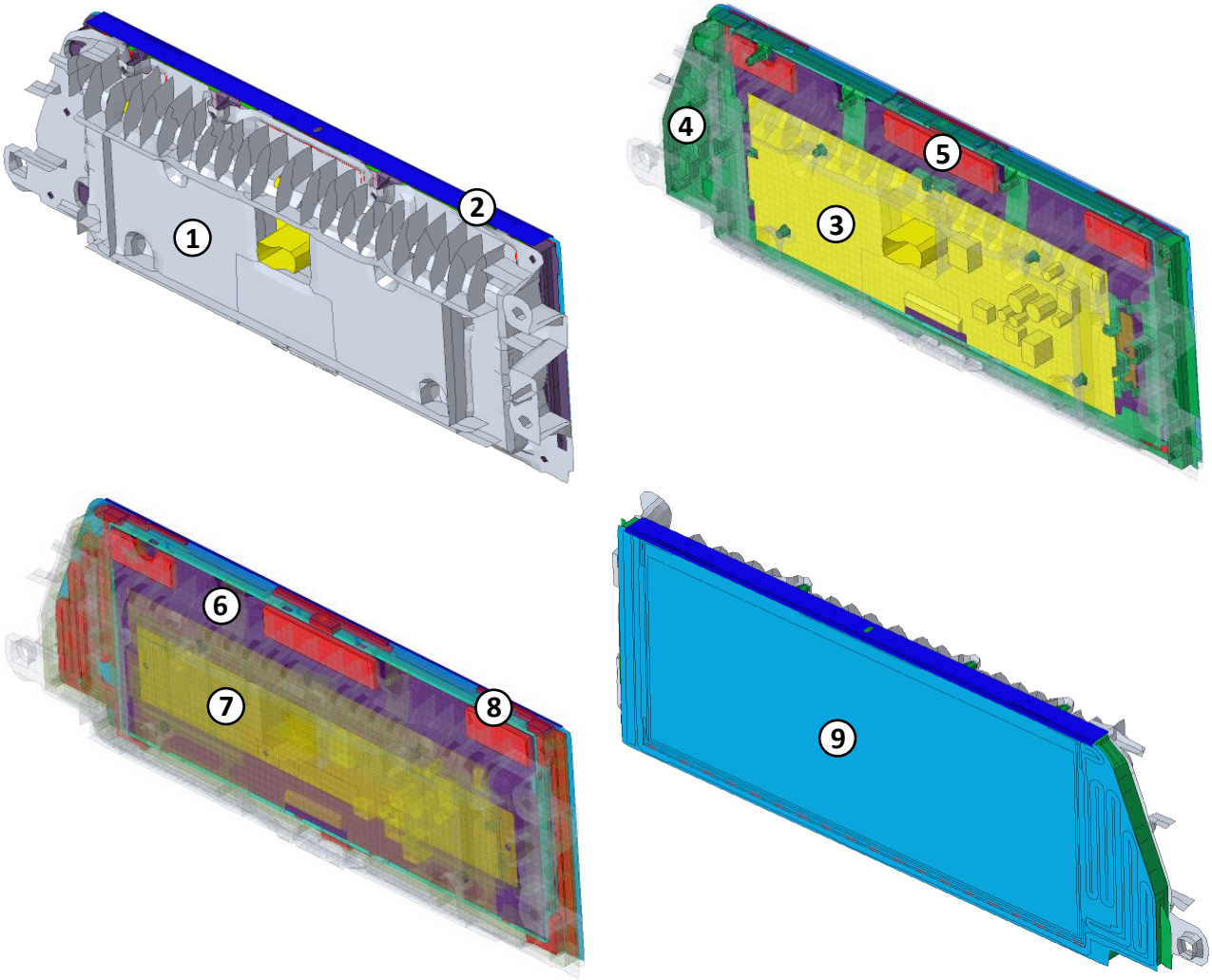

Figure 1.1 - Views of the monitor with the ballooning

Starting from the front view of the monitor, visible in the bottom part of *figure 1.1*, the first component is the front panel, that is the first one to get in contact with the head impactor in the simulation. The front panel is composed by three thin layers that are bonding with the use of glue and these layers are respectively a protective cover glass, a TFT LCD (Thin Film Transistor Liquid Crystal Display) glass module and a polycarbonate optical sheet.

The protective cover glass is bonding with glue to the front frame of the monitor, that is adjacently glued to the front case and the back case. These components, together with the front panel and the soft component glued on top of the front frame, form a unique element that represents the display of the monitor. The connection between the front case and the back case is also obtained with plastic additional fixations.

The front frame presents some screw housing and in these points there is the screwing of the front frame on the rear cover, that is the component located in the bottom part of the monitor.

The free space between the back case and the rear cover is occupied by the electronic board and the PCB (Printed Circuit Board), that is adopted to connect the different electronic components.

1.2 GEOMETRY CLEANUP

The pre-processing phase up to the creation of the mesh is described only for the front frame, but the same procedure is adopted for all the other components.

The first step is the import of the CAD model in the Hypermesh software. This is performed using the *Import* icon in the toolbar of the software, as shown in *figure 1.2*, where it is possible to select, among the different options, the type of model that has to be imported. In this case it is selected the option *Import Geometry*, that permits the import of CAD models that are obtained by design software, and Hypermesh is able to detect it automatically. Once the model is imported, it is necessary to rename all the different elements of the monitor. Each element is identified by a specific name and code and they are organized in assemblies, in order to easily identify all the structural components, that has been described in paragraph 1.1.

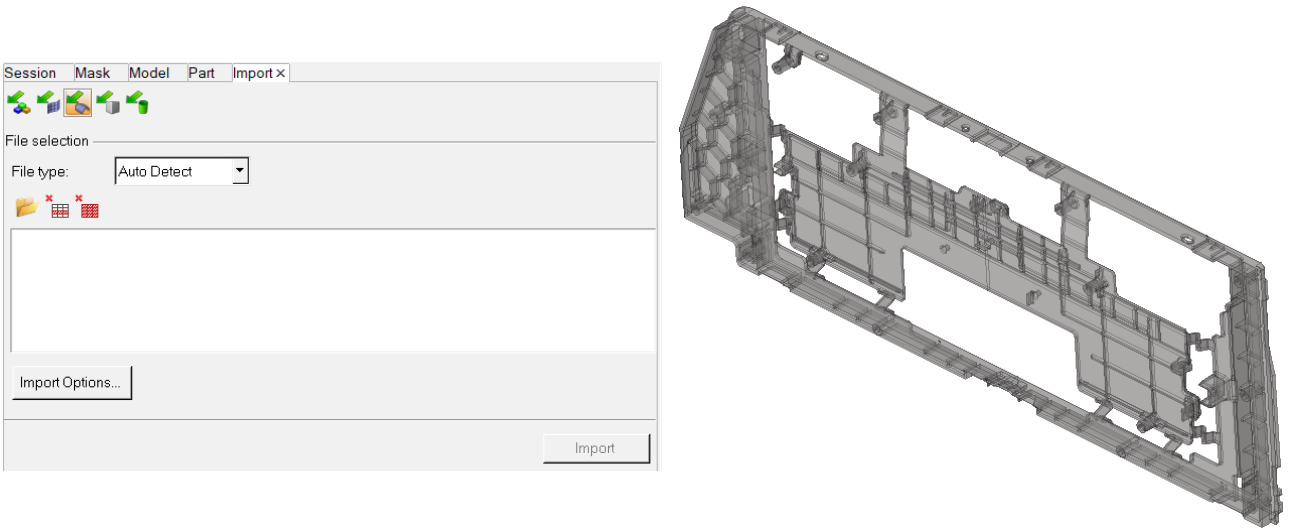

Figure 1.2 - Import window of Hypermesh and model of the front frame imported

After the import and subdivision of the different geometric elements of the model respectively into components and assemblies, the monitor is not yet ready for the mesh, but there are some operations to perform in order to solve geometric issues that may arise from the imported model.

The first step is to remove the solid elements that usually are present, in order to have only the external surfaces of the model. This operation is needed, due to the way in which Hypermesh works, based not on solid geometries but on the external surfaces of the components.

Due to the working principle of the software, since the geometry of the model is made of a solid component or a sequence of surfaces that defines a closed volume, for some components of the monitor, it is necessary to use the *Midsurface* window to extract the middle surfaces from the solid part. The original geometry of the model is unchanged but the new one with the introduction of the middle surfaces is collected in a new component, where Hypermesh also automatically stores the thickness for each middle surface, that is assigned considering half on the top side and half on the bottom one. The mesh on these surfaces is easier and with better accuracy and quality.

Before performing the discretization of the model using finite element method, in order to obtain the mesh

of the monitor, the strategy that is adopted to solve geometric issues is the geometry cleanup, following the topology repair. The topology repair consists in the correction of the errors that may be present in the way in which the surfaces of a part are connected to the adjacent ones, for example adjacent surfaces that are not connected or that are missed. The aim of this repair is the simplification of the model in order to have an improvement of the quality of the mesh. The main window of the software that is used for this purpose is *Quick Edit*, shown in *figure 1.3*, where the most rapid tools for the topology repair are present but, in case of specific corrections, it is possible to use other panels such as *Edge Edit*, *Lines Edit* and *Surface Edit*.

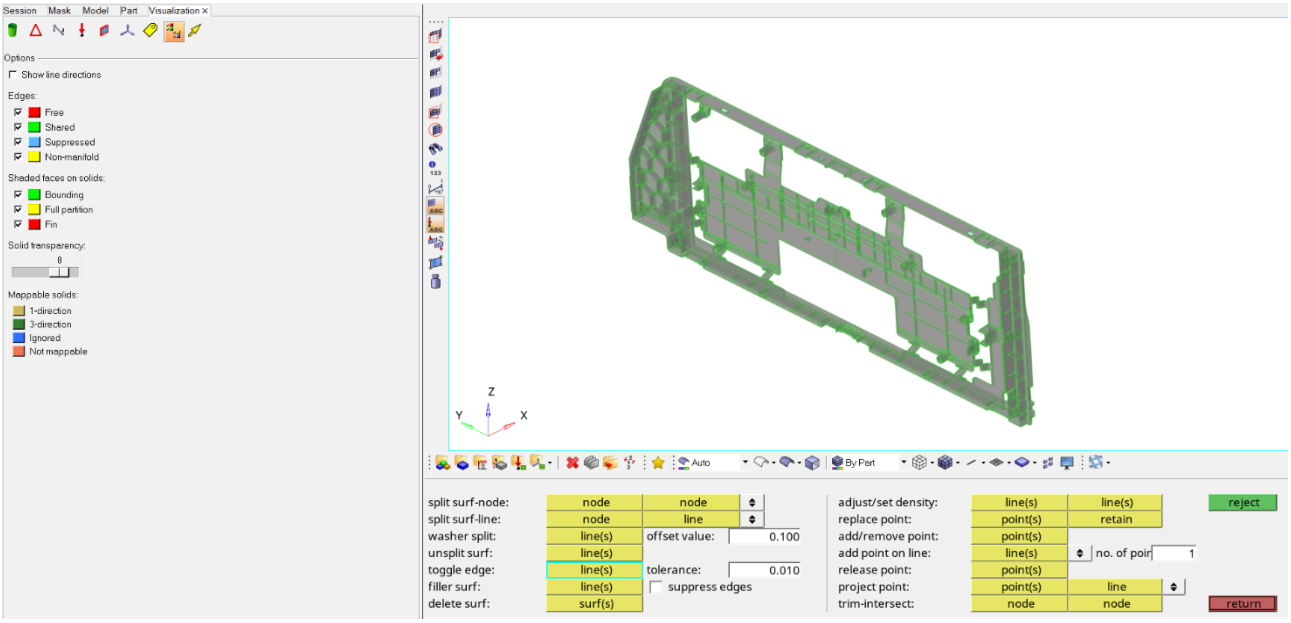

Figure 1.3 - Geometry cleanup of the front frame with quick edit panel

The *Quick Edit* panel allows to have a visualization of the topology of the component and there are some steps to perform in order to conclude correctly the geometry cleanup:

- Select a proper cleanup tolerance, based on the global element size of the mesh that is defined by the car manufacturer. This tolerance is the largest dimension of the gap that is possible to close using the different topology options. It is usually suggested not to exceed 15 % of the global element size because this may cause possible distortions in the meshing.
- Use the *Defeature* function on the software to check if there are some duplicate surfaces and if they are present, delete them.
- Use the equivalence function in the *Edge Edit* panel in order to combine possible free edge pairs but it is also important to perform a check on the component in order to avoid that the surfaces are not correctly collapsed. If there is still the presence of some free edge pairs, a suggested operation can be of using the function toggle in the *Quick Edit* panel.

Once these preliminary steps are performed, in the topology visualization of the model, as visible on the left window of *figure 1.3*, it is possible to observe that there are different colors that the lines of the model can have. Each color is associated to a different condition:

- Green line indicates a shared edge that connects two adjacent surfaces, this guaranties nodal continuity between the two surfaces and during the meshing the nodes are located on this edge.
- Blue line is very similar to the green one since it guaranties nodal continuity between the surfaces, but the edge is ignored in the meshing
- Yellow line indicates an edge that connects three adjacent surfaces.
- Red line indicates a free edge that separates two adjacent surfaces and this condition does not guarantee nodal continuity. This condition must be avoided and so topology repair is needed.

In *figure 1.3* it is possible to observe that all the lines of the front frame are green and this is the best condition that can be achieved. It is, thus, important to check accurately the topology visualization of the component and avoid red lines, since they may cause irreversible problems in the numerical solution of the model.

1.3 MESH

Once the geometry of the model, after the correction of all the geometry issues, is considered appropriate for the discretization using finite element method, the next operation is the meshing of the monitor.
Since this step approximates the geometry of the component, it is fundamental for the following finite element analysis because the quality of the mesh affects directly the results obtained from the different simulations. On the other hand, a more accurate mesh increases the computational time and so a tradeoff between the quality of the mesh and the computational time requested.
The main requirement to obtain a discretization of the model with shell elements, as suggested by the car manufacturer, is to have each component with a single surface without thickness and this is achieved, as previously described, with the creation of middle surfaces from the original geometry and in these surfaces it is possible to perform a bidimensional mesh. It is considered each component separately for the mesh of the monitor to achieve better results from the analysis.
The *Automesh* panel, visible in *figure 1.4*, allows to create rapidly shell mesh at the same time in all the surfaces of a component and the connectivity of the mesh is guaranteed by a properly connected geometry. It is also possible to select among different methods of meshing and in this case, considering the structural analysis and impact crash tests that have to be performed, the choice of the method is *size and bias*. This method allows to mesh again an existing mesh in order to manually improve the quality of the discretization in particular areas of the component, according to the criteria that are defined by the car manufacturer and must be respected. This choice is related to the fact that it is not possible to obtain a mesh with 100 % of the elements that are of good quality and so, in this case, with the use of *Mesh Edit* window it is possible to fix

the elements with poor quality, performing a topology refinement and avoiding to distort significantly the original geometry.

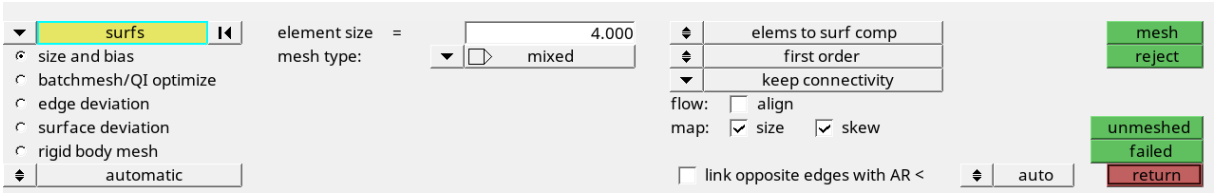

Figure 1.4 - Automesh window on HyperMesh

In the panel of *figure 1.4* it is possible to select different parameters, that permits to have a higher control on the mesh:

- Element size: it is the average dimension of each element of the mesh and this dimension must be selected according to the complexity and size of the component. A finer mesh with very small element size allows a better approximation of the geometry with more accurate results but this causes an increase of the computational time, that is not always acceptable.
- Mesh type: it indicates the kind of element that is created such as triangles, squares or a mix of triangular and squared element. A choice of a mixed mesh allows to have a smoother mesh.
- Order of the element: it is connected to the order of the function that is used in finite element method. It is possible to choose between linear elements of first order or quadratic elements of second order. The second order leads to more accurate results but this, in most cases, does not justify the consequent increase of the computational time.

The mesh size selected by the car manufacturer is 4 mm and the elements of the mesh are linear of first order and mixed, both of triangular and squared shape.

The *Automesh* panel is adopted for the discretization of all the different parts of the monitor, except the front frame, where, due to the complexity of the geometry, it is very difficult to extract the middle surfaces from the original model. In this situation the strategy that is adopted is to use the *Midmesh* window, where it is possible to generate a mesh in the midplane of each surface of the solid part, without the need to create the mid-surfaces. With respect to the traditional approach used, this choice leads to a lower quality mesh and so it is necessary to fix manually the issues that are caused by elements that do not respect both the original geometry and the criteria imposed, as visible in *figure 1.5.*

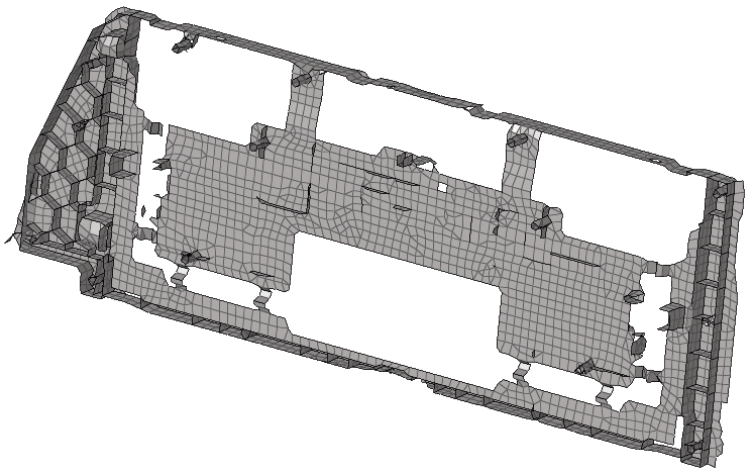

Figure 1.5 - Midmesh of the front frame

1.4 MESH QUALITY CHECK

It is not possible to obtain all the elements of the mesh with good quality and so it is necessary to perform a quality check on the mesh and then modify the elements that do not respect the requirements. In order to control if the values of the upper or lower limit of the different parameters of the mesh are respected, it is used the *Check Elements* window, as visible below in *figure 1.6.* Among all the different quality parameters, the most important is the Jacobian ratio and it indicates the distortion of the element with respect to the ideal shape. It ranges from 0 to 1, where 1 indicates an element with perfect shape but for structural analysis a value higher than 0.6 is considered acceptable.

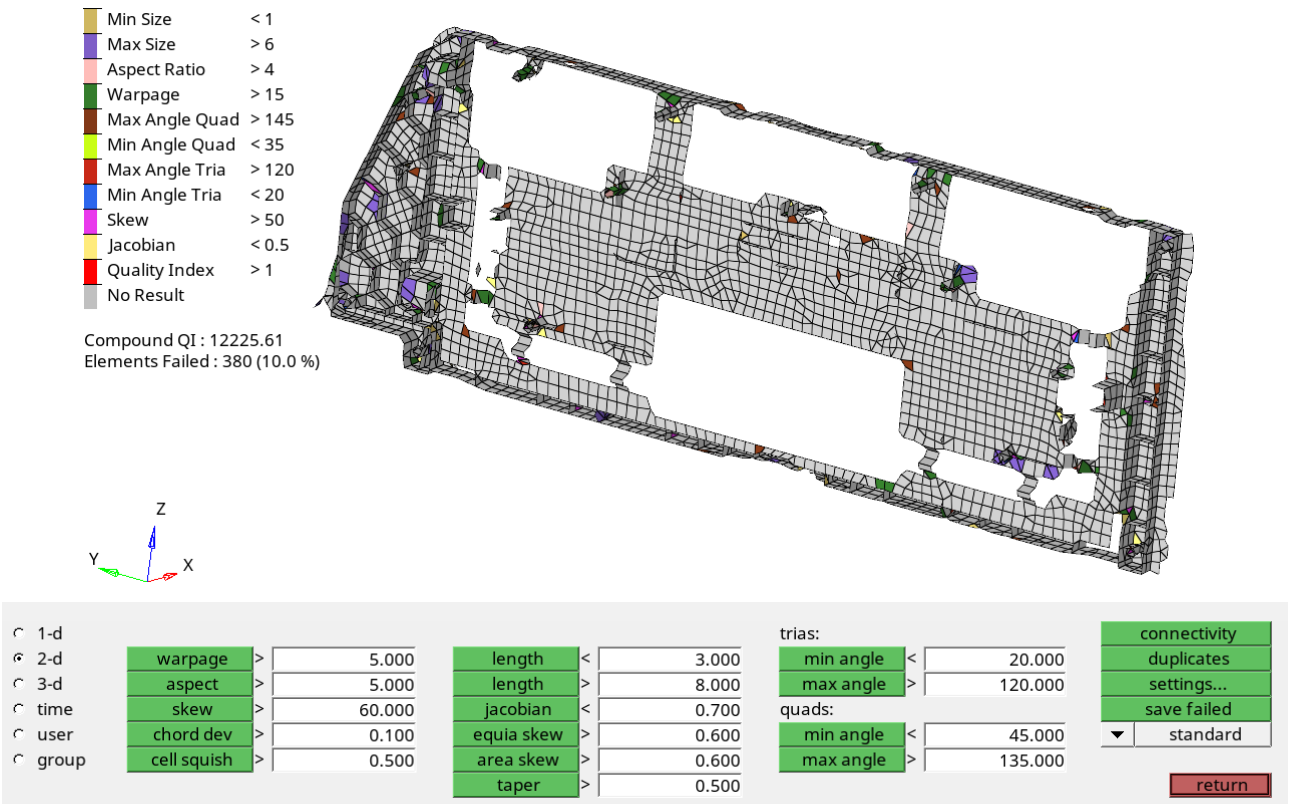

Figure 1.6 - Mesh quality check of the front frame with Check Elements panel below

In *figure 1.6* it is possible to observe that the 10 % of the elements of the mesh of the front frame does not respect the requirements of the geometric quality of the mesh and the Jacobian ratio is below 0.6. For these reasons, there are some operations to perform in order to modify the shape and the size of the failed elements and pass the mesh quality check:

- Check the nodal connection: this check consists in finding the free edges in order to detect possible problems of connectivity. The free edge is considered an issue if it is located within a portion of elements of the mesh, because it represents a discontinuity in the mesh, while it is not a problem if located on the external perimeter of the component. This issue can be solved by using the *Check Nodes* window in *figure 1.7,* by setting a tolerance within which the nodes are equivalenced. This tolerance must not be too large because it may cause the collapse of some elements.

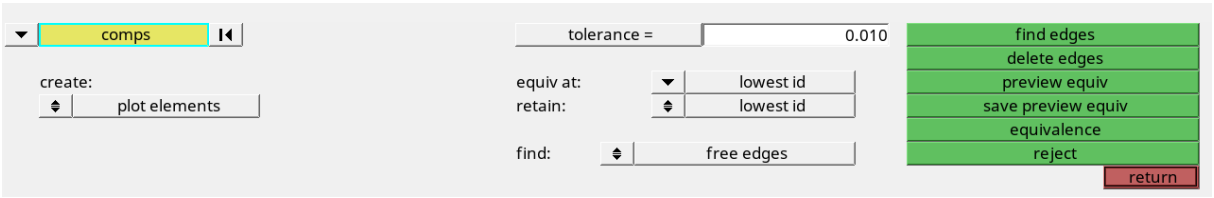

Figure 1.7 - Check Nodes panel on HyperMesh

- Quality index: the value of this single parameter represents the quality of the mesh, based on the different quality parameters shown in *figure 1.6*; higher is the value and lower is the quality of the mesh. In the *Quality Index* window in *figure 1.8* are highlighted the elements that fail, where the red element indicates a worst condition than the yellow one.

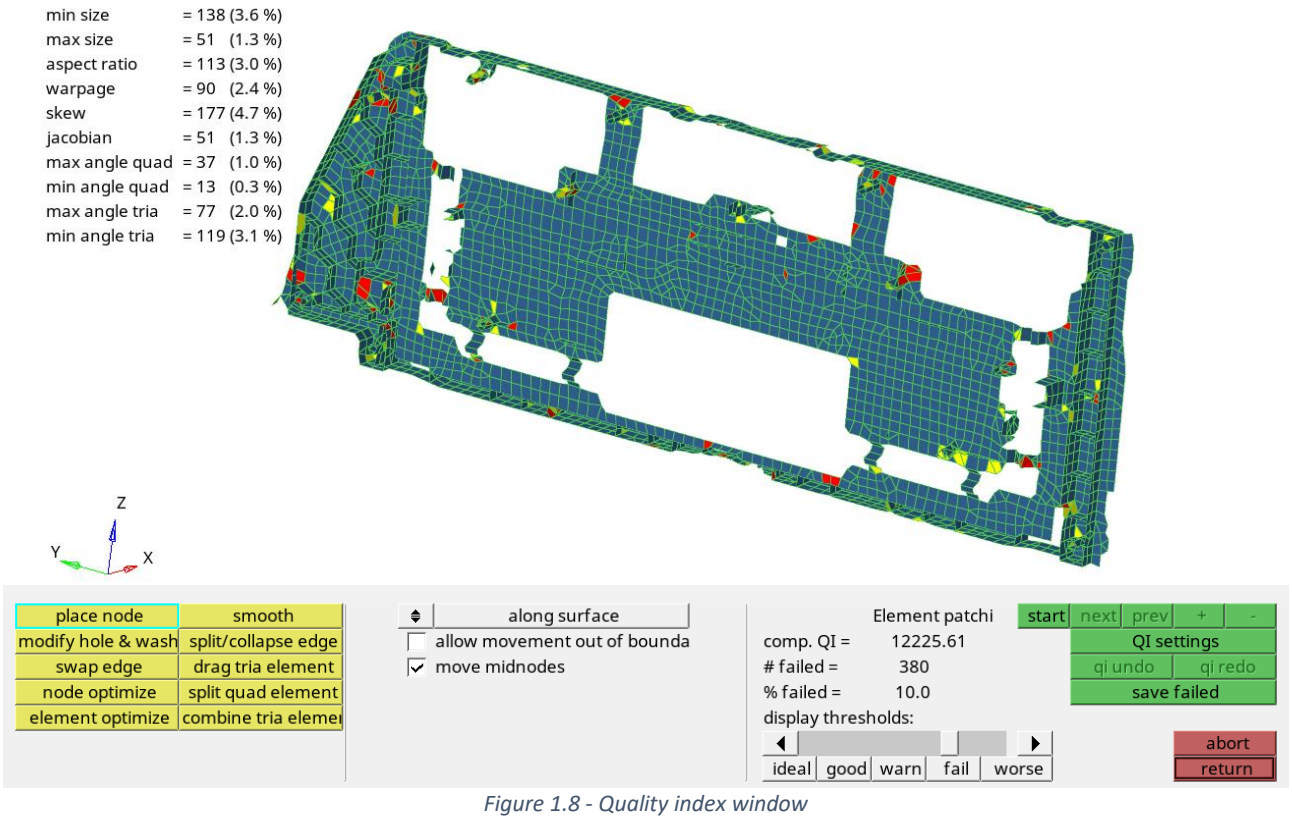

Figure 1.8 - Quality index window

In *figure 1.8* in the bottom part, it is also shown the *QI cleanup tool* panel, where it is possible to see among different tools to improve locally the quality of the mesh with the modification of the shape of the elements.

- If after all the previous steps there are still elements that do not respect the mesh criteria, it is necessary to modify manually the elements for example with the translation or rotation of the nodes of a single element or with a re-mesh of only a portion of the component that is characterized by poor quality mesh.

The final results of the mesh of the front frame of the monitor, after the mesh refinement, is shown in *figure 1.9*, where it is possible to observe that there are no more elements that fail, and the quality index is almost zero and this highlights the good quality of the mesh and the Jacobian ratio is acceptable, with a value higher than 0.6.

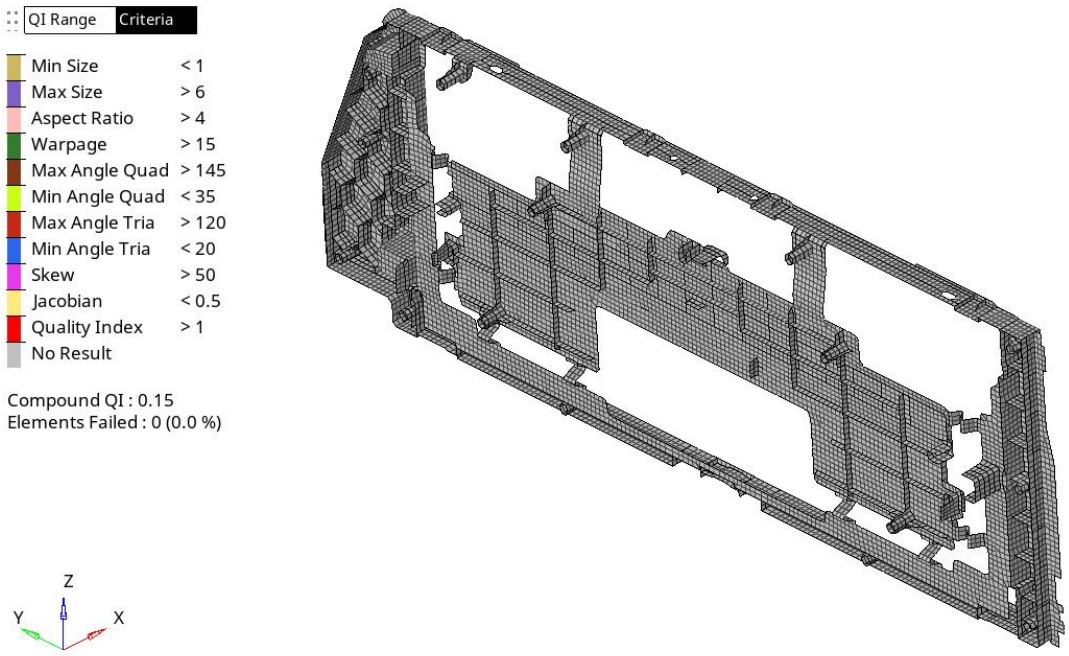

Figure 1.9 - Final mesh of the front frame of the monitor

1.5 Model discretization with Hypermesh (OptiStruct)

Once the mesh of all the different components of the monitor is completed, the next step is to define how the different components are connected each other and in this case some components are bonded with the use of glue and some others through threaded connections.

Some simplifications are applied to the model in order to better understand and analyze the results obtained from the finite element analysis, avoiding to make computations heavier. These assumptions are shown in the next paragraphs.

1.5.1 Definition of the rigids

In the definition of the numerical model for the analysis, the rigids (RBE2) are introduced in order to easily simulate the connection between the nodes, avoiding the approximation of the threaded connections with specific discretization using finite element method. RBE2 is a unidimensional element that rigidly links an independent node to one or more dependents nodes and in this way it is possible to transfer the load. For the model of the monitor, rigids are used to simulate:

- Threaded connection between the board and the back case, as visible in *figure 1.10*. The bolting, made of screw and nut, is simulated with the rigids. In this case the independent node is calculated and located in the middle of the holes to couple while the dependent nodes are the ones that define the holes of the two components. The dependent nodes of the surfaces of the two components has to follow the motion of the independent one with a rigid behavior.

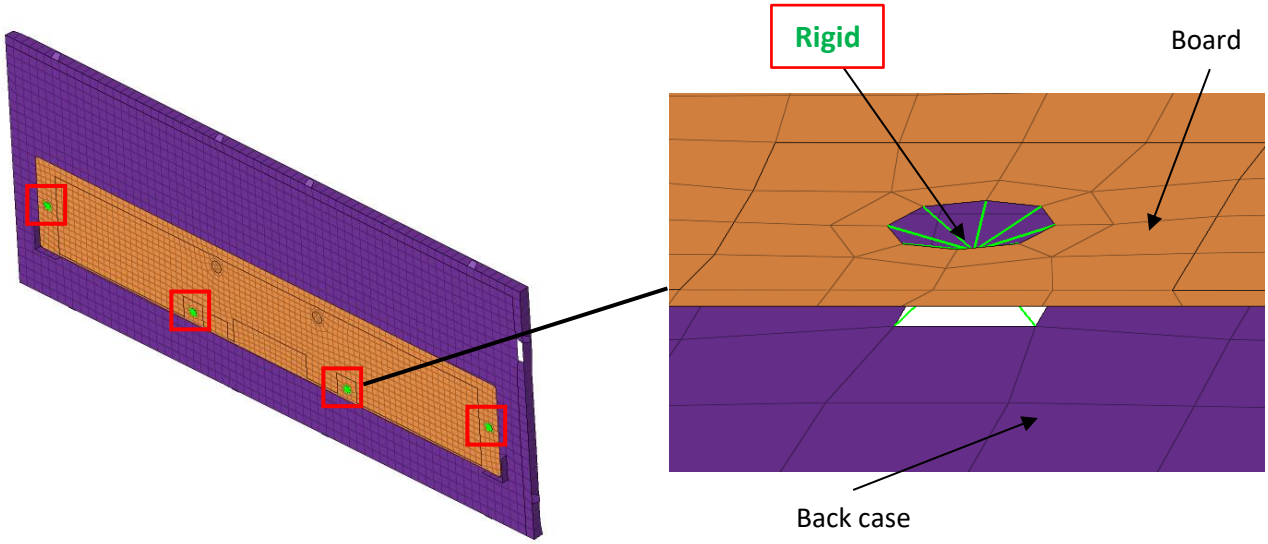

Figure 1.10 - Threaded connection between the board and the back case

- Threaded connection between the rear cover (grey component) and the front frame (green component), as shown in *figure 1.11,*

Figure 1.11 - Threaded connection between the rear cover and the front frame

- Plastic additional fixation to connect the back case and the front case, as shown in *figure 1.12,*

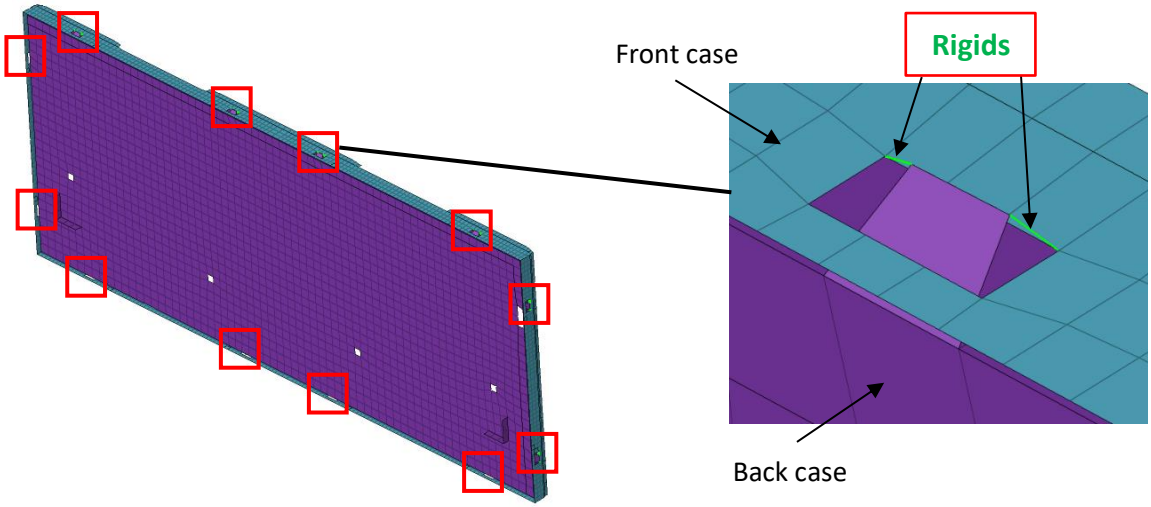

Figure 1.12 - Plastic additional fixations between the front case and the back case

- Contact edge to edge between the components that are not connected, otherwise there may be irreversible problems when the simulations are run. In particular, the rigids are used to connect the screw housing of the front frame and the holes in the PCB, as visible in *figure 1.13*, and to connect the optical sheet and the TFT glass module in the front panel, as shown in *figure 1.14*.

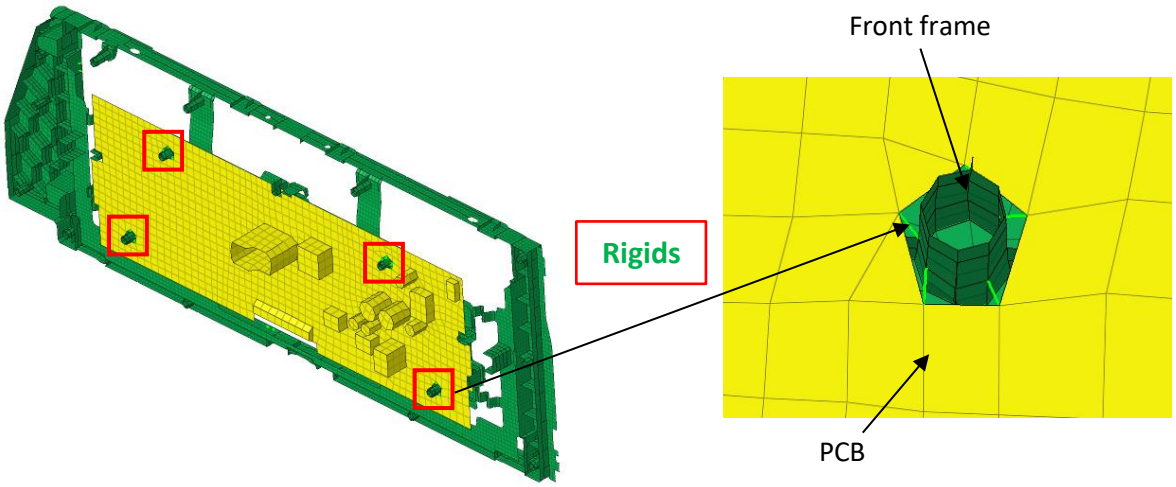

Figure 1.13 - Connection between the front frame and PCB

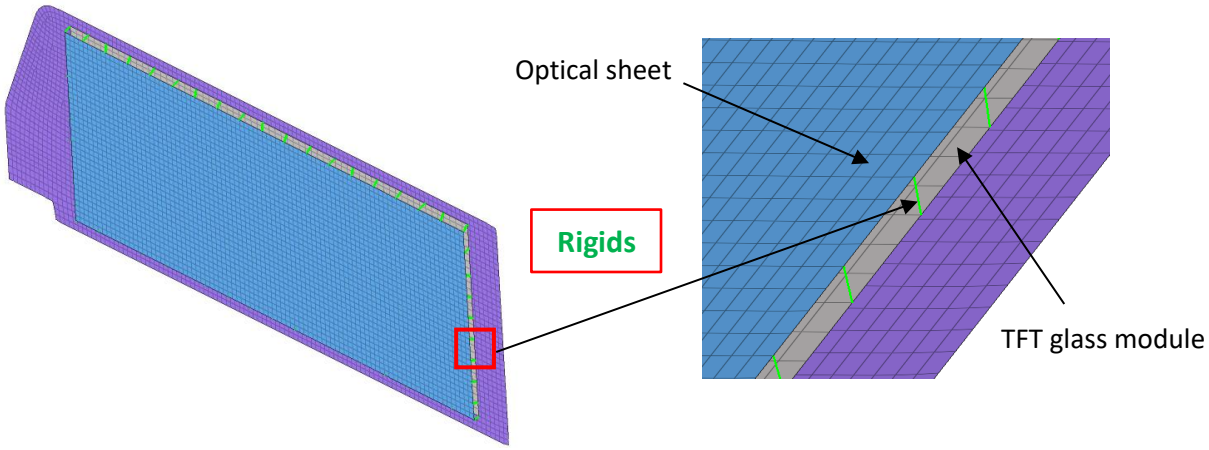

Figure 1.14 - Connection between the optical sheet and the TFT glass module

1.5.2 Definition of the freeze contacts

Glues are modeled as solid elements and it is necessary to create bonding between different components in the model. The bonding with the use of glue is modelled with freeze contact.

In the freeze contact there is not relative motion between the two surfaces that are in contact and the gap between them is fixed during the structural analysis.

This linear contact is a pure kinematic coupling of nodes with surfaces where a defined number of slave nodes has to follow exactly the same movements of the master surfaces. It is a purely linear artifice because no viscosity and friction are defined and so non linearities are not considered, but it is used for modal and linear static analysis on the model since it anyway guaranties reliable results.

In the creation of the contact, it is also important to define search distance criterion for creating contact condition, where only nodes that are within this distance from master surface will have contact condition checked. The freeze contact is adopted to simulate:

- Bonding with glue in the front panel, as shown in *figure 1.15,*

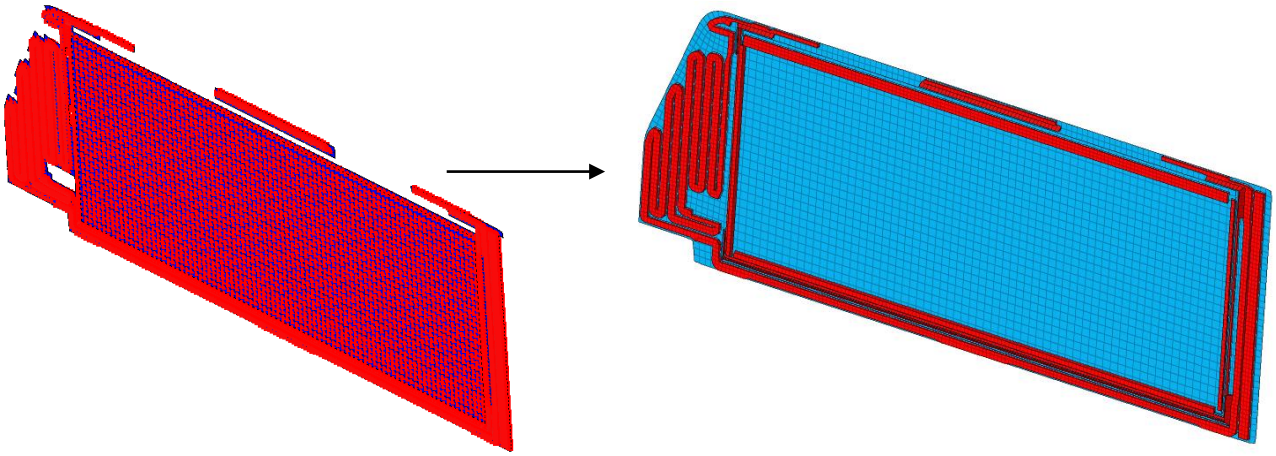

Figure 1.15 - Bonding with glue in the front panel

- Bonding with glue in the front case, as shown in *figure 1.16,*

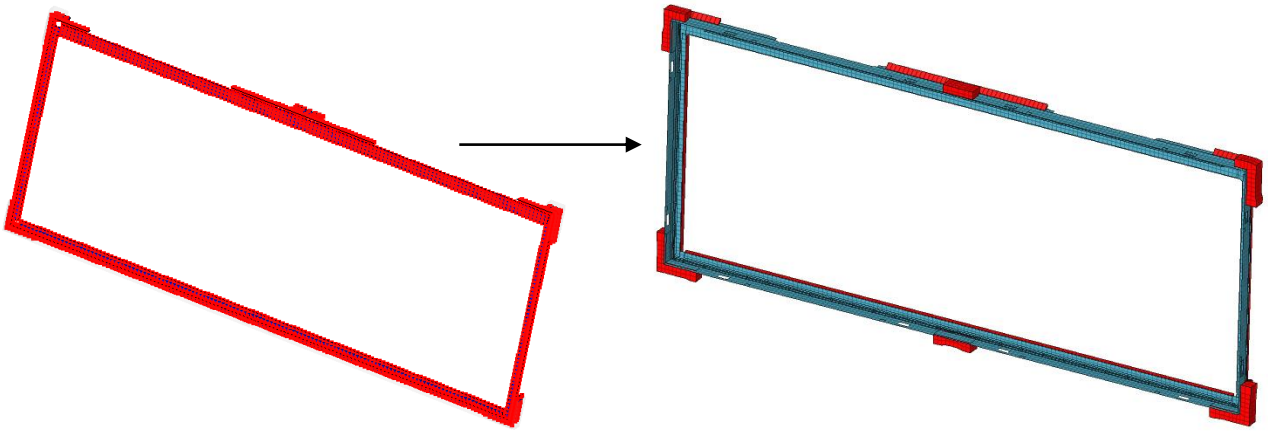

Figure 1.16 - Bonding with glue in the front case

- Bonding with glue in the rear cover and in the back case, as shown in *figure 1.17,*

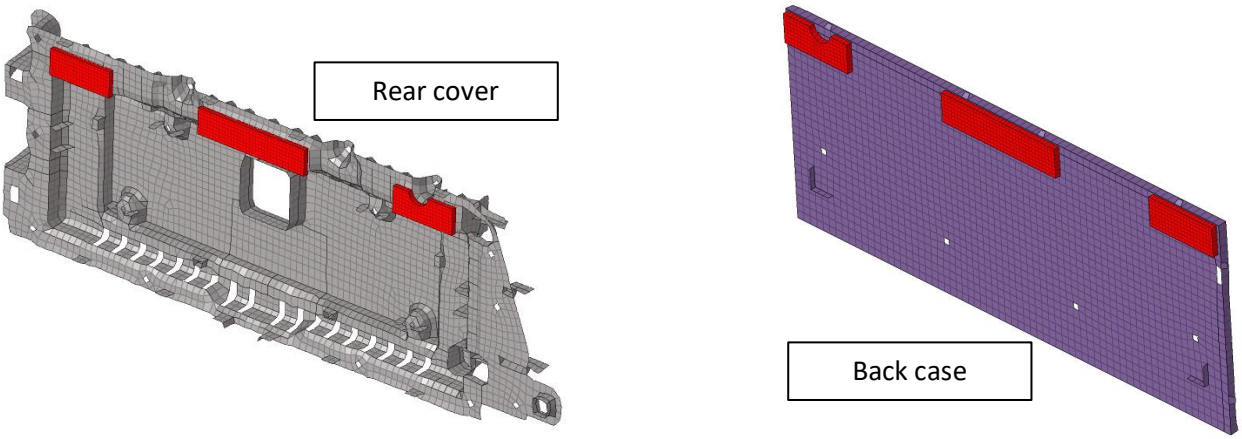

Figure 1.17 - Bonding with glue in the rear cover and in the back case

- Bonding with glue in the front frame, as shown in *figure 1.18,*

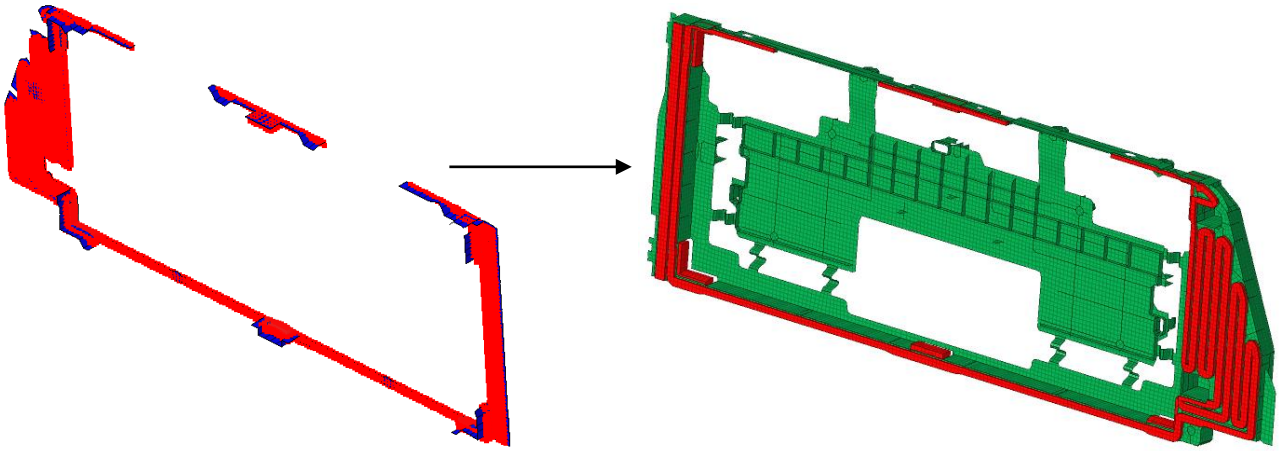

Figure 1.18 - Bonding with glue in the front frame

- Bonding with glue in the soft component, as shown in *figure 1.19.*

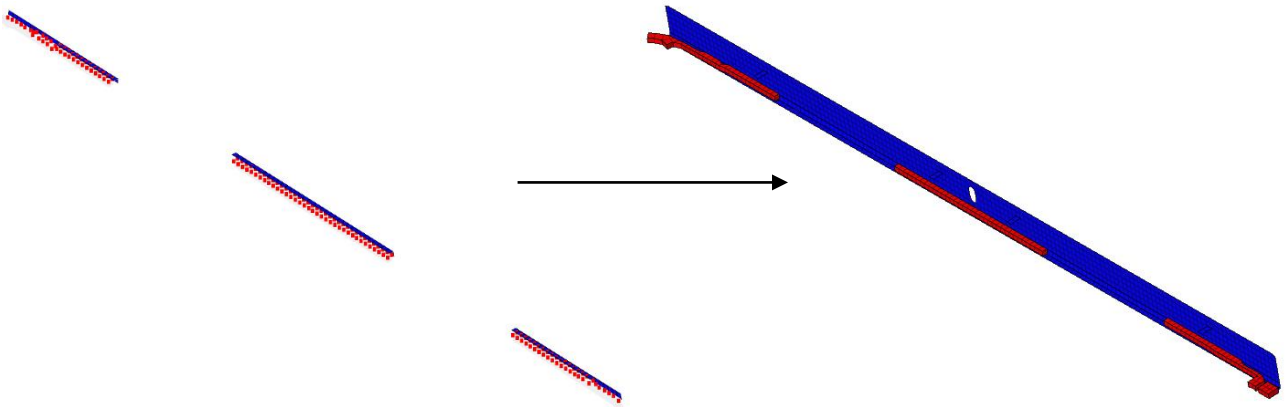

Figure 1.19 - Bonding with glue in the soft component

1.6 DEFINITION OF THE MATERIALS AND THE PROPERTIES

For the structural analysis it is necessary to consider only some parameters for the characterization of the different materials and each material is then associated to the correspondent component with a specific property. In fact, in the OptiStruct solver it is sufficient to define for each material the Young modulus, the Poisson ratio and the density. The card image that is selected in the solver is MAT1, meaning that all the material are modelled as linear isotropic and so the solver considers only the linear-elastic trend of the stress-strain curve. The structural analysis, in fact, has the purpose of computing the static stiffness of the system or its natural frequencies and corresponding structural modes and so the plastic trend after the achievement of the yielding point is not of interest.

The parameters of the different materials of the components of the monitor are reported in *table 1.2*.

Component	Material	Density [kg/m^3]	Young modulus [GPa]	Poisson ratio [-]
Back case	Magnesium alloy AZ91D (die casting)	1810	41.5	0.33
Rear cover	Magnesium alloy AZ91D (thixomolding)	1810	44.8	0.33
Front case and optical sheet	PC	1200	3.5	0.34
Front case and board	PC+ABS	1130	3.0	0.34
PCB	FR4 (composite made of flame retardant epoxy resin and glass fabric)	1900	18.6	0.13
Soft component	TPV (thermoplastic rubber vulcanizate)	1200	1.3	0.35
TFT glass module	TFT (Thin Film Transistor)	2480	7.4	0.23
Protective cover glass	Dragon Trail Pro	2503	73	0.22
Cushion foam (glue)	Foam	86.21	0.0233	0.3
Thermal gapfiller (glue)	Gap filling material	65	0.01	65

Table 1.2 - Properties of the materials of the monitor

Once the definition of the materials is completed, since the discretization of the components of the monitor, with the mesh, is obtained in the middle surfaces, it is necessary to build the thickness map of each component. This step has the function of identifying the different thicknesses present in one component, in order to better assign the corresponding property.

After this step it is possible to assign a property for each component and the properties are adopted to identify the features of the finite elements of the mesh. In this way it is possible to completely characterize

each component of the monitor, also considering the characterization of the material.
The properties that are used in the software (OptiStruct) are:

- PSOLID: this card image is used for the different glues, since they are modelled as solid elements,
- PSHELL: this card image is used for all the other components of the monitor. For each property, aside from the assignment of the material, it is necessary to define the thickness obtained from the thickness map.

For the rigids instead, no property is assigned since the aim of these unidimensional elements for structural analysis is only to create a rigid link between different components.

2 MODAL ANALYSIS OF THE MONITOR OF THE DASHBOARD WITH OPTISTRUCT

The first preliminary analysis that can help to have an idea of the general behaviour of the system, before any structural simulation, is the modal analysis. With a modal analysis it is possible to identify the natural frequencies of the monitor and the corresponding mode shapes but also to check if the connections between the different components are set correctly and verify the rigid modes of the system.

It is necessary that the natural frequencies of the monitor are far from the characteristic frequencies of the external forces, otherwise it is possible to have resonance and the amplitude of the oscillations can increases too much up to the rupture of the component.

2.1 FREE – FREE CONDITION

The first modal analysis is performed without the application of any constraints. The aim of this modal analysis is to verify that all the components of the monitor are correctly connected each other. This is verified only if there are six rigid mode shapes, that correspond to the three translations and the rotations about the three-axis x, y and z. If there are more than 6 mode shapes with a natural frequency of 0 Hz, this means that not all the components are linked correctly, it is, thus, necessary to correct this issue before performing other analysis. The six rigid mode shapes are:

- Translation along y (mode 1) and translation along z (mode 2), as visible in *figure 2.1*,

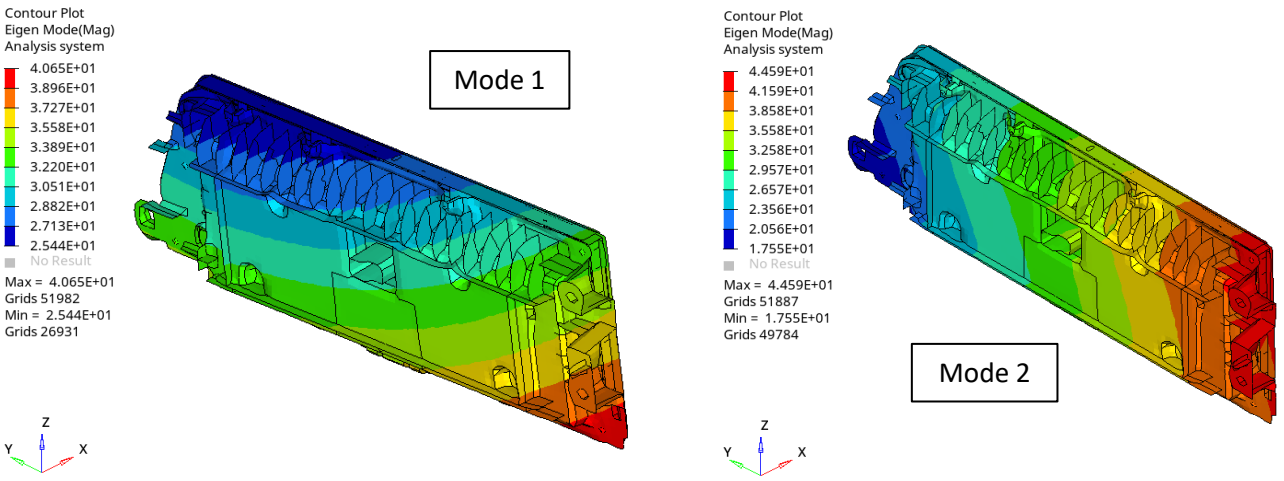

Figure 2.1 - Mode shape 1 and 2 in free- free condition

- Translation along x (mode 3) and rotation about x (mode 4), as visible in *figure 2.2*,

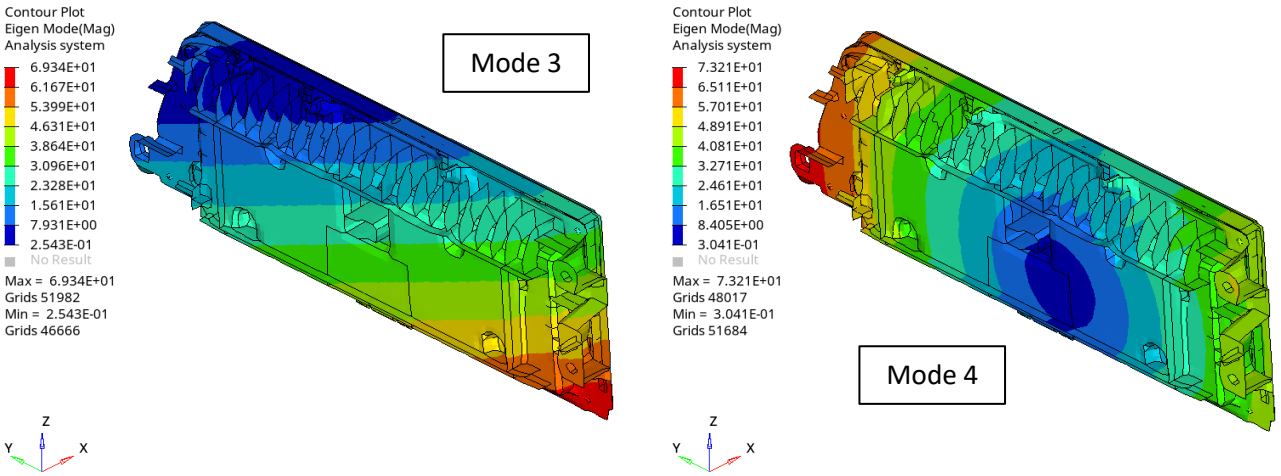

Figure 2.2 - Mode shape 3 and 4 in free- free condition

- Rotation about y (mode 5) and rotation about z (mode 6), as visible in *figure 2.3*.

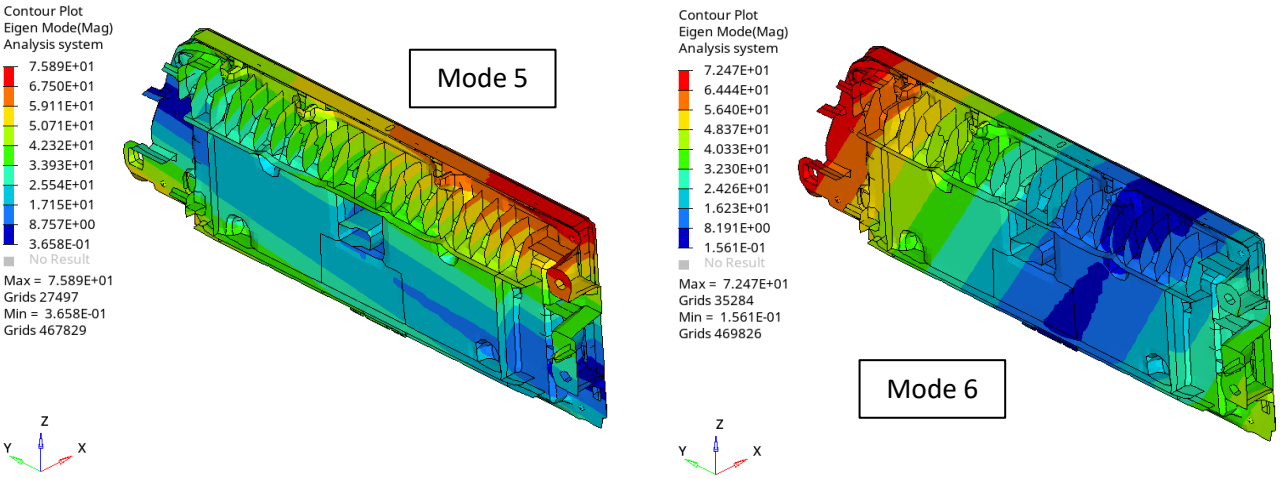

Figure 2.3 - Mode shape 5 and 6 in free- free condition

2.2 CONSTRAINED CONDITION

A second modal analysis is performed but in this case the monitor is constrained in the rear cover, in order to simulate the fixture of the monitor on the dashboard. In this way it is possible to analyze the influence of the constraints on the natural frequencies and corresponding mode shapes.

Constraints are set by considering RBE2 rigids that connects a series of dependent nodes and then they are applied on their corresponding centered independent node, as visible in *figure 2.4*. In the two holes located in the right end side of the rear cover, all the six degrees of freedom are constrained while in the two pins located in the left end side only the translations along x (degree 1) and z (degree 3) as well as the rotation about z (degree 6). In this case not all the degrees of freedom are fixed because the pins are screwed on the dashboard with a rotative motion.

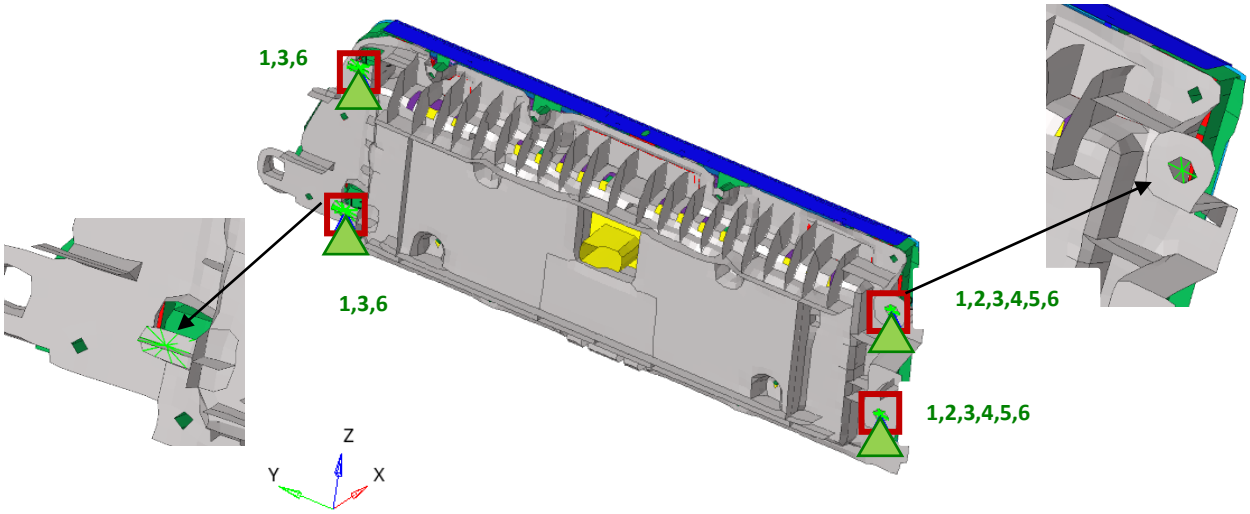

Figure 2.4 - Constraints in the rear cover of the monitor

2.3 COMPARISON OF THE STRUCTURAL MODES

The first comparison that is considered is the one between the first mode in the free- free condition and the constrained one with a natural frequency different from 0 Hz. As shown in *figure 2.5*, it is possible to figure out that the first mode after the rigid ones in the free- free condition has almost the same behaviour as the first mode in the constrained condition case. This is a localized mode shape due to the tilting effect of the PCB (Printed Circuit Board) and may be caused by the connection between the rear cover and PCB, since the link is applied only in four screw housing through rigids. It is also possible to highlight that the constraints, in this case, have a minor effect because the frequency in the two cases is almost the same as well as the motion of the component.

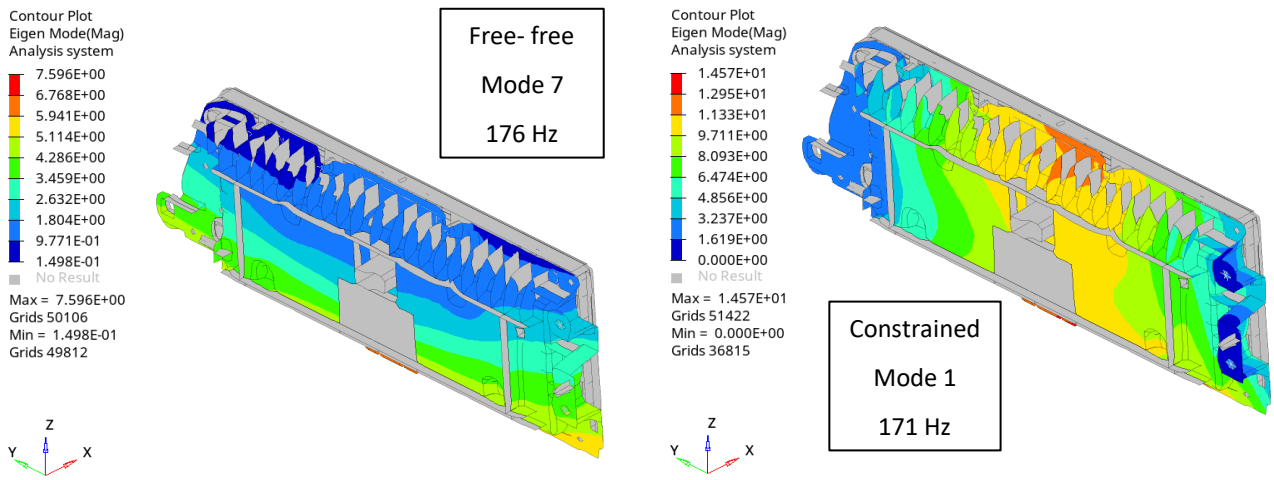

Figure 2.5 - Comparison between mode 7 in free- free condition and mode 1 in constrained condition

The next comparison is to consider the first structural mode of the monitor in the two cases, in particular in *figure 2.6* it is shown the first structural mode of the monitor in free- free condition and the corresponding one in the constrained condition.

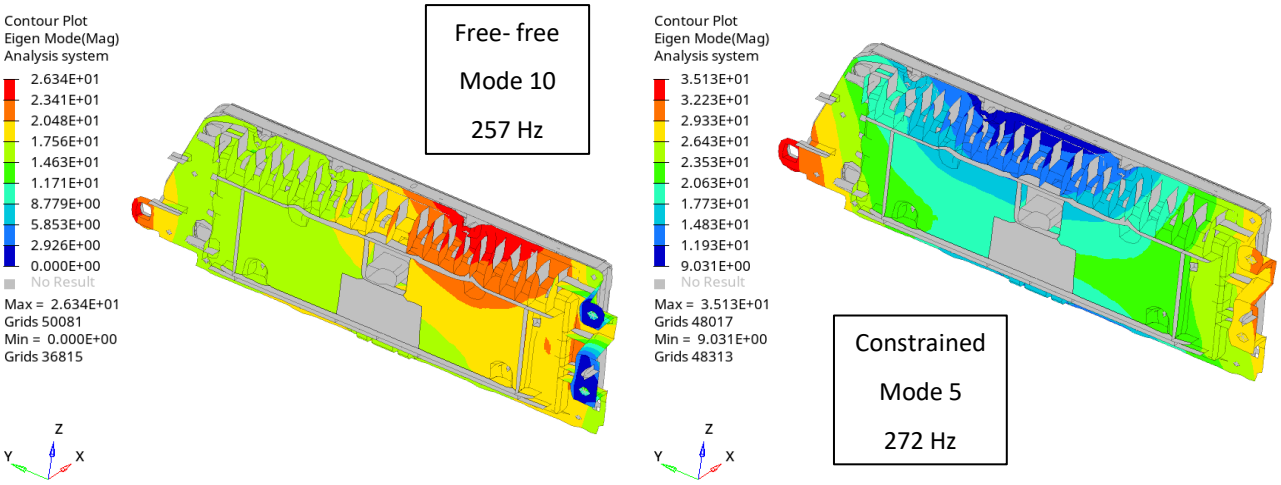

Figure 2.6 - Comparison between mode 10 in free- free condition and mode 5 in constrained condition

As it is possible to see, the first structural mode in the free-free condition is due to the tilting bending moment of the entire structure and not localized only on the PCB while in the constrained condition is due to a torsional moment of the entire structure. Since the first structural modes are different in the two conditions, it is not possible to compare them and so the final comparison is to analyze the structural mode in the constrained condition that is more similar to the first one in the free- free case (mode 7), as visible in *figure 2.7*.

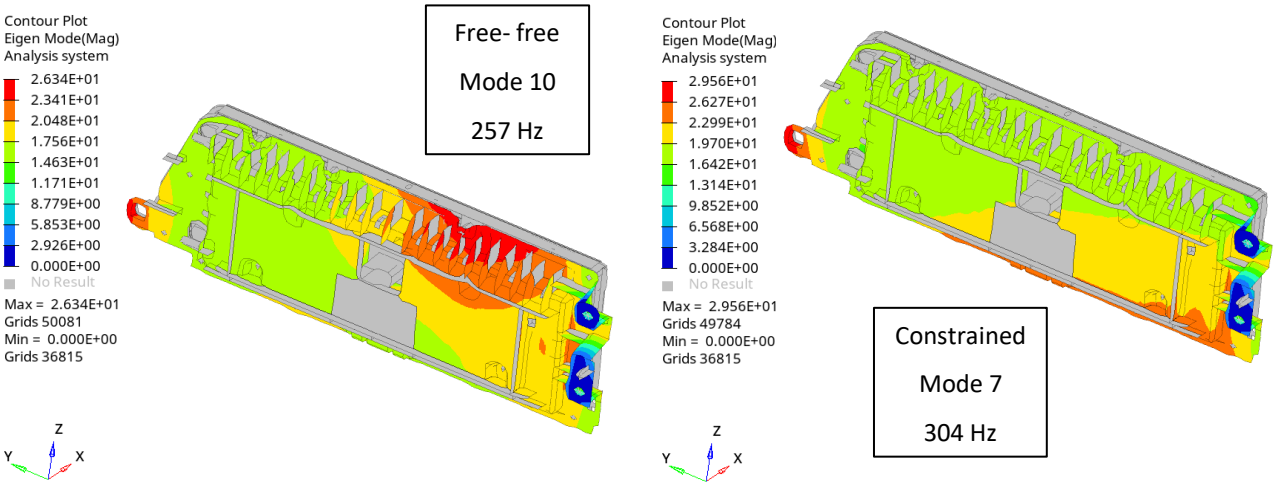

Figure 2.7 - Comparison between similar structural modes in the free- free and constrained condition

The seventh mode shape in the constrained is similar to the tenth one in the free- free condition since it is possible to observe the presence of the tilting bending moment but in the seventh mode shape there is also the presence of a torsional moment that is not present in the other case. The frequency of the constrained case, where constraints are applied on the left and right end part of rear cover, is higher than the similar mode in free-free condition because the oscillations of the extreme parts of the rear cover are limited and this causes an increase of frequency.

After the analysis of the different modal analyses, it is possible to conclude that the natural frequencies of the component are higher than the value of acceptable limit (35 Hz), that is the typical frequency of the engine and gearbox coupling. They are consequently out of dangerous range for perceived quality and far from characteristic frequencies to have resonance.

Also squeaks and rattles problems are avoided. This problem is caused by some components of the vehicle that are not connected correctly and creates annoying noises.

3 LINEAR STATIC ANALYSIS OF THE MONITOR WITH OPTISTRUCT

Based on the constraints applied in the modal analysis in order to simulate the fixture of the monitor on the dashboard, two linear static analysis are performed, by applying a load of 10 N along x axis in the same position but on different components, in order to compute the static stiffness and understand the influence of force in the different components of the monitor:

1) Application of a force of 10 N along positive x axis on the rear cover: a patch of a defined number of nodes, in order to distribute the load, in the center of the rear cover is considered and based on this patch a RBE2 rigid is created in order to define the centered independent node; in this node the force is applied,

2) Application of a force of 10 N along negative x axis on the protective cover glass of the front panel: a patch of the same dimensions of first case is considered and the same approach is used.

The point of application of the force in the two cases is shown in *figure 3.1*, where for the first case is visible the bottom view of the monitor while for the second case the front view.

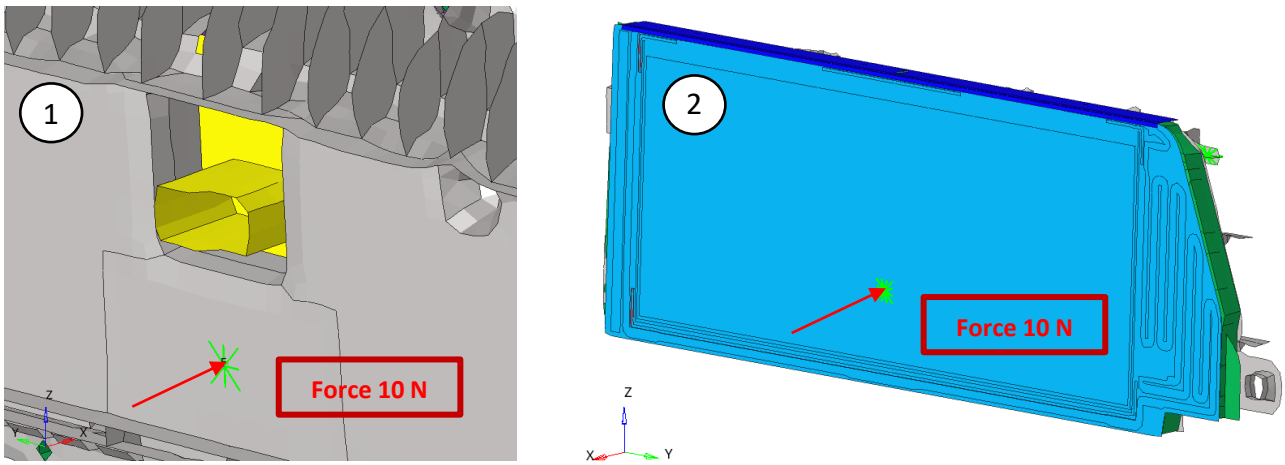

Figure 3.1 - Location of the force in the two different linear static analysis

Once the linear static analyses are completed, it is possible to observe the influence of the force looking at the contour plot of the displacement that is caused by the application of the force in the different components of the monitor. Focusing on the first case, in *figure 3.2* it is possible to check that the force is correctly applied in the centre of the rear cover, since the maximum displacement is located in the point of the load application. The load causes its propagation through the different components that are located behind the rear cover and consequently the displacement, from the largest value on the point where the load is applied, decreases through the thickness of the monitor and as the component considered is far from the application of the force.

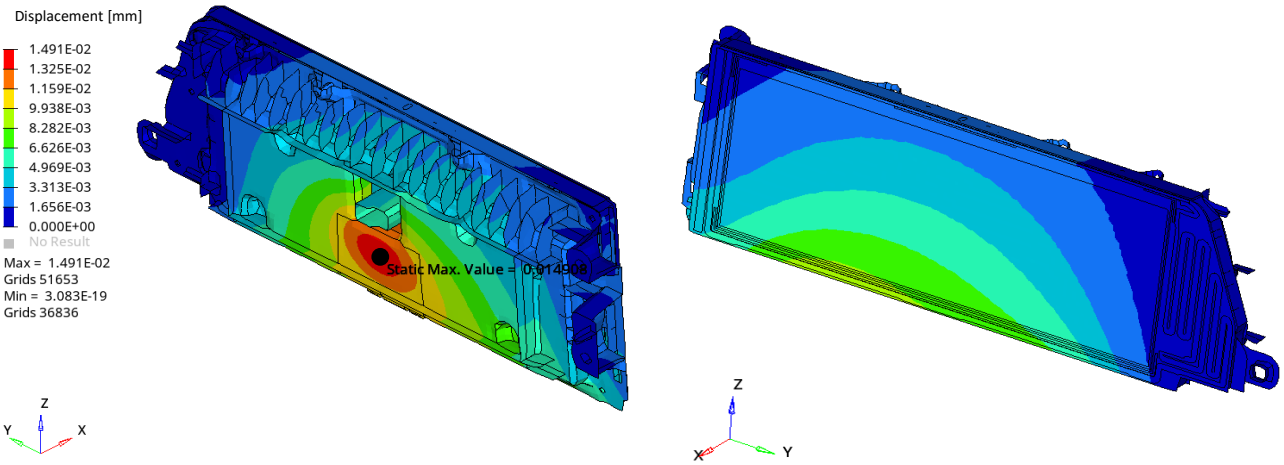

Figure 3.2 - Contour plot of the displacement in the bottom and front view of the monitor with force on rear cover

Focusing instead on the second case, where the force is applied on the protective cover glass, in *figure 3.3* the maximum displacement is located, as expected, in the point of load application but the value is higher with respect to the case of the rear cover. The propagation of the load through the different components located behind the cover glass is more evident, using the same scale for displacement as the one adopted for the first case.

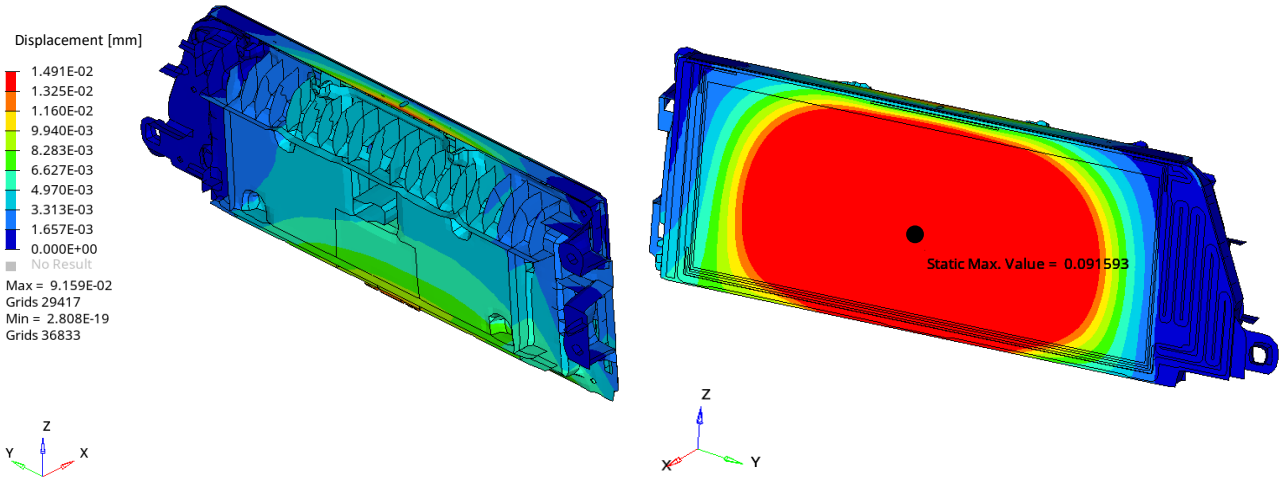

Figure 3.3 - Contour plot of the displacement in the bottom and front view of the monitor with force on cover glass

Since from the contour plot of the displacement it is possible to identify the value of the maximum static displacement, the static stiffness on the rear cover and the protective cover glass can be computed as the ratio between the force magnitude applied (10 N) and the maximum displacement. The values of the maximum displacements and the corresponding static stiffnesses are reported in *table 3.1*.

Force	Maximum displacement [mm]	Static stiffness [N/mm]
Application on rear cover	$1.491 \cdot 10^{-2}$	670.7
Application on cover glass	$9.159 \cdot 10^{-2}$	109.2

Table 3.1 - Values of the maximum displacement and stiffness in the two linear static analyses

Even if the Young modulus of the protective cover glass (E=73 GPa) is higher than rear cover (E=44.8 GPa), the static stiffness of the protective cover glass is lower than the one of the rear cover.

This result may be caused by the fact that the cover glass is one of the 3 sheets of the front panel and these sheets are all bonding with glue. Since the Young modulus of the glue is very small (E=0.1 GPa), this may cause an important decrement of the stiffness of the cover glass.

4 SETUP OF THE DASHBOARD FOR HEAD IMPACT WITH LS-DYNA

Since for the preliminary structural analyses has been adopted the implicit solver Optistruct, the explicit solver Ls-Dyna is instead necessary for the following analyses to simulate the head impact on the dashboard. The modelling of the monitor of the dashboard is no more suitable for the impact simulations and so some steps in the modelling of the monitor are needed, in order to convert the previous model in the OptiStruct environment into a model in the Ls-Dyna environment.

Before converting the OptiStruct model of the monitor using the *Convert* option in the toolbar of the HyperMesh software, it is better to remove the properties, freeze contacts, connections and load steps that were present in the previous model. Even if the materials are the same, for the impact analysis a more accurate characterization of the materials is needed, with more parameters to define, and consequently it is better also the removal of the materials. This operation allows to avoid issues that may arise after the conversion.

After the conversion, the new model in the Ls-Dyna environment contains only the mesh of the different components of the monitor. The same approach, adopted with OptiStruct, is followed also in this case for the model discretization and setup of the monitor of the dashboard.

The same procedure described in paragraph 1.5.1 is adopted to locate the rigids that simulate the threaded connections and the plastic additional fixations between different components.

For the definition of the contacts to simulate the bonding with the use of glue, as well as for the characterization of the materials and definition of the properties, instead, the software Ls-Dyna uses a different nomenclature, that will be explained in the following paragraphs.

4.1 DEFINITION OF THE MATERIALS AND PROPERTIES

The software Ls-Dyna assigns a specific number to each material model, according to its specific behaviour. For the modelling of the monitor, the choice of the different material cards is made in order to have a balance between time requirements for the analysis and the accuracy in simulating the behavior of the material, because a more detailed characterization of the material implies more parameters to define and a better simulation of its real behavior but, on the contrary, this causes an exponential increase of the computational time in the analysis. The material cards that are used for this model are:

- MAT 3 *(MAT_PLASTIC_KINEMATIC)*: it is suitable for materials that present kinematic hardening plasticity and it is adopted for the characterization PCB, TFT glass module and glues in the monitor. It is not sufficient to define Young modulus, Poisson ratio and density as parameter for the characterization but also the yield stress, the tangent modulus and the hardening parameter, the latter equals to 0 to simulate the kinematic hardening.

- MAT 57 *(MAT_LOW_DENSITY_FOAM):* it is suitable for density foams that are characterized by low density and high compressibility and in the model is adopted for the cushion foam. In the characterization of the material, apart from the definition of the density and Poisson ratio of the foam, it is also loaded a curve that defines the nominal stress as a function of the nominal strain.
- MAT 100 *(MAT_SPOTWELD):* it is suitable to beam element type 9 for spot welds, that is the property that is adopted for the rigids of the threaded connections and so it is used for steel screws and plastic additional fixations. The parameters that must be added, apart from the Young modulus, the Poisson ratio and the density, are the plastic hardening modulus and the yield stress.
- MAT 24 *(MAT_PIECEWISE_LINEAR_PLASTICITY):* it is suitable for modelling elasto-plastic material with stress as a function of strain curve and it is adopted for all the other components of the monitor. For these materials, a table defines for each strain rate value a load curve giving the effective stress as a function of effective plastic strain for that rate. The failure of this material model is based on the maximum plastic strain and when this upper value is reached, the element fails and is deleted from the calculation.

In *table 4.1* are reported the different material cards that are adopted for the components of the monitor.

Component	Material	Material card
Back case	Magnesium alloy AZ91D (die casting)	MAT 24
Rear cover	Magnesium alloy AZ91D (thixomolding)	MAT 24
Front case and optical sheet	PC	MAT 24
Front case and board	PC+ABS	MAT 24
PCB	FR4	MAT 3
Soft component	TPV	MAT 24
TFT glass module	TFT	MAT 3
Protective cover glass	Dragon Trail Pro	MAT 24
Cushion foam (glue)	Foam	MAT 57
Thermal gapfiller (glue)	Gap filling material	MAT 3

Table 4.1 - Material cards of the components of the monitor

After the characterization of the materials, it is necessary to assign a property to each single component and for this explicit solver more parameters must be defined, such as the nodal thickness, the formulation of the elements and the cross- sectional properties. In the monitor the following card images are adopted:

- SECTION BEAM: the rigids, adopted in the monitor to simulate steel screws and plastic additional fixations, are modelled as beams and in particular type 9 element formulation is selected in the software, since they are spotweld beams. It is selected the two-point Gauss quadrature rule, as default for beam, and the section of the beam is tubular (only circular).
- SECTION SOLID: it is adopted to define the section properties of solid elements and it is used for the different glues present in the monitor.
- SECTION SHELL: it is used for all the other components and define the section properties of the shell elements. It is considered a full integrated shell element formulation (type 16) that is the typical formulation adopted, since it is the best in terms of accuracy but also very fast in terms of computational time required. It is also defined the thickness and the number of integration points through the thickness of the element, in this case equal to 5 points. It is finally necessary to introduce a shear correction factor to compensate the error that is caused by the theory that is behind the different element formulations adopted in Ls-Dyna for shell elements. The shear deformation theory considers constant transverse shear strains along the thickness of the element; this violates the condition of absence of traction on the bottom and top surface and so this error must be taken into account.

4.2 PLACEMENT OF THE MONITOR IN THE MODEL OF THE DASHBOARD

The setup of the monitor of the dashboard is completed and the next step is to place it in the model of the dashboard provided by the car manufacturer, as shown in *figure 4.1*.

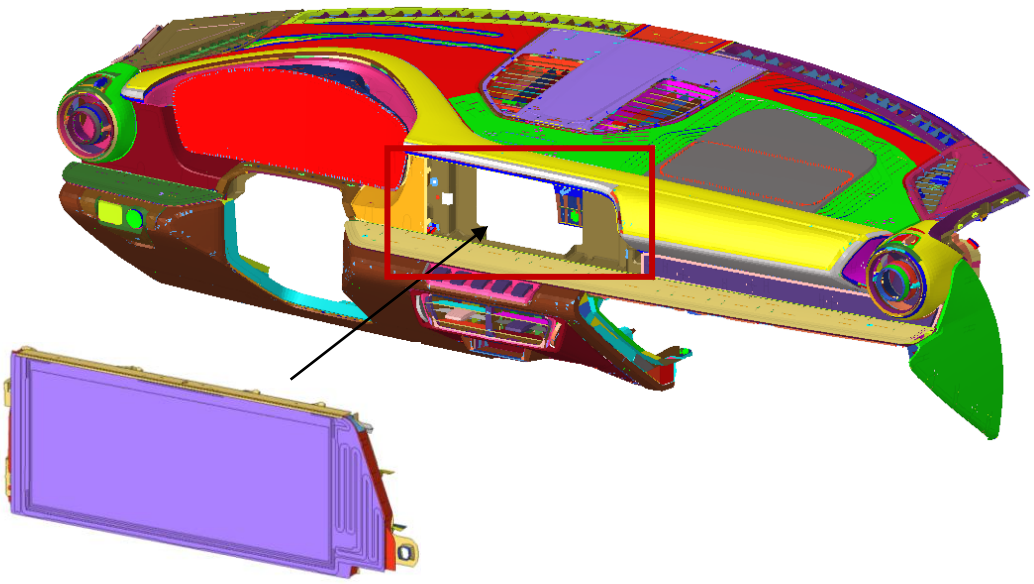

Figure 4.1 - Placement of the monitor on the dashboard

The connection between the monitor and the dashboard is obtained through rigids on the left end side of the monitor. These rigids simulate the threaded connections between the rear cover of the monitor and the dashboard. The independent node is located in the middle of the holes to couple while the dependent nodes are the ones that define the holes of the two components, as visible in figure *4.2.*

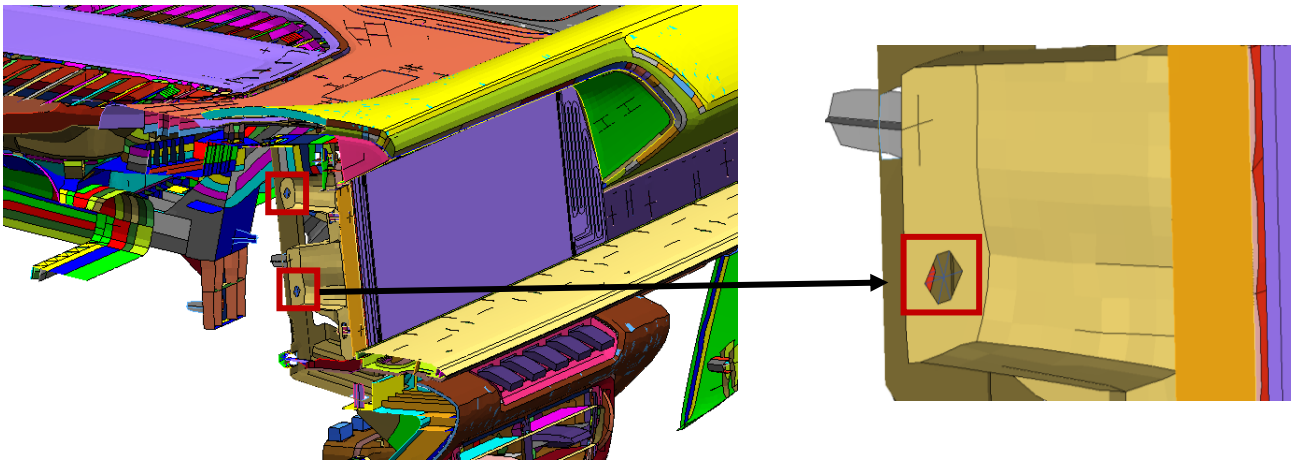

Figure 4.2 - Threaded connections between the monitor and the dashboard

This is not the only way in which the monitor and the dashboard are connected but there are also the two following contacts:

- CONTACT TIED SHELL EDGE TO SURFACE: this contact is adopted to simulate the bonding between the components in the monitor with the use of glue. This tied contact creates a kinematic constraint to tie the slave nodes of the solid elements of the glues to the master surfaces of the finite elements of the components in contact with the glues. It is adopted this kind of contact because it is the most suitable for surfaces that are very closed each other, as this case, and it constrains both the translational and rotational degrees of freedom.
- CONTACT AUTOMATIC SINGLE SURFACE: this contact is recommended for crash impact analysis because deformations can be very high and it is very difficult to determine where and how is the contact between different components. For this reason and due to higher probability of a lot of initial penetrations in the model of the dashboard, that is made of many components, this automatic contact is adopted. It is a single-surface contact where only the slave surface is defined while the master surface is considered the same as the slave one. In the slave surface are considered all the different components of the dashboard, including the ones of the monitor. This kind of contact is not only between the different components of the slave surface, but it considered also self-contact of each component.

There is another contact that has to be defined when the head impactor is located in the head impact area, before starting the simulation of the head form on the dashboard of the vehicle:

- CONTACT AUTOMATIC SURFACE TO SURFACE: this is another automatic contact that is suggested for crash test simulations. In these simulations the components can have large deformations and it is not easy to predict the orientation of one component with respect to the adjacent one. This contact allows to detect possible penetration present in both sides of the shell element and so the check for penetration is performed not only on the slave nodes but also on the master ones.
  The slave set is the head impactor while the master set is composed by the protective cover glass of the monitor and the lower shell of the instrument panel of the dashboard, as it is possible to see in *figure 4.3*. In this way it is possible to transfer the compressive load, caused by the impact of the head impactor, to the dashboard and so there is transfer of force between the slave set and the master one.

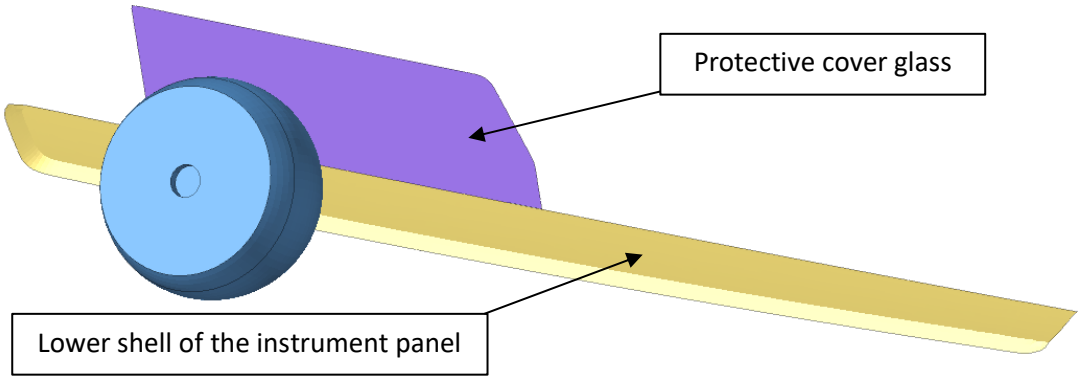

Figure 4.3 - Contact automatic surface to surface

4.3 LOAD COLLECTORS IN THE DASHBOARD

It is finally necessary to define some load collectors, to complete the setup of the model of the dashboard:

- LOAD BODY (solver keyword in Ls- Dyna): since the mass of the dashboard is not negligible, the effect of the acceleration of gravity is considered and a gravitational force is applied in the centre of gravity of the dashboard along the vertical direction,
- CONSTRAINTS: in order to simulate the fixture of the dashboard on the ground, it is placed a rigid element in each hole located all over the model of the dashboard. The independent node is located in the middle of each hole while the dependent nodes are placed in a larger area with respect to the one that defines the hole, as visible in figure *4.4.* In these rigids all the six degrees of freedom are constrained and consequently each rigid behaves as a hinge.

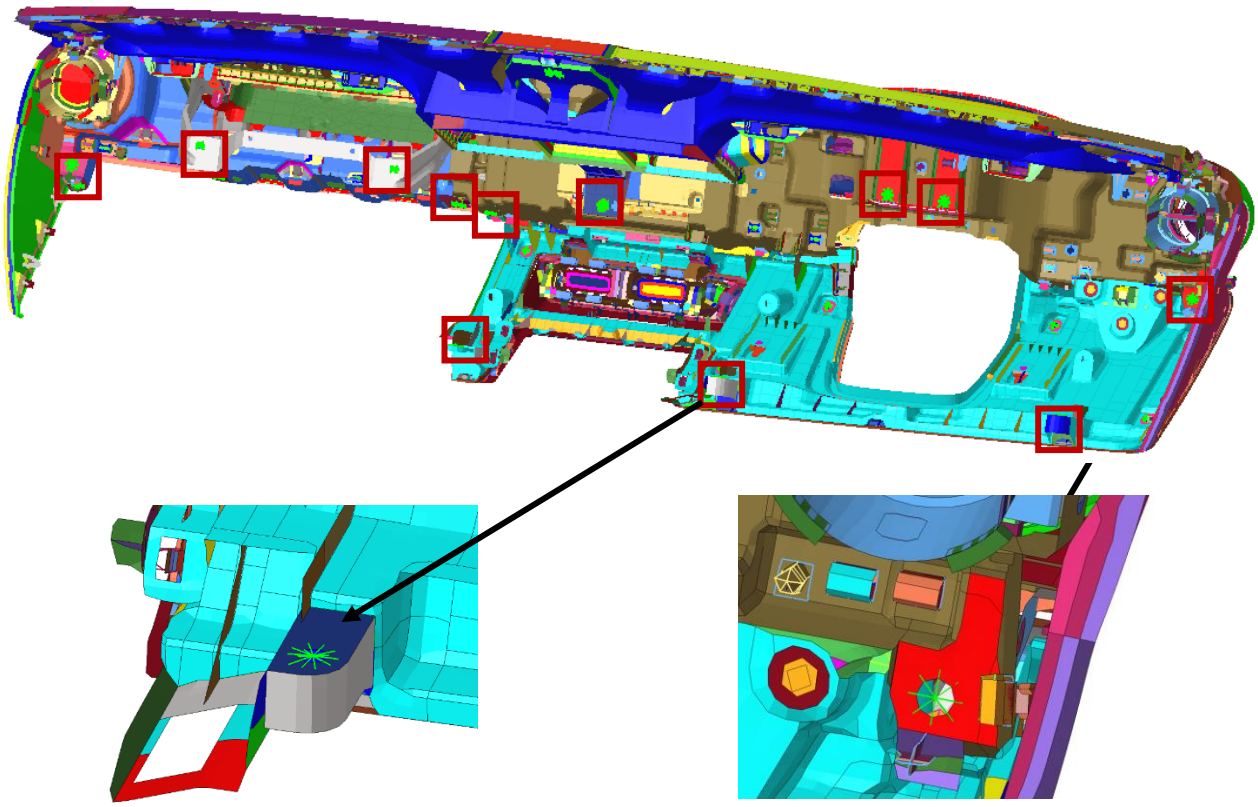

Figure 4.4 - Constraints to fix the dashboard on the ground

Before running the impact simulation, it is important to perform the model checker to see if errors and warnings are present and eventually correct them starting from penetration and intersections check.

5 SIMULATIONS OF HEAD IMPACT ON THE DASHBOARD

This chapter is focused on the description and analysis of the different simulations of the head impact on the dashboard, in order to understand the behaviour of the system in the interaction between the head impactor and the monitor and with the final aim of its virtual validation.

5.1 IMPACT CRASH TEST AND PASSIVE SAFETY

The interest in crash test simulations has increased in the last years and its evolution has been very rapid. Thanks to better and better computers in terms of power and storage, it is possible to perform simulations with higher reliability and sensitivity but also with a reduction in terms of time and money.

However, simulation is only an approximation of reality and it is not possible to predict all the possible injuries that can occur in real crashes, due to uncertainty of human response.

The main purpose of the crash test is to check if a sufficient level of passenger safety has been reached. When the vehicle is subjected to a crash, the resistance of the different components of the vehicle reduces its speed up to the point where the vehicle is stopped. Higher is the stiffness of the different components, more resistance is produced with high deceleration and more transfer of energy.

There is the presence of deceleration pulses that affects respectively the vehicle, then the components of the interior and finally the occupants; the probability of possible injuries increases as well as the deceleration becomes more abrupt. According to the different regulations in the world, there are some requirements to satisfy in terms of average deceleration for a certain time duration during the crash and the aim of each car manufacturer is to keep deceleration as low as possible to reduce possible injuries of the passengers and eventually compensate for possible unwanted accelerations that may occur to the occupants. This objective of the resistance of the vehicle to crashes is achieved with a correct management of energy and control of the pulses caused by crash deceleration. So, it is fundamental vehicle safety, both active, to prevent possible accidents, and passive, to reduce at minimum injuries that mat occur in crashes. Focusing on passive safety, seat belts and airbags are the protections that are used in the interior parts of the vehicle in order to avoid additional injuries in the contact with the passenger of the vehicle. In addition to these restraints systems, there are some requirements to fulfil in the vehicle compartment in terms of occupant protection and one is related to the occupant cell.

In the dashboard, in fact, it is possible to identify the area of head impact and in this thesis different impact test investigations are performed using FEM calculation.

5.2 FMVSS 201L REGULATIONS

The vehicle safety is strongly influenced by different government legislative institutions all over the world and is the combination of three different factors: traffic routing, vehicle performance and the education of traffic participants. The important point is that the requirements specify criteria of performance that must be achieved with the use of objective tests.

Focusing on automotive legislation in all the countries of the world, the role assigned to each factor relevant for the safety was different at the beginning. For example, in the United States the passengers of the vehicle should be protected in the case of a crash caused by the vehicle design because the education of the traffic participants was limited. In Europe, instead, the responsibility of the driver was higher and the key point was the prevention of possible accidents.

From the middle of the 1960s, the United Nations Economic Commission for Europe (ECE) starts to work with the goal of standardizing the different requirements and rules all over the world and reducing at minimum barriers among the different continents and increase trade relations. The number of rules that can be standardized can be very high if the car manufacturers accept the level of the safety that can be reached in some countries in the world.

Since the objective of this work is the virtual validation of the dashboard of the vehicle, the American rule of the United States that must be considered is FMVSS 201L, related to occupant protection in interior parts. Focusing on the impact protection requirements for the instrument panel, the regulation states that *"a point within the head impact area is impacted by a 15-pound (6.8 kg), 6.5-inch (165 mm) diameter head form at the velocity of 11.8 mph (19 km/h). The deceleration of the head form shall not exceed 80 g continuously for more than 3 milliseconds"* [1].

5.2.1 Head impact area

FMVSS 201L regulations define the area of the instrument panel that has to be investigated and consequently the one that has to be excluded, as it possible to see in *figure 5.1*. The possible head impact area is identified in the dashboard, according to FMVSS 201L, as *"all nonglazed surfaces of the interior of a vehicle that are statically contactable by 6.5-inch diameter head form of a measuring device having a pivot point to "top—of-head" dimension infinitely adjustable from 29 to 33 inches."* [1]

The regulations describe the procedure for the determination of the area of possible head impact but not the exact location of the points. The general requirement, in terms of deceleration, must be fulfilled in all the points within the impact zone and the car manufacturer is responsible. Since the points of impact that can be selected are infinite, the car manufacturer identifies the worst-case points for virtual validation and verification. With CAE analysis it is possible also to select other point and reject the ones that do not satisfy the requirements.

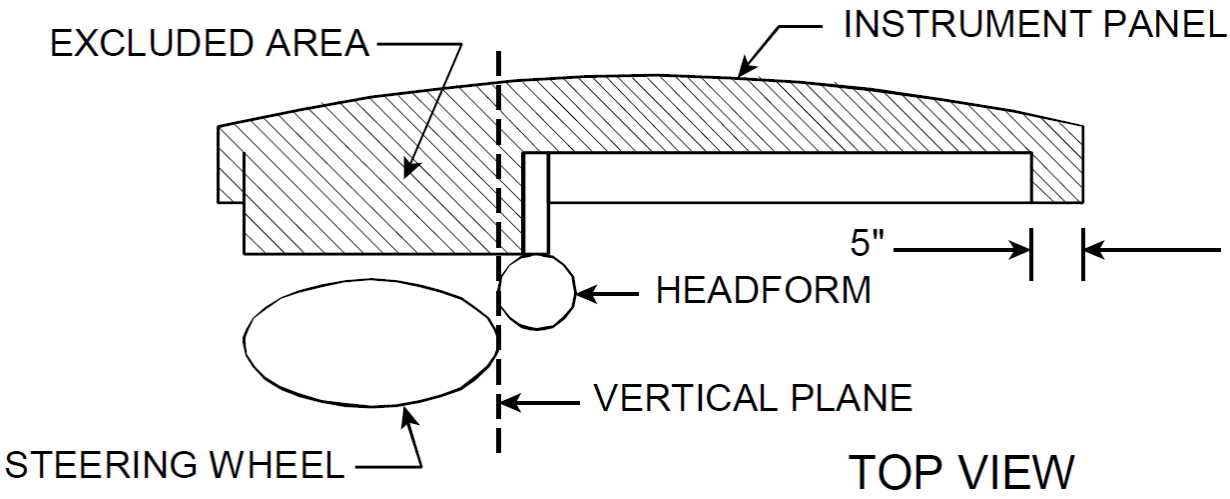

Figure 5.1 - Top view of the instrument panel [1]

The location of this area is determined with the use of a head impact location fixture, represented in *figure 5.2*. It is composed by an arm that presents on one end side a pivot and on the other one a head form that is rigidly attached. The steps to follow are:

1) Locate the base of the fixture in the right front seating position and adjust it and the pivot until the pivot is positioned at the Seating Reference Point (SRP) or point H, the theoretical position of the hip of the passenger of the vehicle.

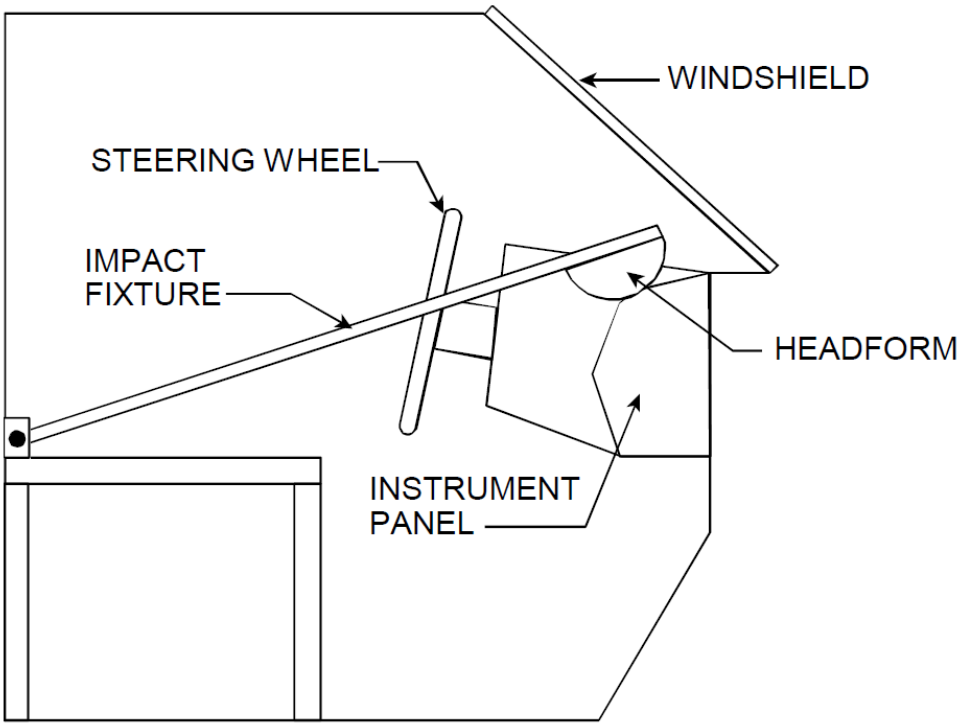

Figure 5.2 - Section of the right-side view of the vehicle with the impact fixture [1]

2) Fix the arm of the head impactor fixture to the base.
3) Place the head form at 33 inch radius position with respect to the pivot and regulate the arm in a position where it can oscillate in a plane that is parallel to the vehicle centre line, as it is possible to see in *figure 5.3*.

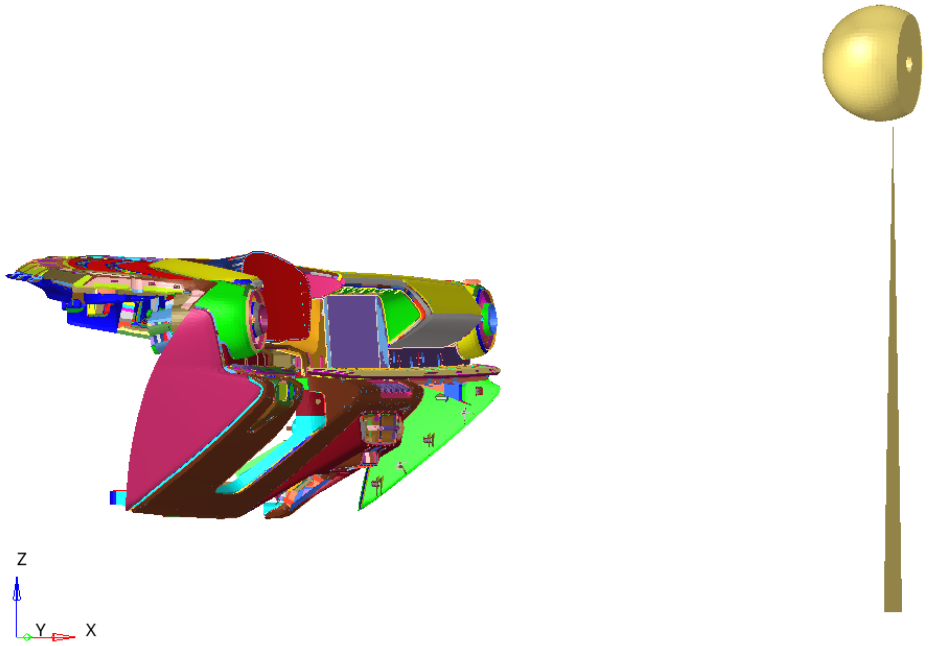

Figure 5.3 - Regulation of the impact fixture

4) Rotate the arm until there is the contact of the head form with the instrument panel, as shown in *figure 5.4*.

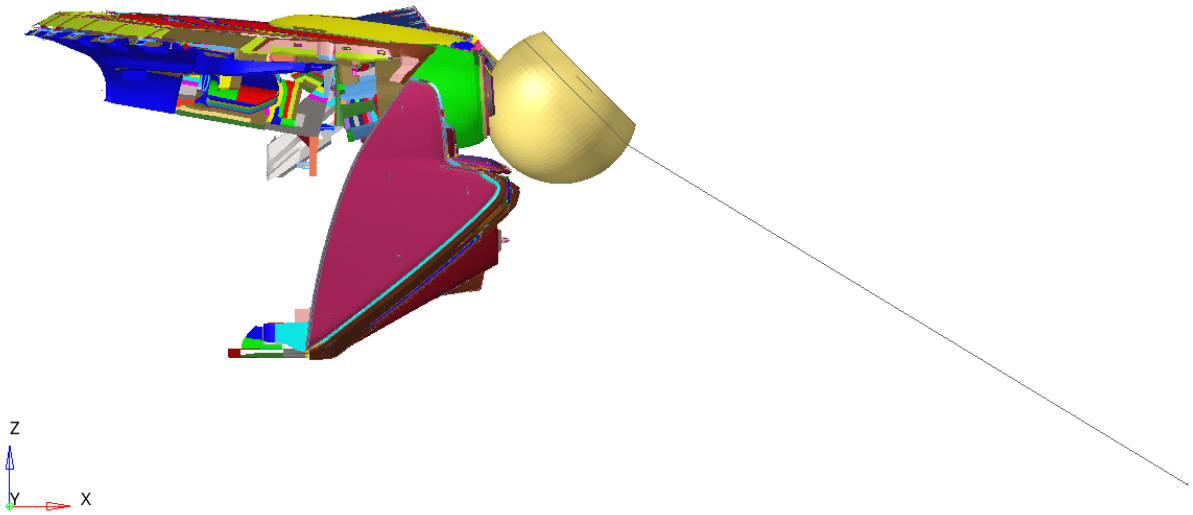

Figure 5.4 – Rotation of the impact fixture until the contact with the dashboard

5) Maintain the contact with the instrument panel and swing the arm, about the vertical axis through the pivot, to the left and to the right in order to find the area of the points for head impact.

6) Repeat the same procedure but place the head form at 29 inch radius position with respect to the pivot. In this way the white dashed line in *figure 5.5* identify the top of the impact zone for the 33 inch arm while the bottom for 29 inch and only the points that are located inside the area that has to be investigated are admissible.

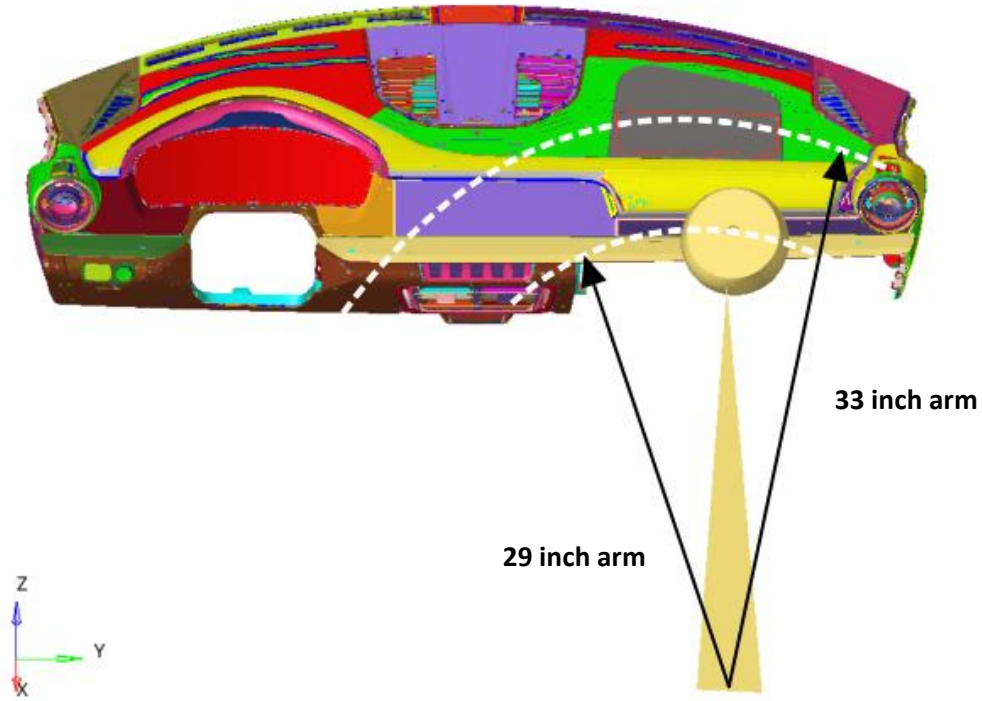

Figure 5.5 – Identification of the possible head impact area

5.2.2 Definition of the head impactor and approximation

According to FMVSS 201L regulations, the head impactor is a hemispherical sphere of 6.5 inch (165 mm) diameter and weighs 15 lbs (6.8 kg). It is a metallic rigid body that does not deform during the impact with the dashboard. There are steps to performed before running impact simulation:

1) Fix the support of the actuator of the head form behind the head impact zone
2) Select the location of the points of impact ad record for each of them the coordinates.
3) Assure the proper mounting of the triaxial accelerometer in the centre of gravity of the head impactor, with the use of mounting holes (*figure 5.6*) to measure the resultant acceleration and that its output is connected to the recorder.
4) Assign the pressure of the actuator to a level able to achieve 19 km/h speed of impact.
5) Trigger the speed timing trap and verify, when the actuator is turned on, that the assigned speed is achieved.
6) Place the head form actuator and run the impact simulation for each point considered, with a speed of the head actuator of 19 km/h and record the actual speed from the velocity trap.

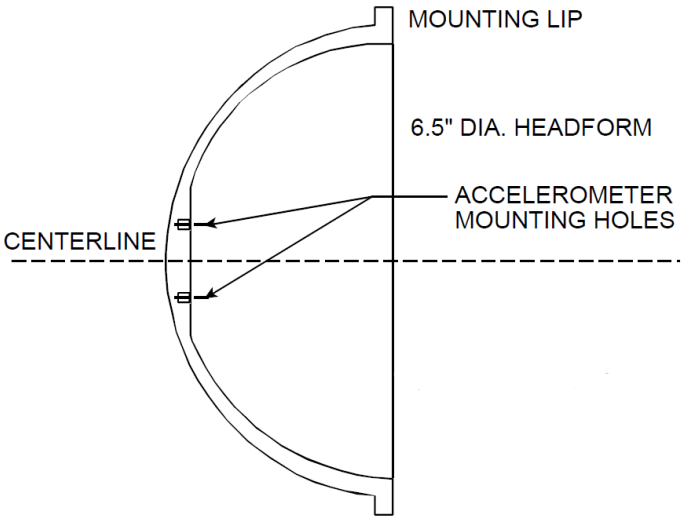

Figure 5.6 - Left side section of the head impactor with the mounting of the accelerometer [1]

According to FMVSS 201L, the movement of the head impact location fixture is a rotation and, to simulate this motion, it is necessary to set on the pivot of the arm of the fixture, located in the Seating Reference Point (SRP), a rotational speed that allows the head impactor to reach 19 km/h. The use of the entire device of the head impactor, with the motion of both the arm of the fixture and the head form, requires a high computational time in the simulation.

The simulations of this virtual validation of head impact have been run on a computer with 8 processors but generally the computer used for these simulations has 40 processors and so the computational time decreases significantly. So an approximation is considered, in order to reduce the computational time : instead of imposing a rotational speed in the black reference system located in the pivot (P) of the impact fixture (on the left side of *figure 5.7*), only the head form is considered and a translational speed in the z direction is set in the red local reference system (on the right side of *figure 5.7*) positioned in its centre of gravity. This approximation allows to keep a good accuracy in terms of results, because for small displacements the rotation can be approximated with a linear translation.

The translational velocity is set on the z axis in the red local reference system, since it is perpendicular to the surface of the dashboard, as it is possible to see in *figure 5.8*.

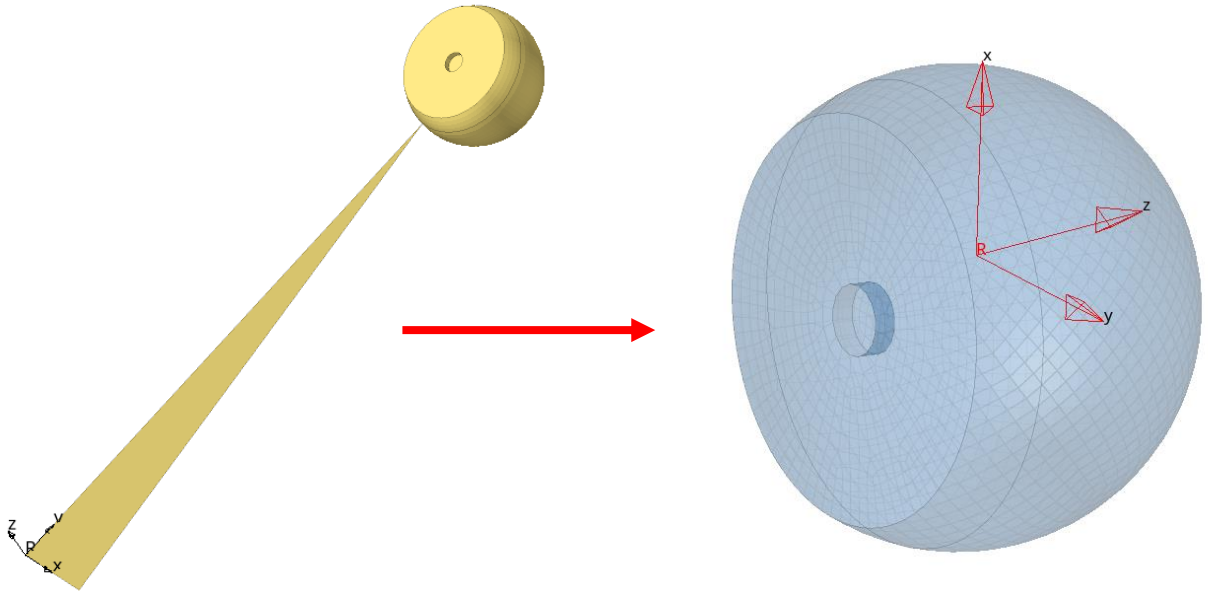

Figure 5.7 - Approximation of the motion of the head impactor

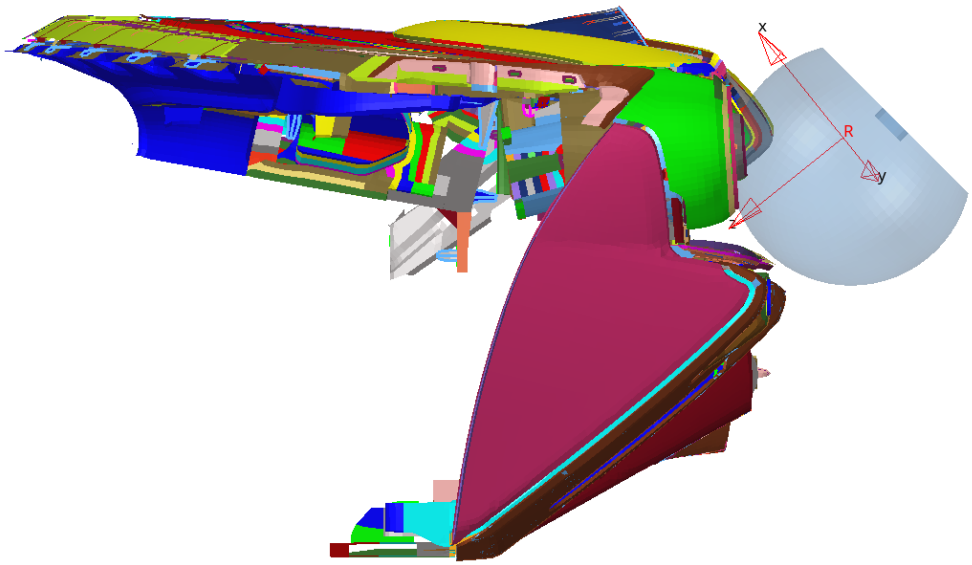

Figure 5.8 -Side view of the dashboard with the placement of the head form

5.3 IMPACT POINTS

The impact points are identified by the car manufacturer and they are the most critical points, for example where there is the joining between different components or change of slope in the geometry. In this case the car manufacturer selects two impact points to see the interaction of the head impactor with the protective cover glass of the monitor. Both the points of impact are located in the lower shell of the instrument panel and are shown respectively in *figure 5.9* and *figure 5.10*. The first impact point is selected to see the interaction in the middle of the monitor while the second one is shifted of 78 mm along the negative y axis of the global reference system of the entire model of the dashboard and it is the most external point of the occupant that can be investigated.

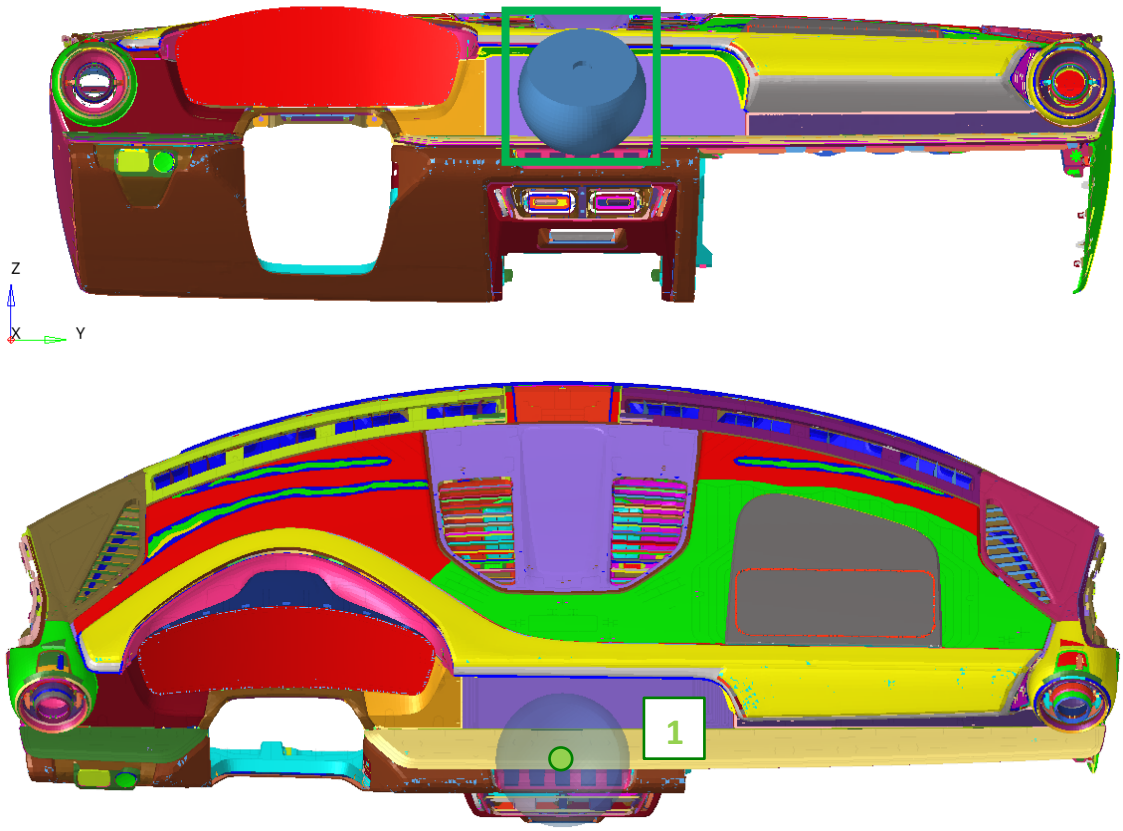

Figure 5.9 - First point of impact

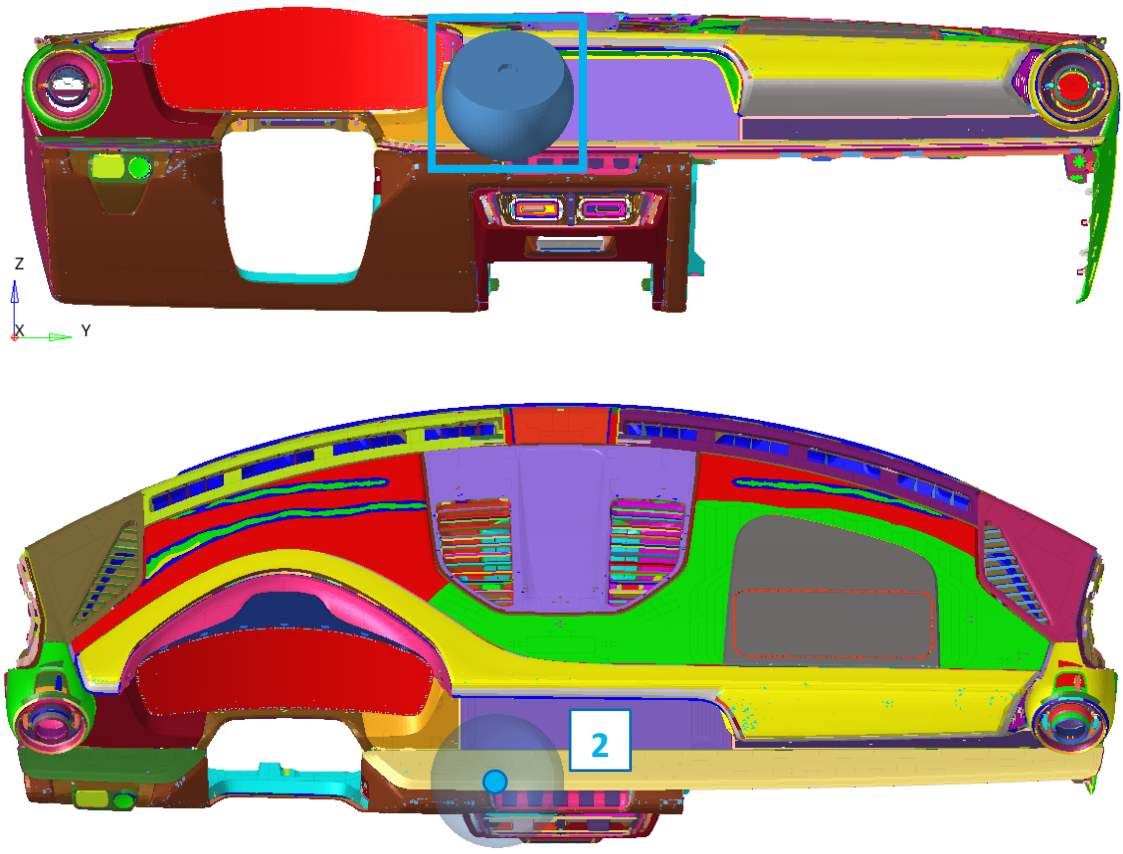

Figure 5.10 – Second point of impact

5.4 POST PROCESSING ANALYSIS

Once the simulation of the head impact on the dashboard is completed, it is necessary to analyze the results obtained in order to understand the general behaviour of the system and check if the requirements of the regulation and the car manufacturer are fulfilled.

As it is possible to see in *figure 5.11*, showing the recording setup, the data recorded from the triaxial accelerometer are collected in the computer and used in the post processing phase to build the plots that are necessary for the analysis. Focusing on the general requirement to achieve, in the acceleration of the head form vs time plot, a 3 ms clip threshold is defined in order to find the maximum value that is achieved and check if the virtual validation is fulfilled. The 3 ms clip is a rectangular window of the integral of 3 ms of the deceleration curve and corresponds to the highest value of acceleration that is kept constant continuously for 3 milliseconds.

From the acceleration data, obtained from the accelerometer mounting on the head form, it is possible also to recover its velocity and dynamic displacement. This is reached respectively by single and double integration of the data recorded from time zero.

In order to understand the general behaviour of the entire dashboard, it is also considered the reaction contact force between the head impactor and the dashboard and finally the energy balance, in order to check if the total energy is conserved and how is the transfer of energy between the components of the system.

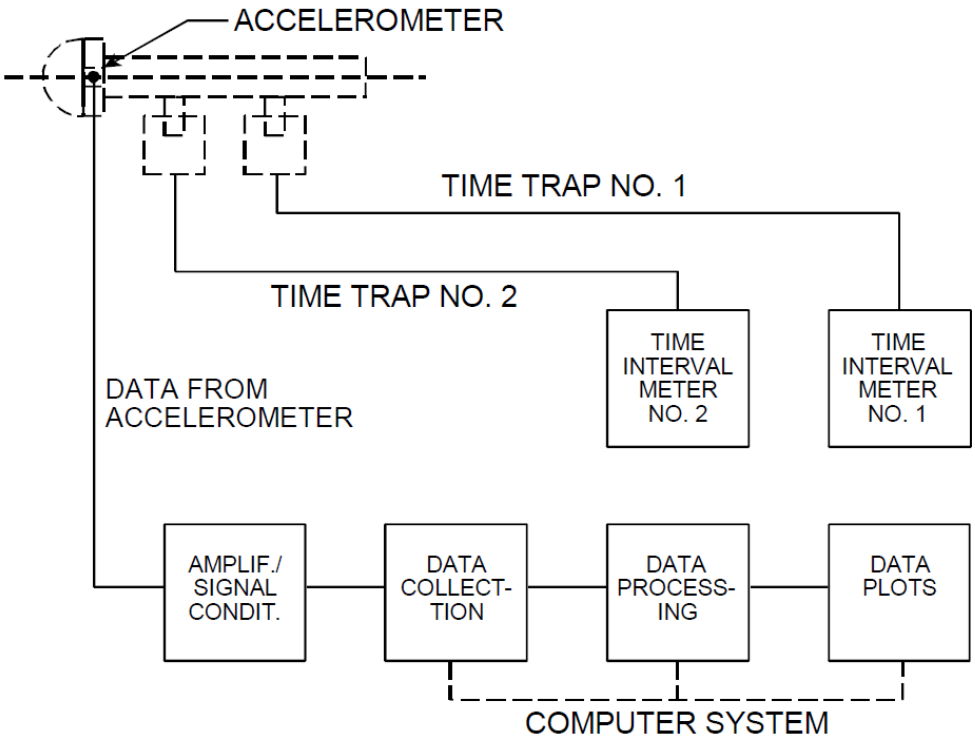

Figure 5.11 - Recording setup of the data of the accelerometer [1]

5.4.1 First impact point

The head impact on the dashboard has been run with an explicit simulation with the use of software Ls-Dyna R12.0. The time interval in which the solver writes the output of the frame animation of the dashboard is 0.1 ms and the total duration of the test is 30 ms. This time interval is defined by the car manufacturer in order to have a better analysis of the different frames of the simulation in the post-processing phase. As first step to observe the behaviour of the dashboard, in *figures 5.12, 5.13, 5.14, 5.15* and *5.16* it is considered the frame of the head impact every 5 ms up to 20 ms and in each figure is visible a full view of the entire dashboard and a left side section, located in the middle plane of the head impactor. They are not shown all the frames up to 30 ms, since the moment when the head impactor reaches zero velocity is at about 15 ms and then the head impactor returns in its initial position.

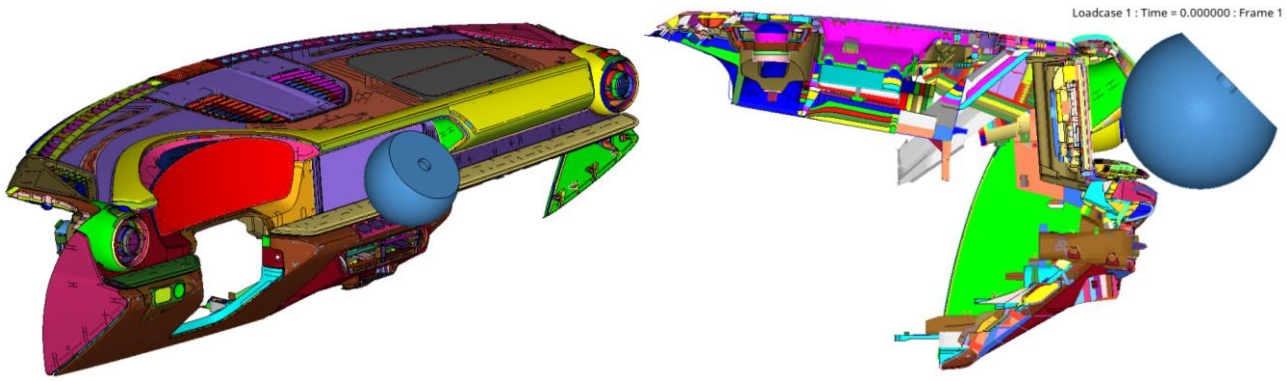

Figure 5.12 – Full view and left side section of the head impact simulation on the dashboard (time 0 ms)

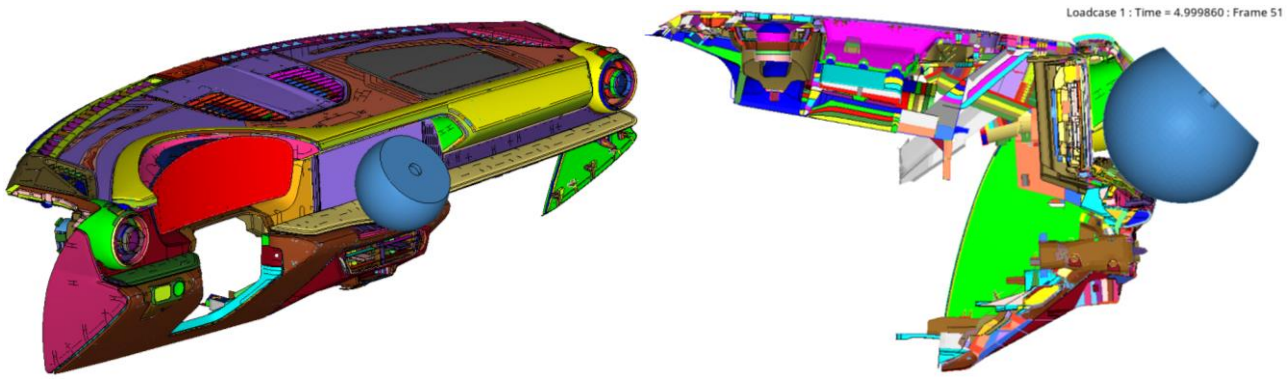

Figure 5.13 – Full view and left side section of the head impact simulation on the dashboard (time 5 ms)

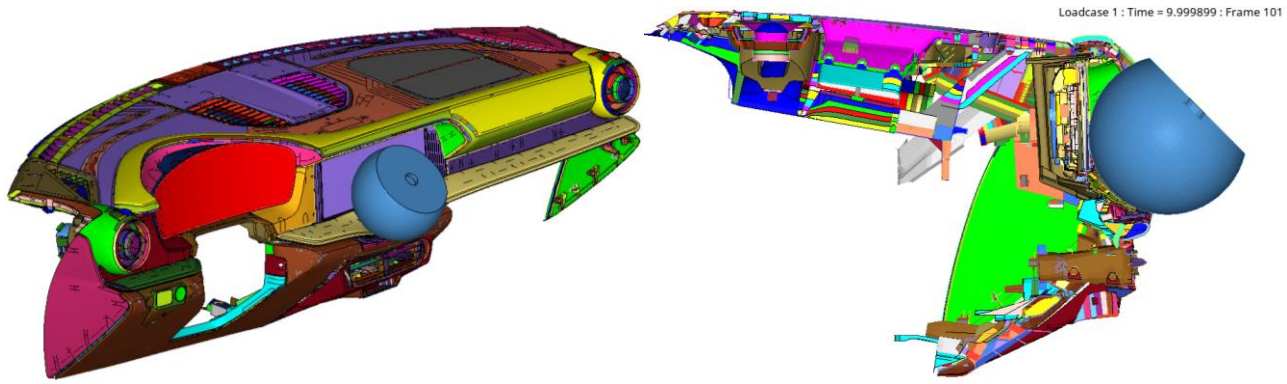

Figure 5.14 - Full view and left side section of the head impact simulation on the dashboard (time 10 ms)

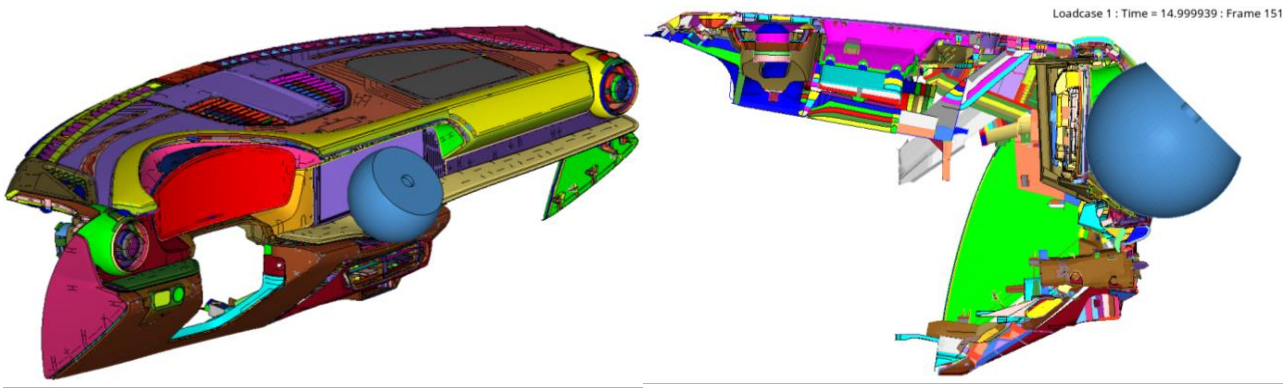

Figure 5.15 - – Full view and left side section of the head impact simulation on the dashboard (time 15 ms)

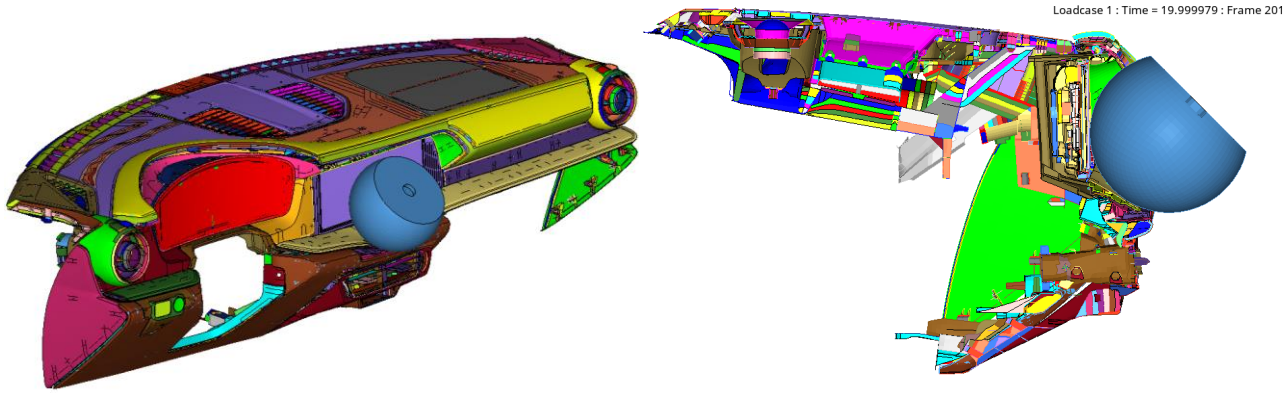

Figure 5.16 - Full view and left side section of the head impact simulation on the dashboard (time 20 ms)

From these frames it is possible to see that the splintering effect is avoided, since there are not dangerous components and fragments of glass that explode in the dashboard.

5.4.1.1 Energy balance

The energy balance graph shows how the energy is transferred from the head impactor to the dashboard, but it is also a way to check that the following equation is respected at any time during all the simulation:

$$E_{kin} + E_{int} + E_i + E_{hg} = E_{tot}$$

where:

E_{kin} : actual kinetic energy

E_{int} : actual internal energy, related to the six components of stress and strain

E_i : actual interface energy, related to the dissipative energy that is generated in the contact between different components of the dashboard and the head impactor

E_{hg} : actual hourglass energy, related to modes that are not physical and with zero energy, stress and strain

E_{tot} : total energy is the sum of all the previous contributions of energy and at t = 0 ms is equal to initial kinetic energy of the head impactor.

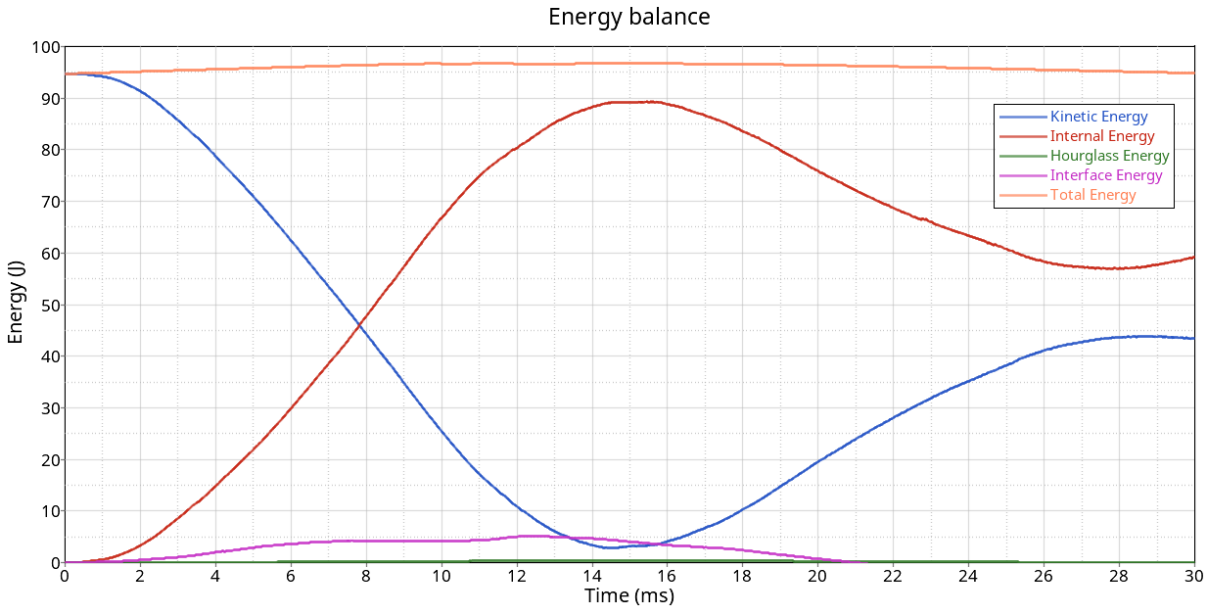

Figure 5.17 – Energy balance of the first impact point

Looking at the energy balance graph in *figure 5.17*, hourglass energy is almost equal to zero for the entire simulation and total energy of the system is conserved; this tells that the simulation runs correctly.

The system at t = 0 ms has a total energy equal to the kinetic one, related to the mass of the head impactor and its initial velocity. Looking instead at *figure 5.18,* from t = 0 ms the velocity decreases since the head impactor gets in contact with the dashboard and the kinetic energy of the head impactor is transformed into internal energy of the dashboard. At about 15 ms the speed of the impactor is null and there is a change of direction of its motion. There is an elastic behavior of the dashboard and from that point there is a release of energy into kinetic one.

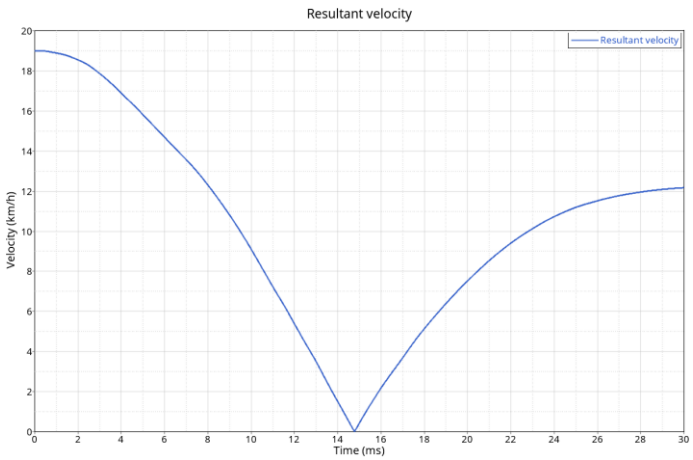

Figure 5.18 – Resultant velocity of the head impactor

The total energy is not perfectly constant but varies in a small range, in particular it increases very slowly up to the point where the velocity of the impactor is zero and then decreases up to have the same value of the initial total energy at the end of the simulation. This small variation can be explained with the trend of the interface energy, since it increases up to when the speed of the impactor reaches zero and then decreases up to null value. The interface dissipative energy is the way in which the solver approximates the contacts between the different components of the dashboard.

5.4.1.2 Deceleration curve

According to FMVSS 201L, the deceleration shall not exceed 80 g continuously for more than 3 ms (a_3ms curve). Looking at the deceleration curve in *figure 5.19*, the general requirement of FMVSS 201L regulation of not exceeding 80 g for more than 3 milliseconds continuously is achieved, since the acceleration reaches 49.1 g (a_3ms). The target of the car manufacturer is also achieved, since it is requested not to exceed the 80 % of what regulation requires (limit* = 64 g).

Acceleration data are not filtered in the graph, using SAE J211 filter class 1000 as suggested in the regulation, because the filter is adopted only if the signal presents a lot of noise. In this case the filter is not used and a more precise value of the a_3ms curve is obtained.

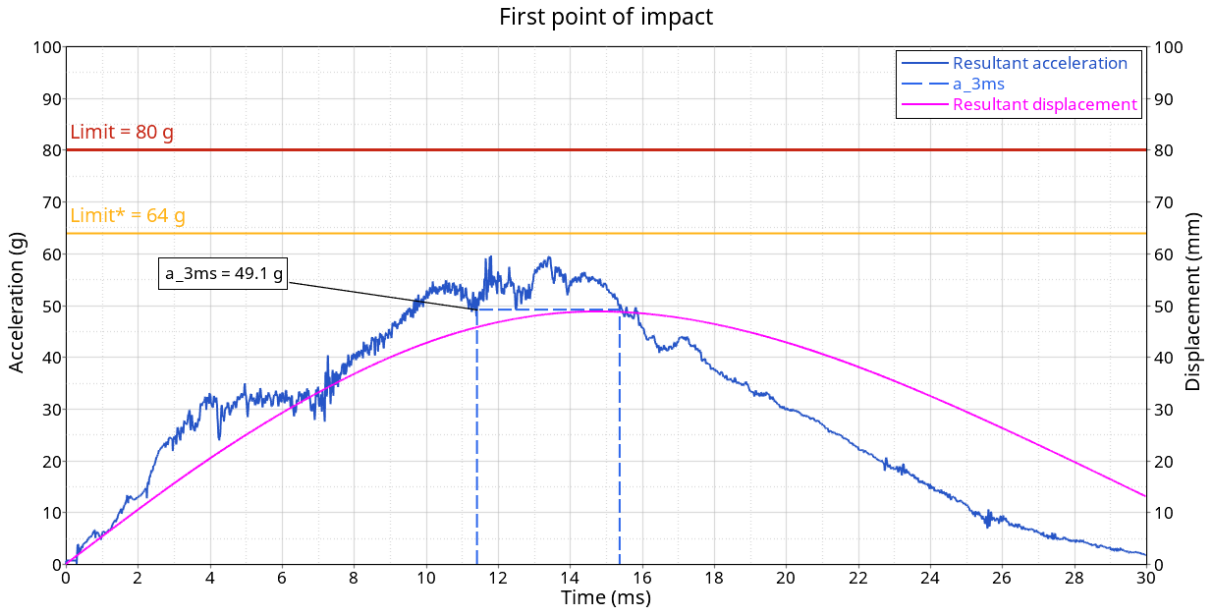

Figure 5.19 – Deceleration curve of the first impact point

5.4.1.3 Contact force between the impactor and the dashboard

On the left graph in *figure 5.20*, there is a curve showing, over time, the contact forces that are transferred between the head impactor and the dashboard. The car manufacturer suggests, for the design and validation of the test, not to exceed 4.2 kN and this requirement is satisfied.

On the right graph of *figure 5.20*, it is shown the trend of the interface force as a function of the resultant displacement of the head form. The contact force increases up to the maximum value when the maximum

displacement and zero velocity is reached. From that point, interface force decreases up to almost zero at the end of the simulation and this is in accordance with the elastic behavior of the dashboard.

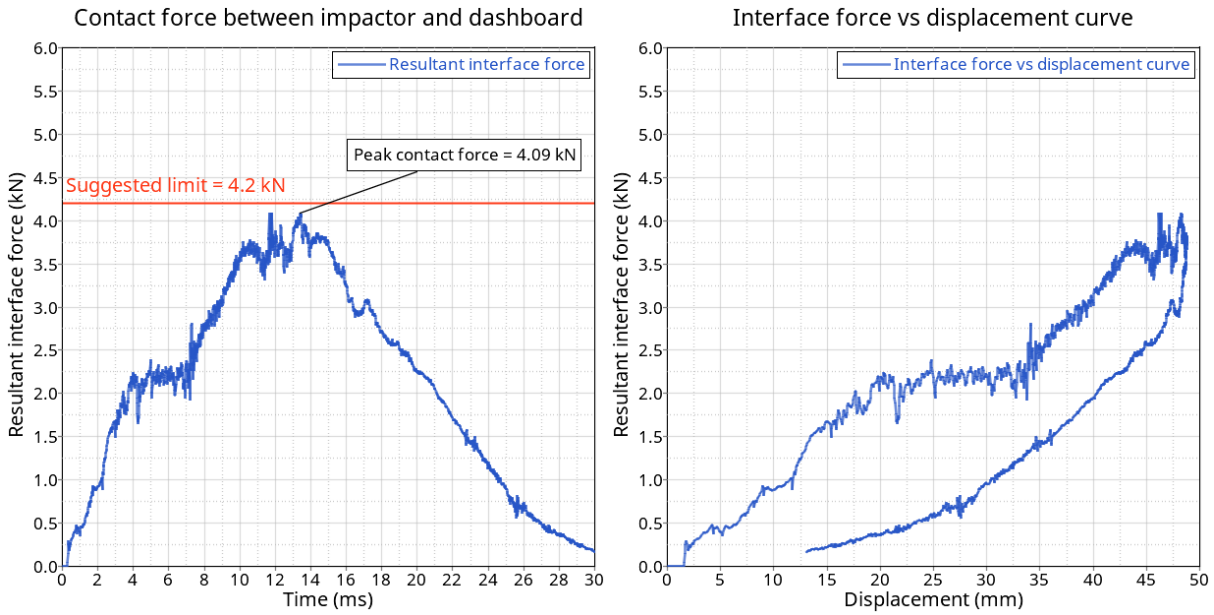

Figure 5.20 – Contact force between the impactor and dashboard curves

5.4.1.4 Discussion

In *figure 5.21* it is shown a detail of the lower shell of the instrument panel, where there are some elements that disappear and fail. This is related to the failure criteria and card image of the material of this component.

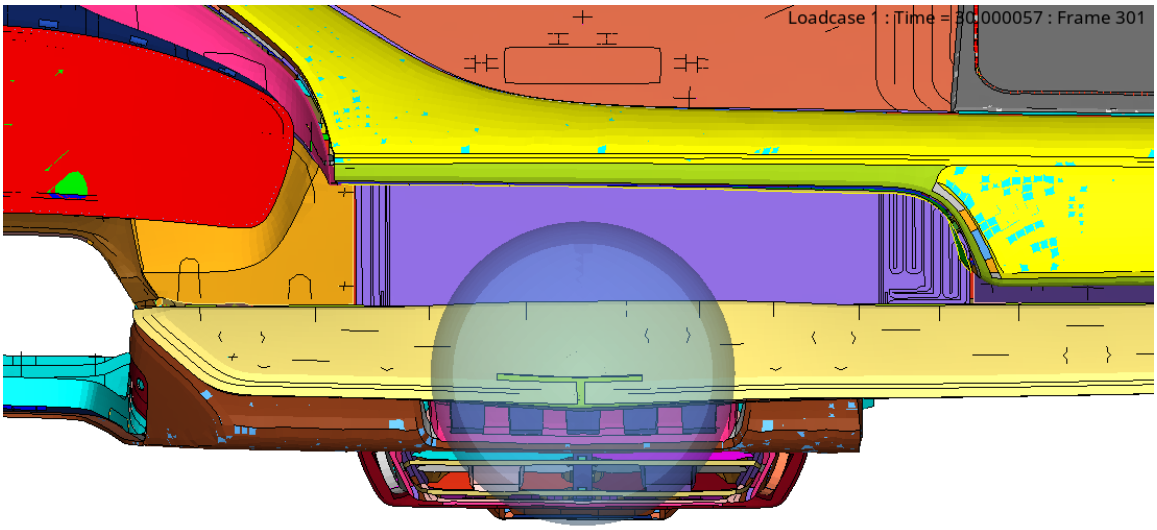

Figure 5.21 – Detail of the lower shell of the instrument panel at the end of the simulation (time 30 ms)

The lower shell is made of composite material (PC/ABS with 20 % of short glass fibers) and is modeled as elasto - plastic (MAT24), with a failure criterion based on the maximum plastic deformation. Once this deformation is achieved in one element, it fails and disappears.

The material modelling is already an approximation that considers a trade-off between the real behavior and the required computational time. This is because a more precise and detailed characterization of the material

would lead to a higher computational time. The fact that there are elements that disappear, due to the achievement of the maximum plastic deformation, is a phenomenon that does not happen in reality but if some sharp edges are present below that shell in the real component, this condition is not acceptable. These simulations are a first virtual validation, where the behavior and possible problems that may arise in the dashboard are highlighted. After the virtual validation, it is necessary to carry out the first physical tests to observe if there is a perfect correlation with the analysis conducted with the simulations.

When the physical tests are analyzed, it is checked whether there are elements of the lower shell subjected to breakage and so if sharp edges are generated or not. If this phenomenon is not present in the real component, the material behavior is not a problem otherwise it is necessary to change the type of material or in case of composite material it is possible to modify the percentage of matrix and fibers.

Later in the development of this thesis, a change of material of the lower shell of the instrument panel is considered to see if this phenomenon is avoided.

5.4.2 Second impact point

The first step to observe the behaviour of the dashboard, as done for the first point of impact, is to consider the frame of the head impact simulation every 5 ms up to 20 ms and this is shown in *figure 5.22, 5.23, 5.24, 5.25* and *5.26*, where in each figure is visible a full view of the entire dashboard and a left side section, located in the middle plane of the head impactor.

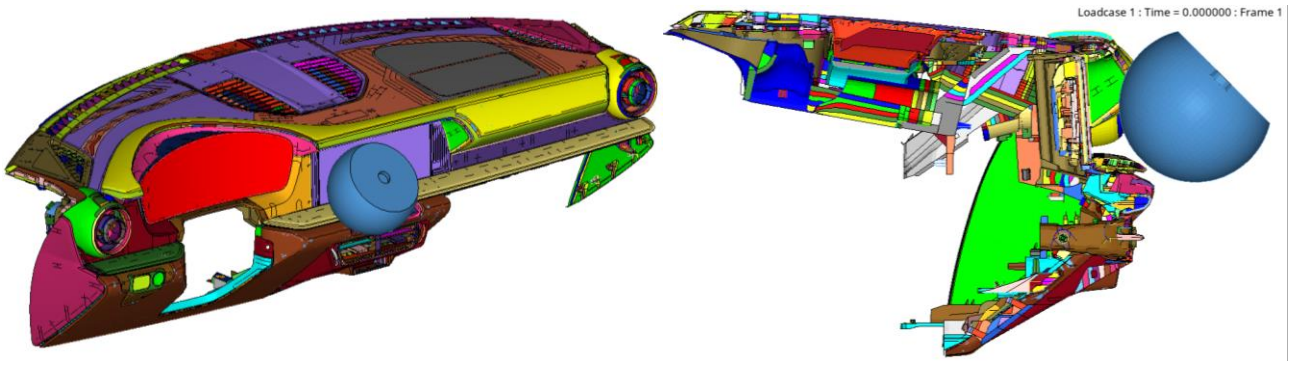

Figure 5.22 – Full view and left side section of the head impact simulation on the dashboard (time 0 ms)

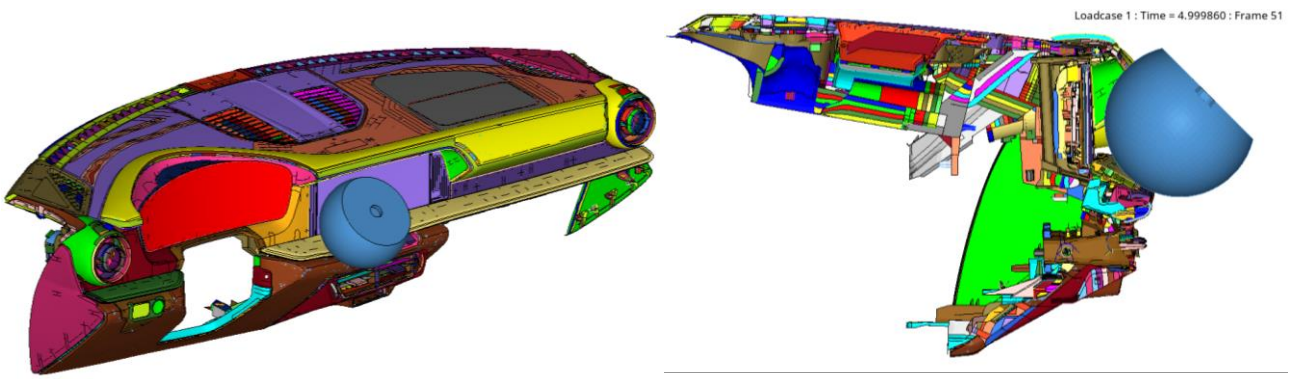

Figure 5.23 – Full view and left side section of the head impact simulation on the dashboard (time 5 ms)

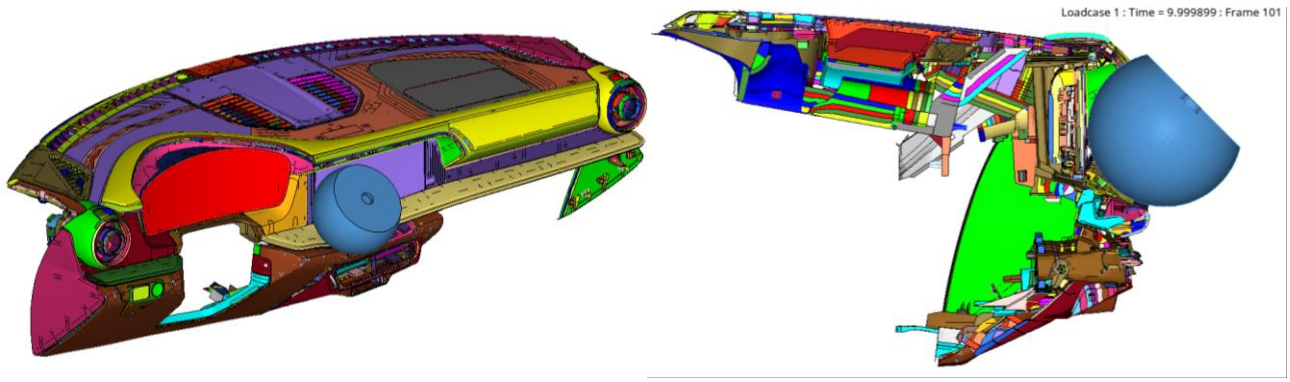

Figure 5.24 – Full view and left side section of the head impact simulation on the dashboard (time 10 ms)

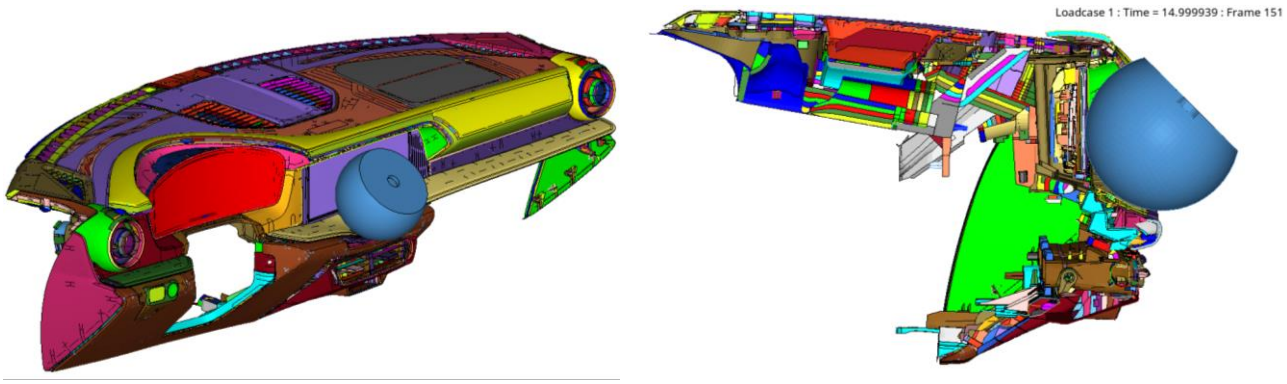

Figure 5.25 – Full view and left side section of the head impact simulation on the dashboard (time 15 ms)

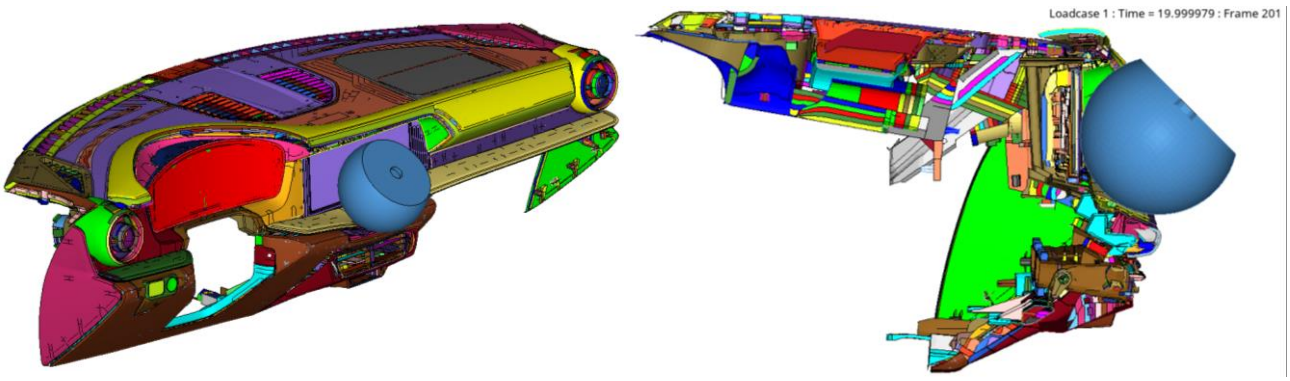

Figure 5.26 – Full view and left side section of the head impact simulation on the dashboard (time 20 ms)

In *figure 5.27* it is shown a detail of the lower shell of the instrument panel at the end of the simulation. For the second impact point, even if less relevant with respect to the first impact point, there is still an element that fails and disappears during the simulation, highlighted in the red circle in *figure 5.27*, due to the achievement of the maximum plastic deformation. It is therefore necessary to check with physical tests the possible occurrence of sharp edges.

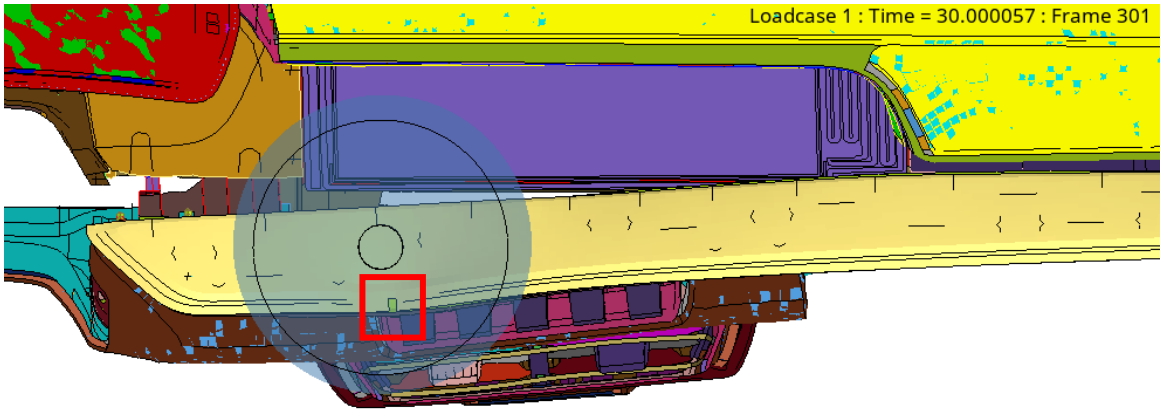

Figure 5.27 – Detail of the lower shell of the instrument panel at the end of the simulation (time 30 ms)

5.4.2.1 *Energy balance*

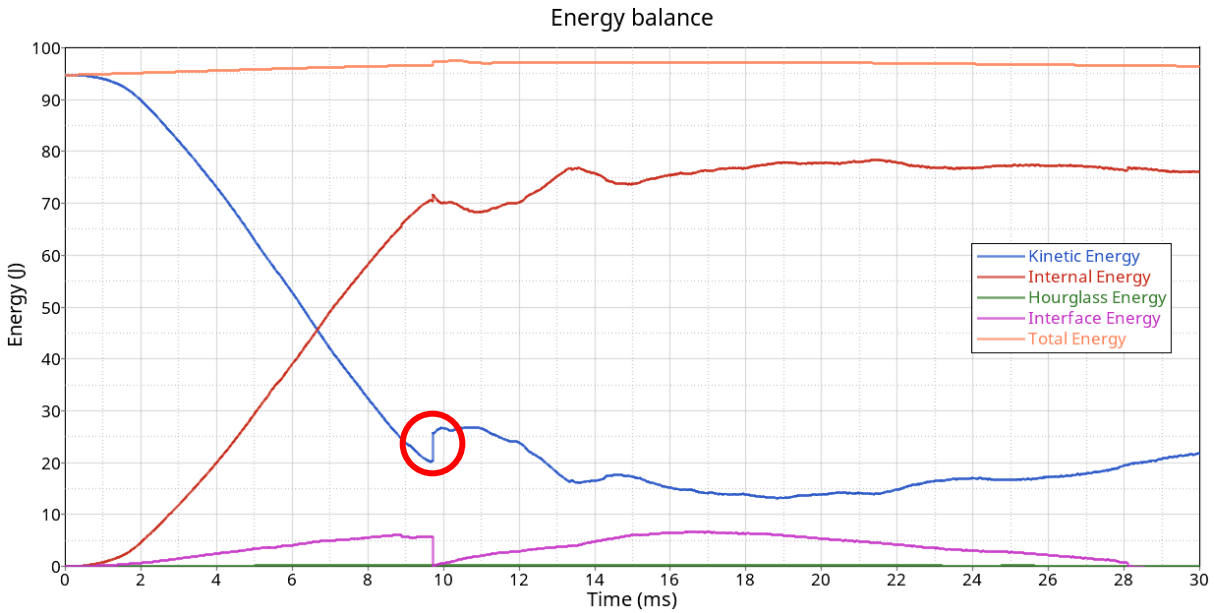

Figure 5.28 – Energy balance of the second impact point

Looking at the energy balance graph in *figure 5.28*, as previously described for the first impact point, at t=0 ms the system has a total energy equal to the kinetic one. In *figure 5.29* below, similarly, the speed of the head impactor decreases as it gets in contact with the dashboard up to null value and, from that point, the head form returns to its initial position. In this case it is possible to observe that the behavior of the dashboard is not as elastic as the previous case. From the point where the speed of the impactor is null, the dashboard is not able to transform its internal energy into kinetic energy of the head form, but the internal energy is almost constant because there is the presence of more permanent plastic deformations in the system. For what concerns the dissipative energy, it increases up to when the impactor speed reaches null value and then decreases and this is in accordance with the trend of the total energy, that is conserved for the duration of the simulation but is not perfectly constant but varies in a small range of values.

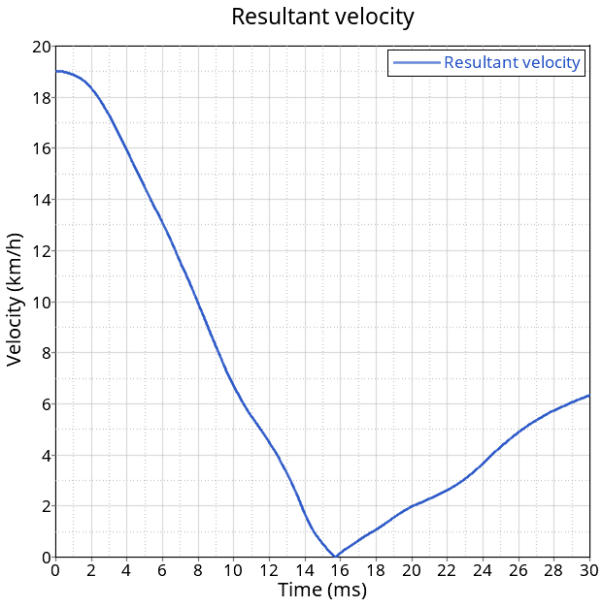

Figure 5.29 – Resultant velocity of the head impactor

In the red circle drawn in *figure 5.28* is highlighted a drop in the kinetic energy at about 10 milliseconds. This is caused by the breakage of the head of the screw below the threaded connection, whose location is shown in *figure 5.30* in the red square. Threaded connections are modeled as 3D solid elements and in this case the connecting element tears with a release of energy that generated a stroke, as it is possible to see in the frames of the simulation in *figure 5.31*. Since the models of the dashboard are adopted for different vehicles, the breakage of the threaded connection is a warning for the car manufacturer, that has to investigate this phenomenon. In fact, it is better analyzed later in the thesis with possible solutions to be adopted to avoid its occurrence.

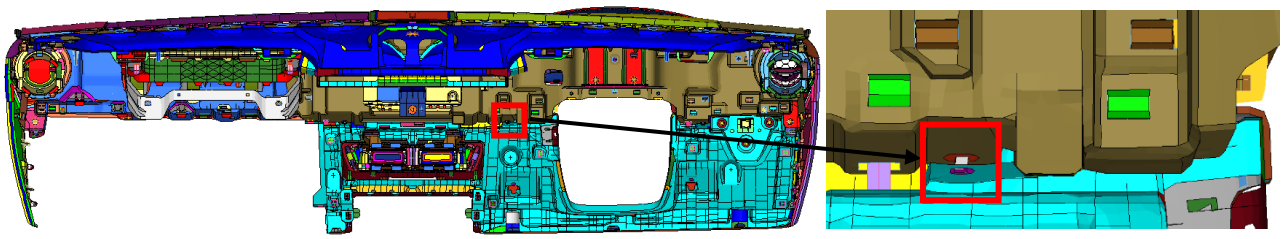

Figure 5.30 – Location of the threaded connection subjected to breakage

Figure 5.31 – Frame of the threaded connection before (left image) and after (right) the breakage

5.4.2.2 *Deceleration curve*

According to FMVSS 201L, the deceleration shall not exceed 80 g continuously for more than 3 ms (a_3ms curve). Looking at the deceleration curve in *figure 5.32*, the general requirement of FMVSS 201L regulation is achieved, since the acceleration reaches 36.2 g (a_3ms). The target of the car manufacturer is also achieved, since it is requested not to exceed the 80 % of what regulation requires (limit* = 64 g).

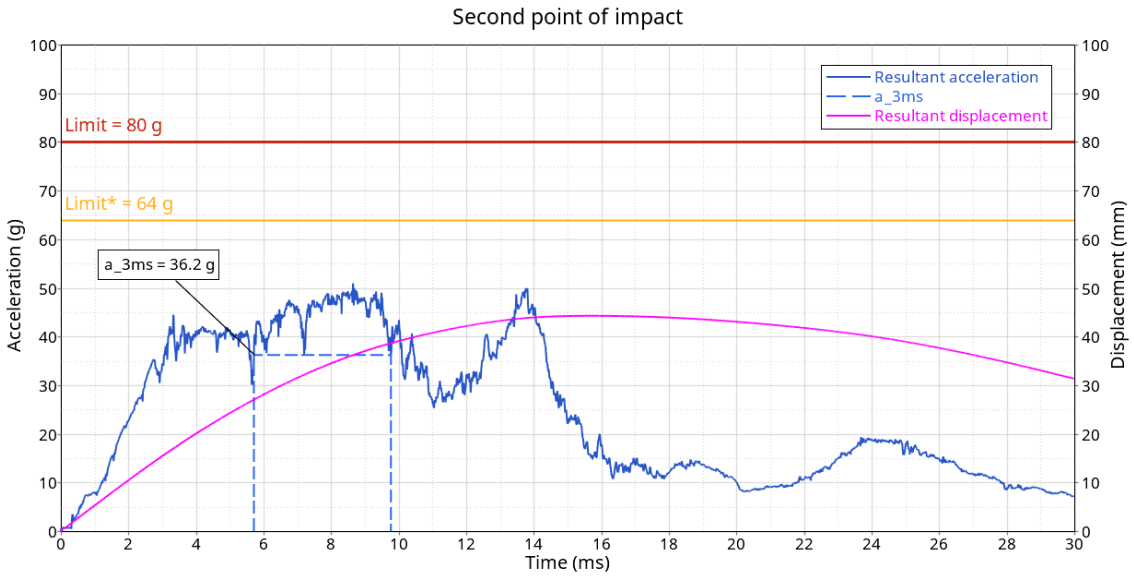

Figure 5.32 – Deceleration curve of the second impact point

5.4.2.3 *Contact force between the impactor and the dashboard*

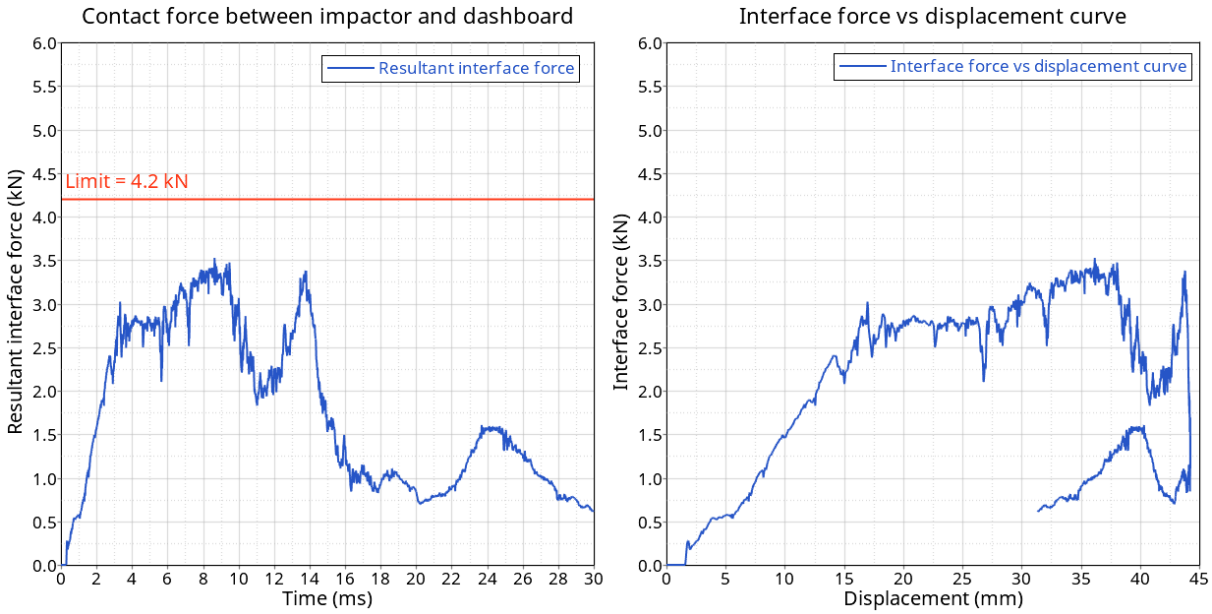

Figure 5.33 – Contact force between the impactor and dashboard curves

On the left graph in *figure 5.33*, there is a curve showing, over time, the contact forces that are transferred between the head impactor and the dashboard. The suggested requirement of the car manufacturer of not exceeding 4.2 kN is fulfilled also for the second point of impact.

With respect to the first point of impact, the contact force does not increase up to the maximum value and then decreases up to almost null value but there is the presence of a negative drop in the range of the simulation between 9.5 and 11 milliseconds and a positive one between 20.2 and 24.6 milliseconds. The negative drop is caused by the detachment of the lower shell of the instrument panel. So, at the beginning of the detachment, the contact between the dashboard and the head impactor decreases, as it is possible to see in *figure 5.34* and 5.*35*, where the sections of the simulation at 9.5 and 11 milliseconds are shown, with focus on the contact between the lower shell (gold component) and the head form (blue component).

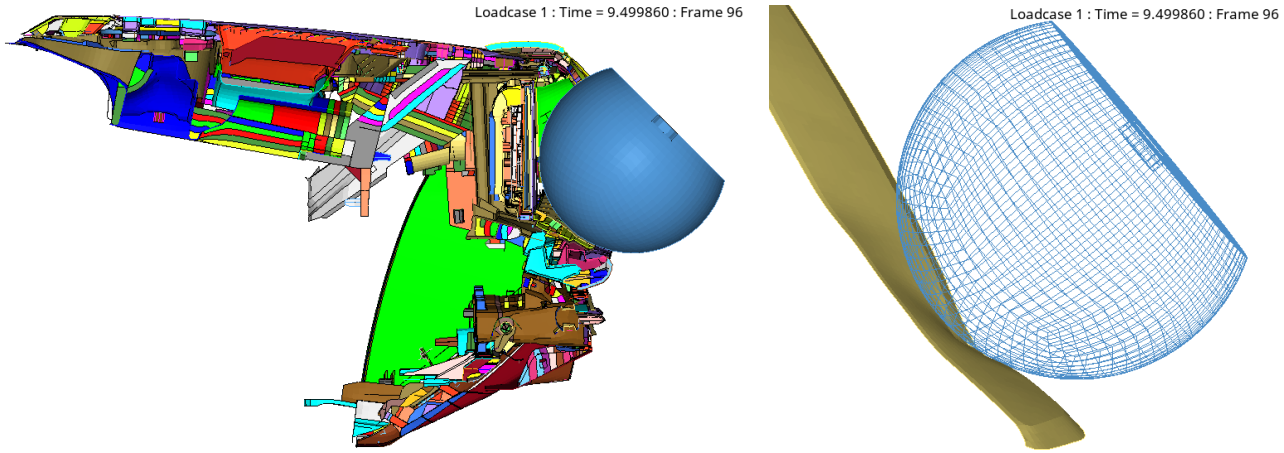

Figure 5.34 –Section of the head impact at time 9.5 ms (left) and detail of the contact (right)

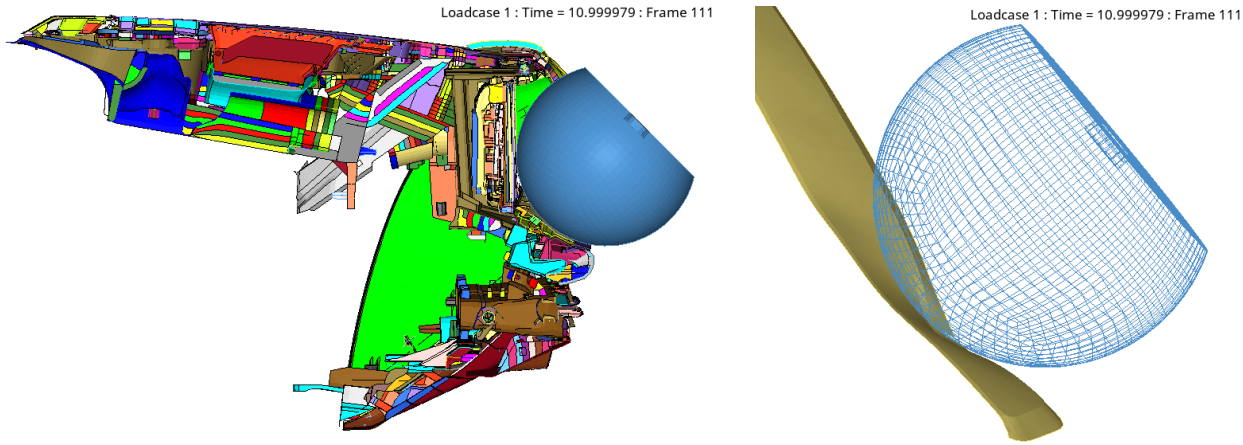

Figure 5.35 Section of the head impact at time 11 ms (left) and detail of the contact (right)

Looking at the section of the dashboard in *figure 5.35*, at 11 milliseconds there is the first contact between the head form and the monitor and so the interface force increases again up to the point where the speed of the impactor reaches zero. From this point, the contact force decreases but there is a positive drop, caused by the tendency of the lower shell of the instrument panel to return to its initial position. So, the contact between the dashboard and the head impactor increases and consequently the contact force, as it is possible to see in *figure 5.36* and 5.*37*, where the sections of the simulation at 20.2 and 24.6 milliseconds are shown, with focus on the contact between the lower shell (gold component) and the head form (blue component).

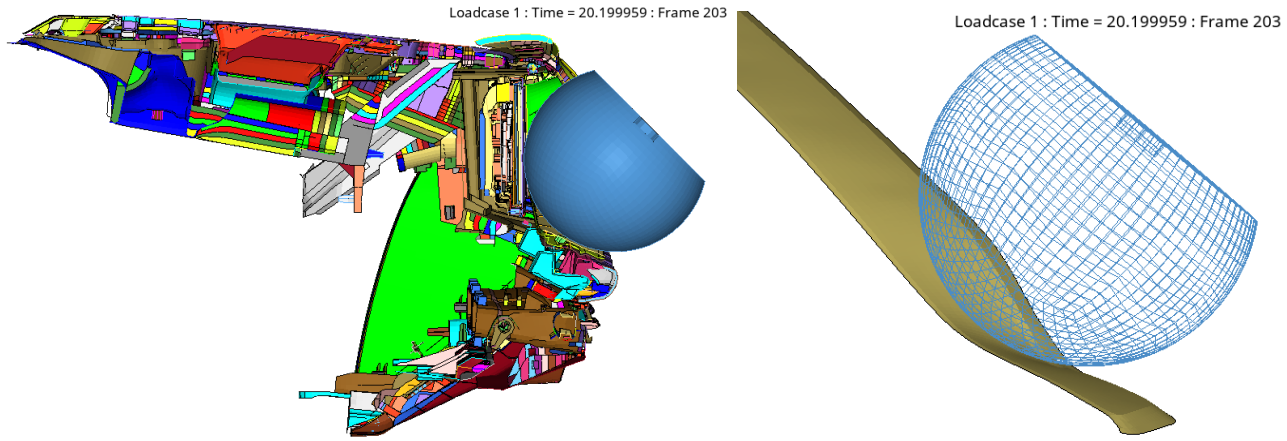

Figure 5.36 –Section of the head impact at time 20.2 ms (left) and detail of the contact (right)

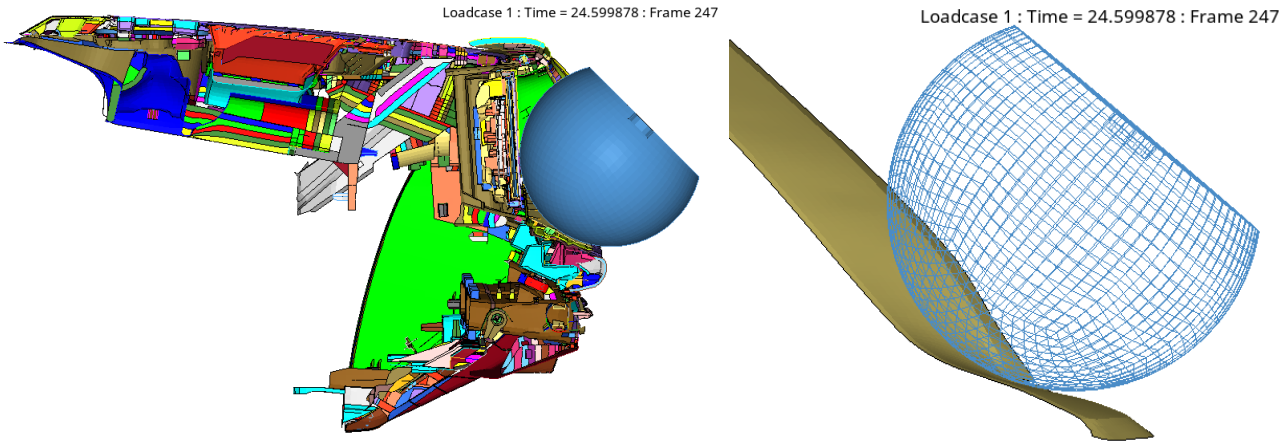

Figure 5.37 –Section of the head impact at time 24.6 ms (left) and detail of the contact (right)

5.4.2.4 Solutions to avoid threaded connection breakage

In terms of FMVSS 201L regulations and virtual validation, every requirement is satisfied but there is the detachment of the lower shell of the instrument panel, due to the breakage of threaded connection, that causes a drop in the kinetic energy. This is a warning for the car manufacturer for a better investigation in order to possibly avoid this breakage. A possible solution can be of using a larger head of the screw and this can be simulated with the use of rigids on a larger area but, as it is possible to see in *figure 5.38*, still the breakage is present.

Figure 5.38 – Frame of the threaded connection before (left image) and after (right) the breakage

The breakage of the rigids is also highlighted in *figure 5.*39 with a black circle, where a positive drop in the kinetic energy is present. With respect to the original case, the breakage of the threaded connection is only postponed in the simulation.

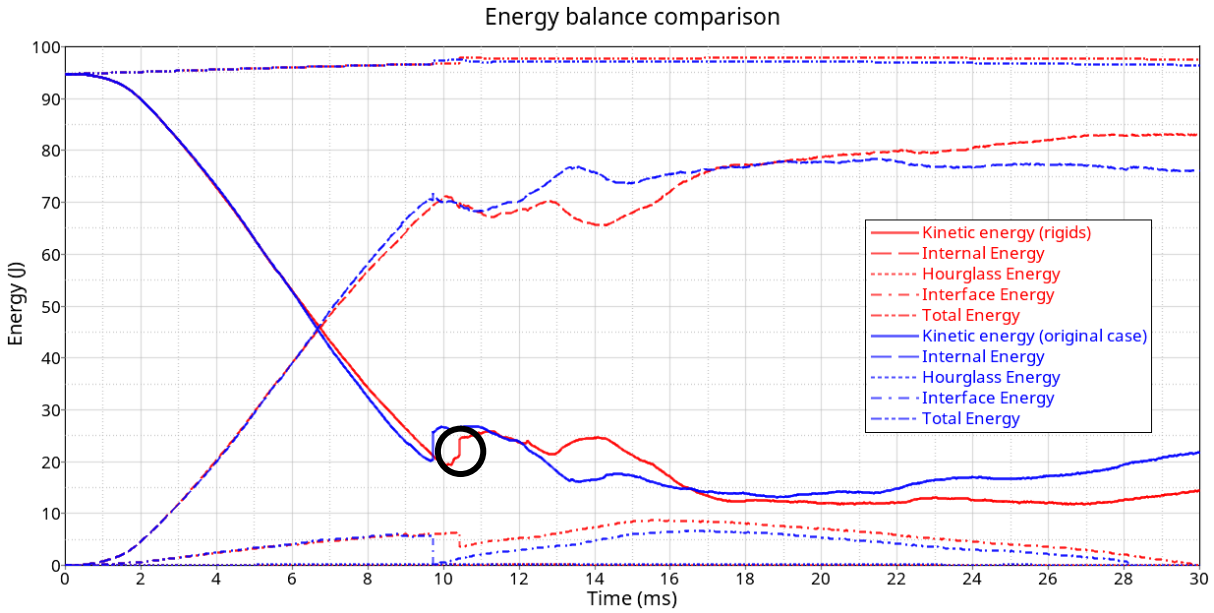

Figure 5.39 – Energy balance comparison

Since threaded connections are normed with specific dimensions and sizes defined by the regulations, the car manufacturer adopts as much as possible screws with the same size with the aim of reducing the costs, because there are many threaded connections located in the entire dashboard. It is, thus, better to consider a possible improvement focusing not on the single threaded connection that fails but, on the assembly, analyzing the general behavior of the entire dashboard.

The best solution is not to change the type of connection but modify the structure by slightly changing the plastic injection mold in order to allow the survival of the component without compromising the structural integrity of the system. It is therefore considered an overall increase of 1 mm of the thickness of the reinforcement part driver side is considered to see the effect on the behavior of the dashboard and if the breakage of the threaded connection is avoided. The reinforcement part driver side is located behind the monitor and its extension is along the entire length of the dashboard, as it is possible to observe in *figure 5.40*.

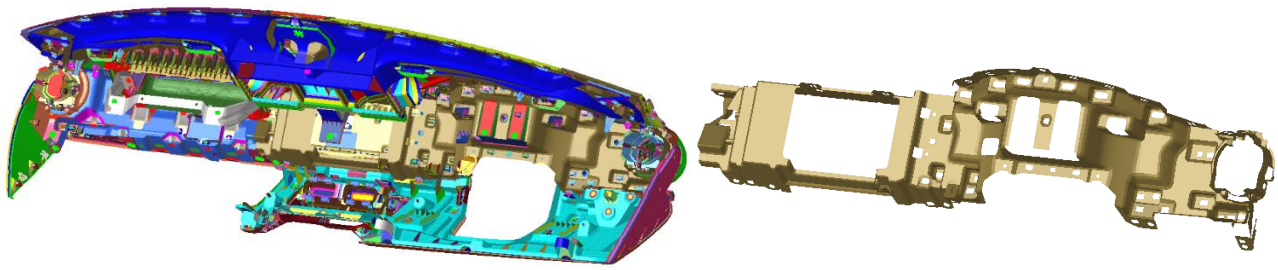

Figure 5.40 – Location of the reinforcement part driver side (left image) and focus (right)

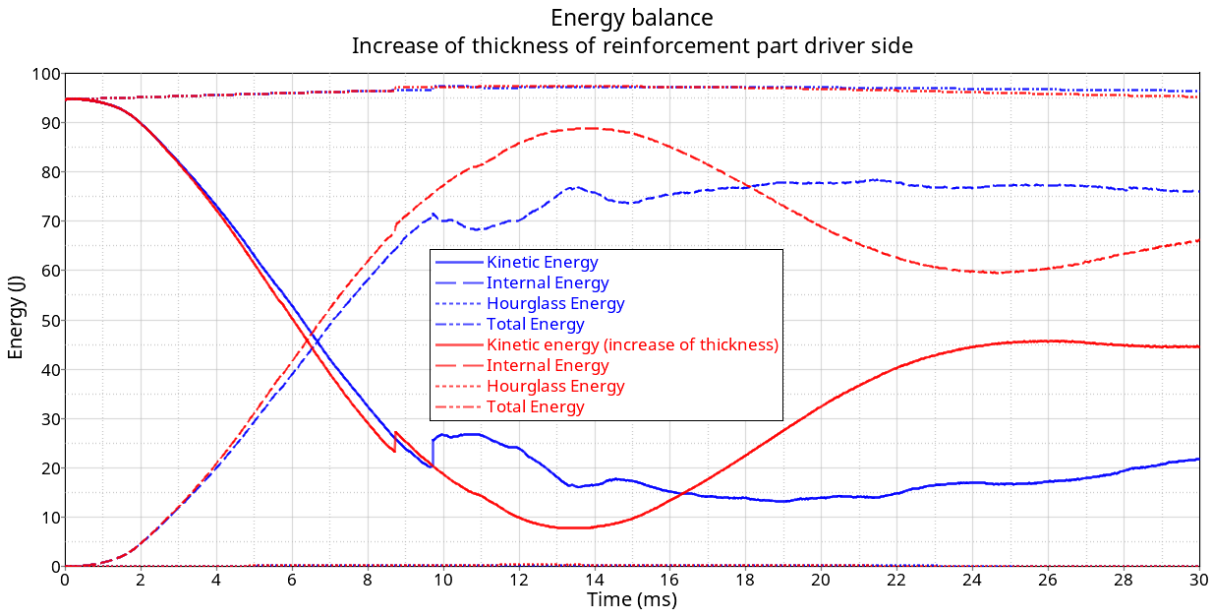

Figure 5.41 - Energy balance comparison

Looking at the energy balance in *figure 5.41*, the increase of thickness is beneficial. The component is stiffer and this is highlighted by the fact that the point where the kinetic and internal energy are equal occurs earlier in the simulation with respect to the original case. The system is able to absorb more energy and deform more in the impact phase and when the head form returns to its initial position, the dashboard has sufficient time to transfer energy to the impactor again and this is the reason why the kinetic energy is higher at the end of the simulation, with fewer components that fail. In the original case, instead, after the impact, the internal energy remains almost constant due to the presence of permanent plastic deformations and so the system is not able to transfer energy from the dashboard back to the head impactor.

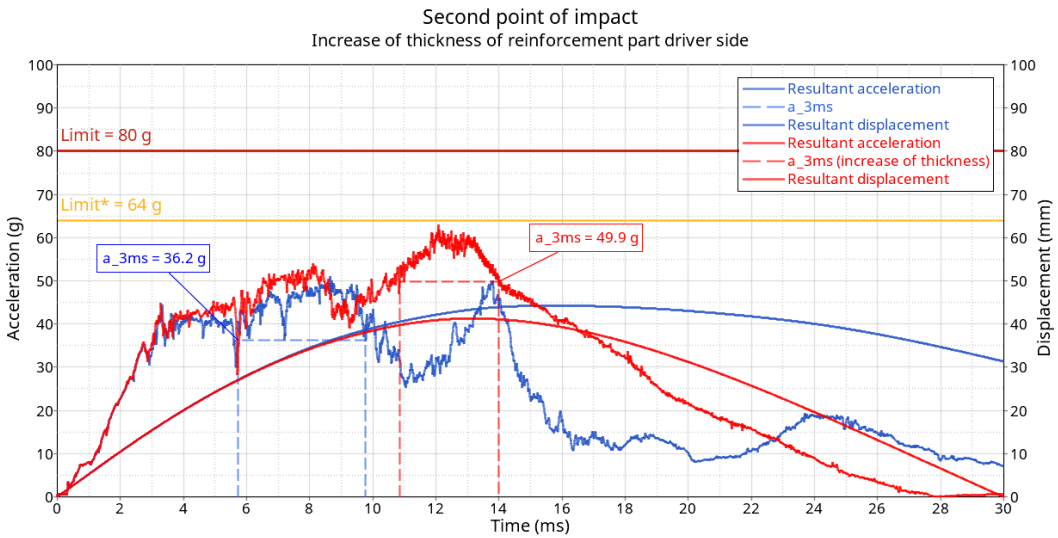

Figure 5.42 – Deceleration curve comparison

Focusing instead on the deceleration curve in *figure 5.42*, the increase of thickness causes higher values of the acceleration, since the structure is stiffer. With respect to the original case, these values are reached in the middle of the simulation, where the speed of the impactor is zero, because the detachment of the lower shell of the instrument panel is avoided and consequently there is not the presence of a negative drop in the acceleration. Even if the deceleration curve is higher, the values are below the limits imposed by the regulations and the car manufacturer.

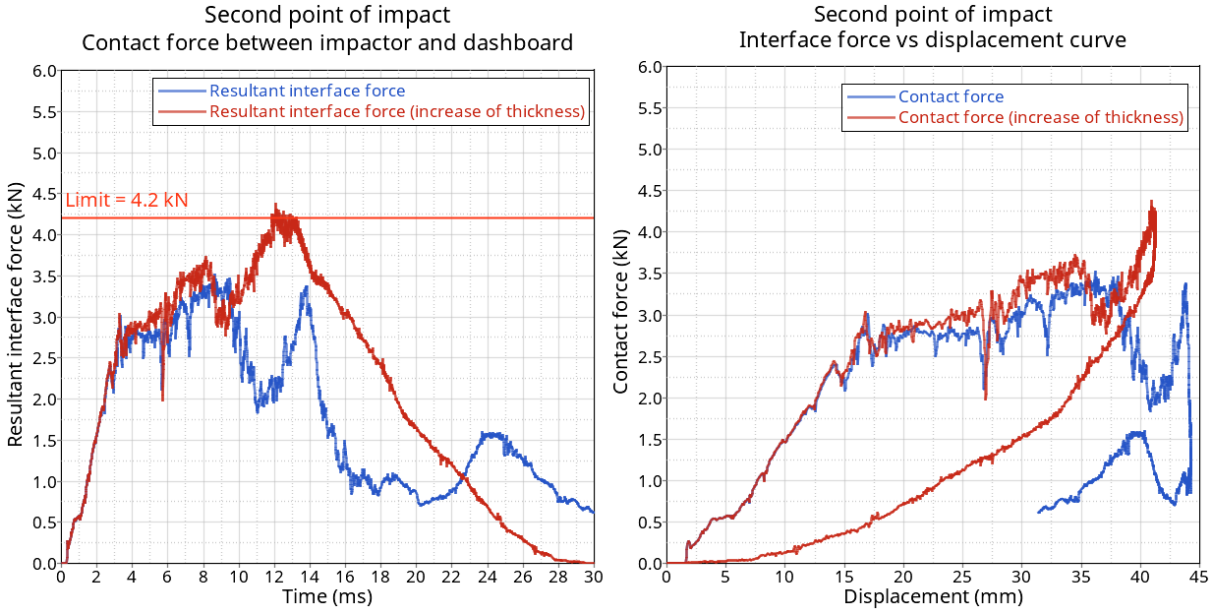

Figure 5.43 - Comparison of the graphs of the contact force between the impactor and dashboard

In the left graph of *figure 5.43* the comparison between the original trend of the contact force between the head impactor and the dashboard and the one with a modification of thickness of the reinforcement part driver side is shown. Because of higher values of the acceleration, there is an increase of the values of the interface forces with respect to the original case, but the maximum values reached during the simulation are acceptable because only few points in a limited range of time are above the suggested limit. The limit of 4.2 kN depends on the stiffness of the dashboard. If the values of the contact force are below this limit, the target is definitely fulfilled but if they are above, it is acceptable in terms of virtual validation if there are only few points that are above otherwise it is a warning for the car manufacturer that has to check if possible problems may arise when physical tests are carried out.

Focusing instead on the red curve of the right graph of *figure 5.43*, where the increase of stiffness is considered, the maximum displacement reached is lower but with higher contact force with respect to the original case, because the system is stiffer. From the maximum displacement, the behavior of the dashboard in this case is elastic since the contact force rapidly goes to zero and with zero displacement and this is in accordance with the considerations extracted from the previous graphs.

In conclusion, the best solution to avoid the breakage of the threaded connection is the increase of the overall

thickness of the reinforcement part driver side, as visible in the red circles in *figure 5.44*. The breakage is avoided because the structure is stiffer but, as a drawback, this causes an increase of weight of the component of 40 %. This proposal can be adopted but it must be feasible in terms of manufacturing process to produce it and so a deeper analysis from various points of view must be performed.

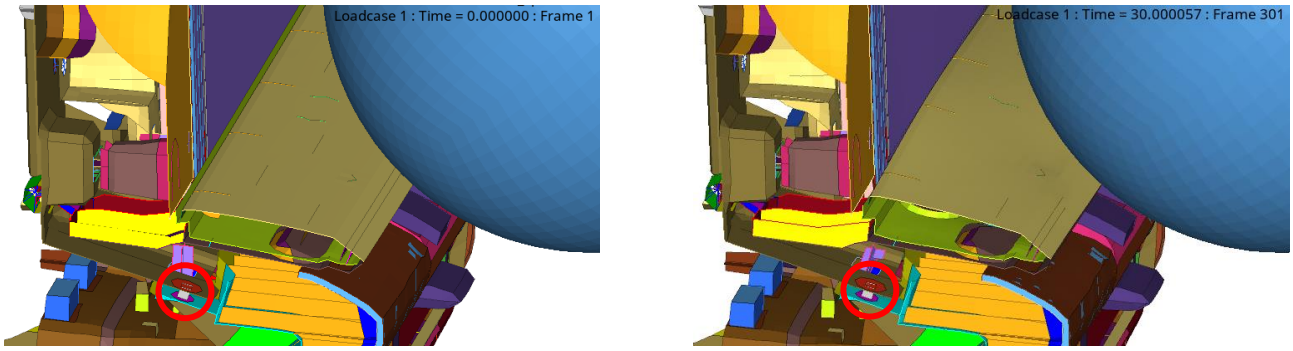

Figure 5.44 – Frame of the threaded connection at the beginning (left) and the end (right) of the simulation

5.5 MODIFICATIONS ON THE DASHBOARD: CHANGE OF MATERIAL

After the analysis of the simulations obtained from the points of impact defined by the car manufacturer, the next step is to consider a change of the materials of some components of the dashboard, since the car manufacturer suggested to investigate other industrial processes, considering variations of weight and stiffness of the system. In particular there is a change of the material of the structural elements of the monitor, such as the rear cover and the front frame, and finally of the lower shell of the instrument panel, that is considered a decorative element and is the first component that gets in contact with the head impactor. The results are then analyzed with a comparison for each point of impact, in order to understand how these modifications influence the general behavior of the dashboard in terms of energy balance, acceleration and contact force between the dashboard and the head impactor.

5.5.1 Lower shell of the instrument panel

The material of the lower shell of the instrument panel, shown in *figure 5.45*, as well as the others adopted in the dashboard, is selected by the car manufacturer according to a tradeoff between different parameters such as mechanical properties, performance and cost. In this case for the lower shell the car manufacturer has selected a composite material, made of PC/ABS matrix with 20 % of short glass fiber.

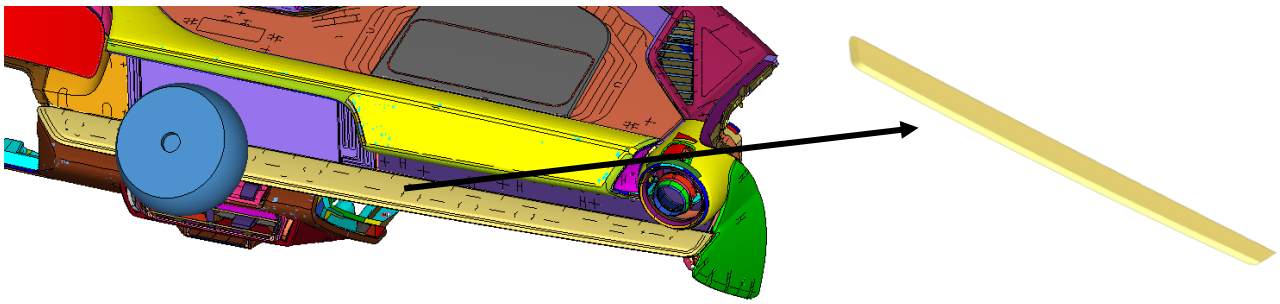

Figure 5.45 – Location of the lower shell of the instrument panel with focus on it

As previously described in the first point of impact, since this material is modeled in the software as elasto - plastic with a failure criterion based on the maximum plastic deformation; at the end of the simulation, it is possible to observe that some elements of the shell fail due to the achievement of maximum deformation. This phenomenon can be potentially a problem with crack propagation if sharp edges are generated and since it is necessary to check the occurrence in the physical tests, a more performing material is selected as alternative solution. From the base model of the dashboard, where the lower shell is made of composite material, in this case it is considered an aluminum alloy with better mechanical properties.

The main mechanical properties of the two materials are reported in the *table 5.1*.

Material	Density [kg/dm^3]	Young modulus [GPa]	Poisson ratio [-]	Yield strength [MPa]
PC/ABS GF20 (original)	1.28	4.5	0.36	100
AlSi7Mg0.3 (modification)	2.47	70	0.33	190

Table 5.1 – Mechanical properties of the original and modified material of the lower shell

The elastic and mechanical properties of the aluminium alloy are better than the ones of the composite material, but the drawback is that the density of the alloy is much higher. In fact, the weight of the lower shell of the instrument panel is 93 % higher than the one of PC/ABS GF20.

The graphs below in *figure 5.46* show the trend of the internal energy, focusing only on the lower shell of the instrument panel, in order to understand how the change of the material influences the behavior of the component. As it is possible to see in both the points of impact, the internal energy in the case of component made of Al alloy is higher than the one made of composite and so the component is able to absorb more rapidly energy in the impact phase and higher transfer of the kinetic energy of the head impactor into the internal one of the lower shell of the instrument panel.

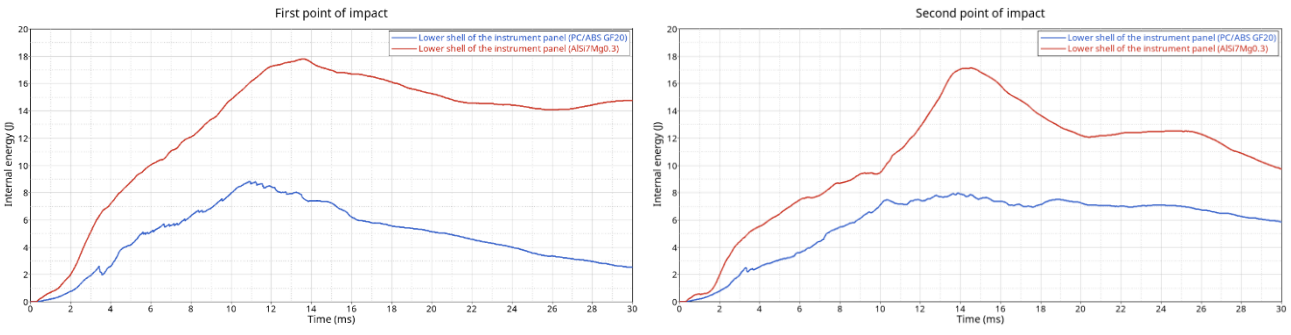

Figure 5.46 – Comparison of the internal energy of the lower shell in the two impact points

This difference in the values of internal energy is due to the different stiffness of the two materials. Since the Young modulus of the Al alloy is higher than the one of PC/ABS GF20, the stiffness of the Al alloy is higher and so it is able to absorb more energy in the impact phase, considering the same deformation. Consequently, in the deceleration curve of the head impactor higher values are reached.

The maximum level of internal energy is achieved when the velocity of the head impactor reaches zero and then it changes direction, losing the contact with the dashboard and so there is again transfer of energy from internal to kinetic one, but some permanent plastic deformations are present.

5.5.1.1 First impact point

The first step to observe the behaviour of the dashboard is to consider the frame of the head impact simulation every 5 ms up to 20 ms and this is shown in the *figures 5.47, 5.48, 5.49, 5.50* and *5.51* where in each figure is visible a full view of the entire dashboard and a left side section, located in the middle plane of the head impactor.

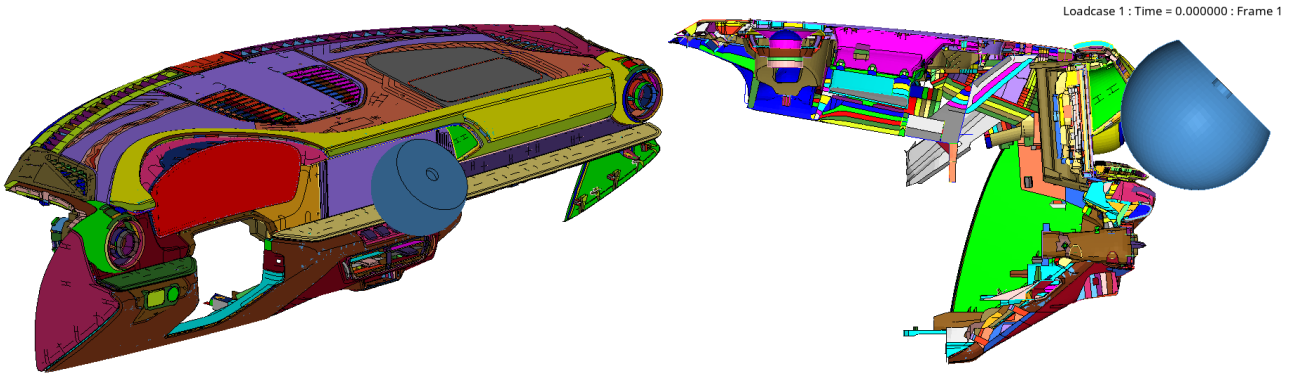

Figure 5.47 – Full view and left side section of the head impact with modified lower shell (time 0 ms)

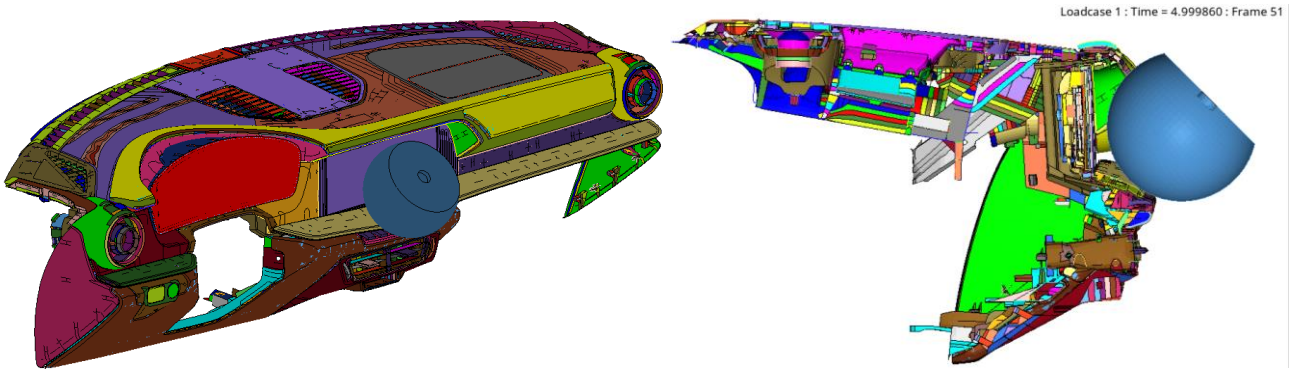

Figure 5.48 – Full view and left side section of the head impact with modified lower shell (time 5 ms)

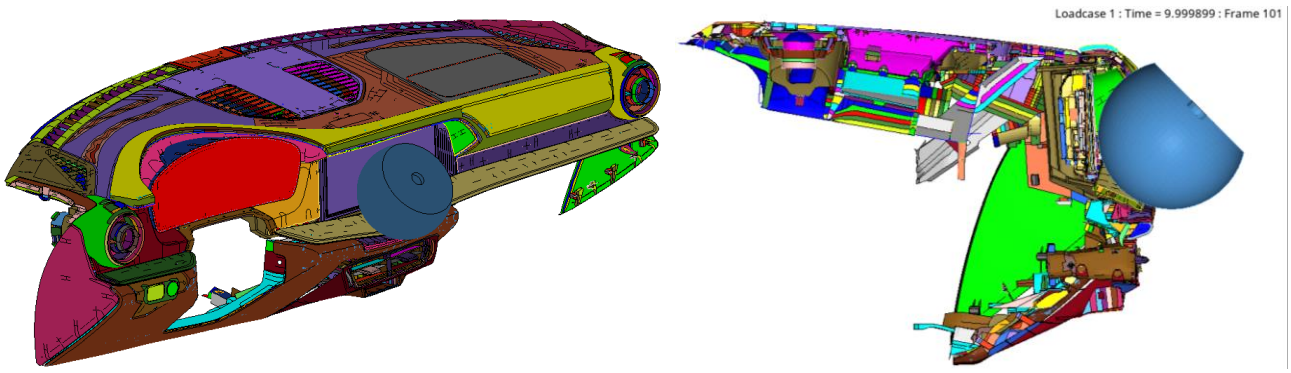

Figure 5.49 – Full view and left side section of the head impact with modified lower shell (time 10 ms)

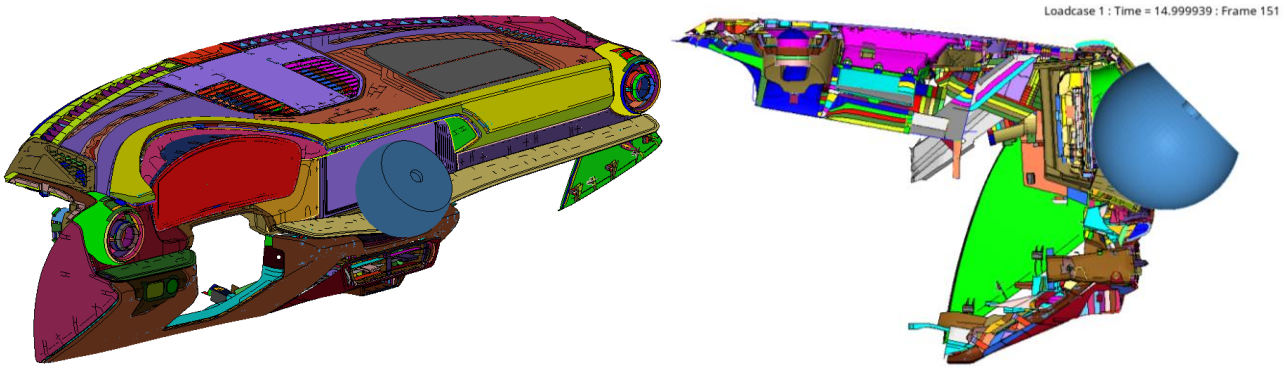

Figure 5.50 – Full view and left side section of the head impact with modified lower shell (time 15 ms)

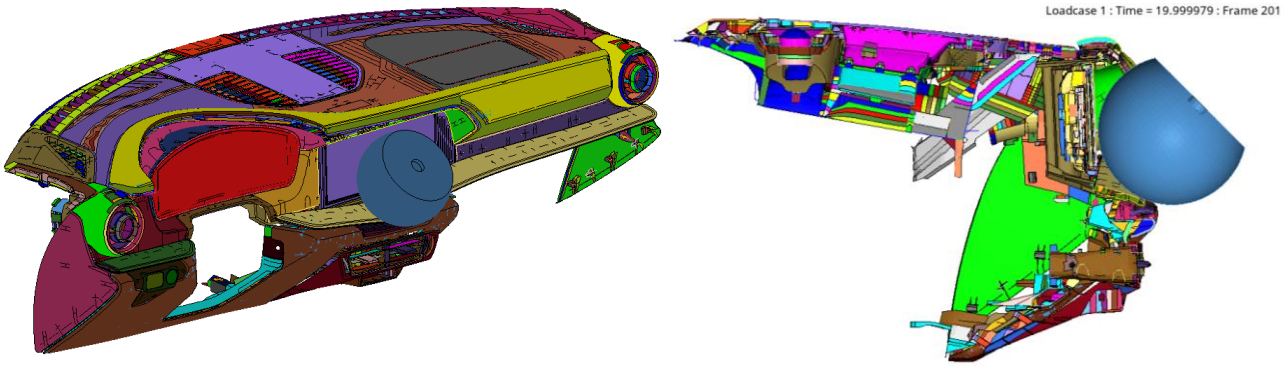

Figure 5.51 – Full view and left side section of the head impact with modified lower shell (time 20 ms)

Finally in *figure 5.52* it is shown a detail of the lower shell of the instrument panel at the end of the simulation. With respect to the original case, it does not present any element that disappears and fails during the simulation, due to the achievement of the maximum plastic deformation, and this is due to higher stiffness of the aluminum alloy. The possible occurrence of sharp edges, in this case, is definitely avoided.

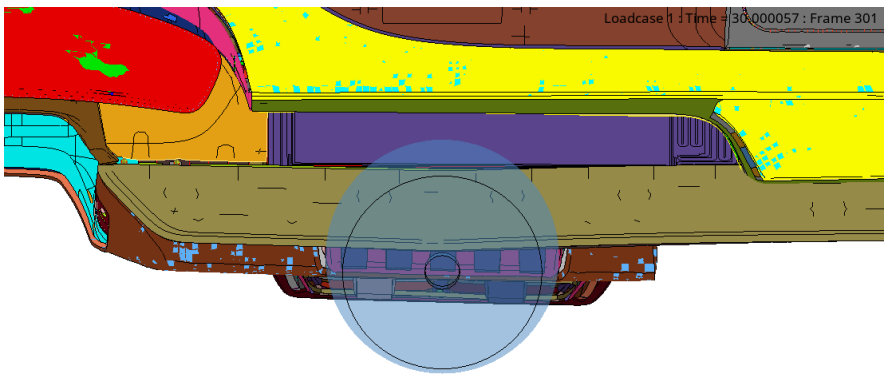

Figure 5.52 – Detail of the lower shell of the instrument panel at the end of the simulation (time 30 ms)

5.5.1.1.1 Energy balance

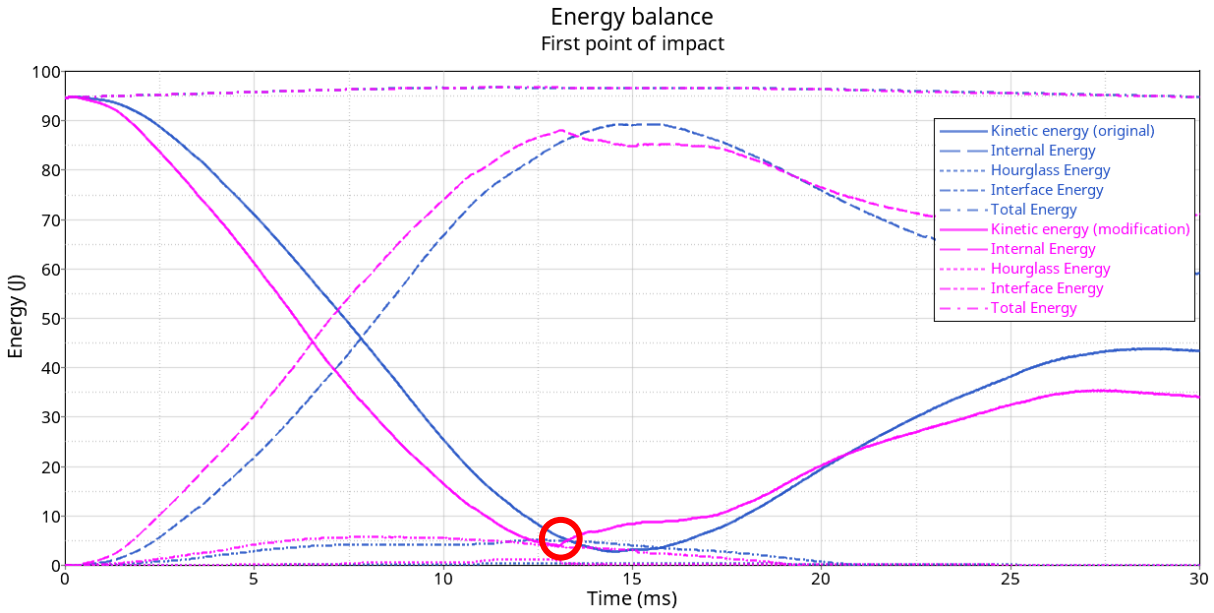

Figure 5.53 – Energy balance comparison

Looking at *figure 5.53*, it is possible to observe that the change of the material of the lower shell of the instrument panel causes some differences in the energy balance of the dashboard, but total energy is conserved in the entire duration of the simulation. Since the curves of the different energies are not superimposed, it is possible to observe the influence of the modification of the material. In this case the effect is also highlighted by the fact that the lower shell is the first component that gets in contact with the head form. The first difference is the shift of the point where the internal energy is equal to the kinetic one. The modification causes the shift to the left because Al alloy has higher stiffness than PC/ABS GF20 and so the system is able to absorb more rapidly energy, considering the same deformation. This is also highlighted by the higher slope of the purple internal energy of the Al alloy with respect to the one of the component made of composite. With respect to the original case, the lower shell of instrument panel made of AlSi7Mg0.3 causes less release of energy from the dashboard to the head form, once the impactor returns back to its initial position, due to the presence of higher permanent plastic deformations. Focusing on the red circle on the graph of *figure 5.53*, it is possible to see a small positive drop at 13.1 ms in the purple curve of the kinetic energy of the lower shell made of AlSi7Mg0.3. This is caused by a partial detachment of the threaded connection between two components of the dashboard. In *figure 5.54* it is shown the location of the threaded connection in the dashboard and the frame at time t=13.1 s and t=13.2 s, respectively before and after the failure of the threaded connection.

A possible solution to solve this small drop, as suggested before for the second impact point, is to increase locally the thickness of the reinforcement part driver side.

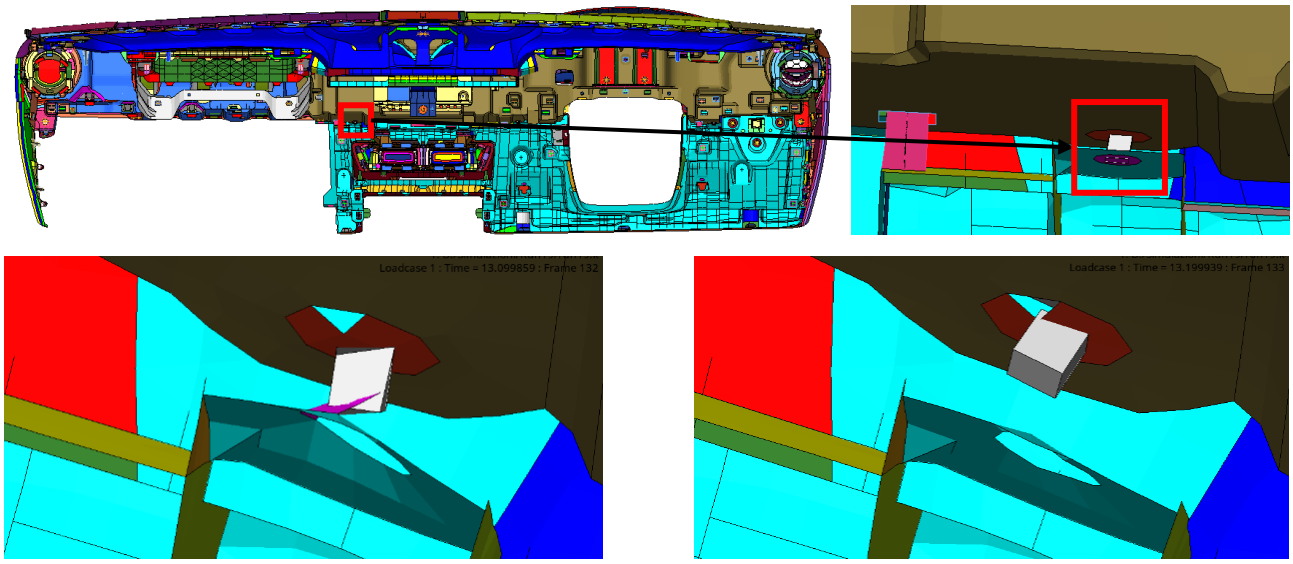

Figure 5.54 – Location of the threaded connection and its frame before (t=13.1 s) and after (t=13.2 s) the breakage

5.5.1.1.2 Deceleration curve

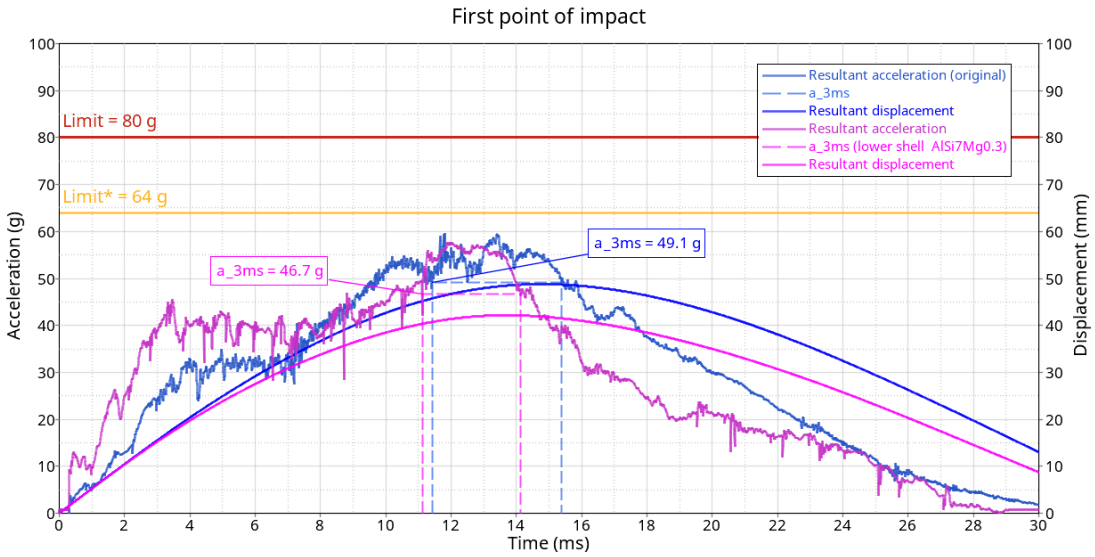

Figure 5.55 – Deceleration curve comparison

Looking at the plot of the resultant acceleration in *figure 5.55*, the general requirement of FMVSS 201L regulations (limit = 80 g) and the target requested by the car manufacturer (limit* = 64 g) are fulfilled. It is important to monitor the acceleration of the lower shell because it is the first component hit by the head impactor and there is the risk of having high peaks above the limit. Since Al alloy is stiffer than PC/ABS GF 20, there is an increase of the acceleration of the purple curve in the first part of the impact phase with respect to the original case, but the values are far below the limits and the maximum value is reached after in the simulation, when additional components of the dashboard are subjected to the influence of the head impact. From the point of view of the deceleration curve, the change of material is also beneficial since the maximum values of the acceleration are lower with respect to the original case.

5.5.1.1.3 Contact force between the impactor and the dashboard

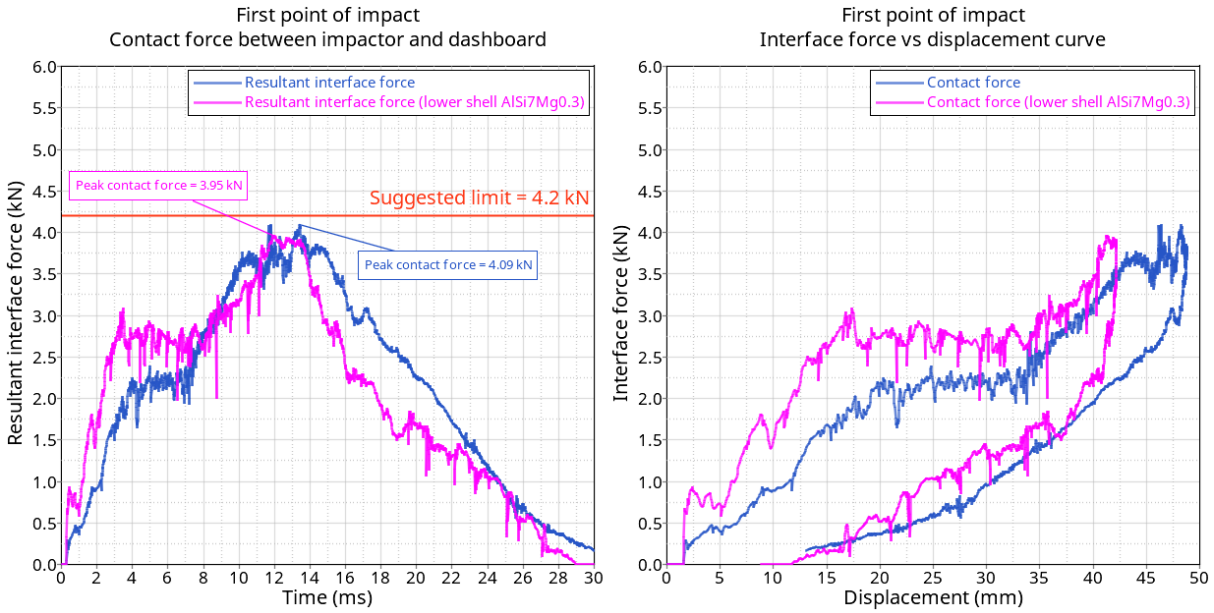

Figure 5.56 – Comparison between curves of contact force between the impactor and dashboard

The requirement of the suggested upper limit of the contact force is also satisfied, as shown in *figure 5.56.* The graphs above are in accordance with the considerations made for the deceleration curve. Focusing on the plot that shows the contact forces as a function of the displacement, the interface force of the lower shell made of aluminum alloy at the beginning is higher with respect to the original case, since it is the first element subjected to contact with the head form, but the maximum values are lower and below the limit. Due to higher stiffness of the new material, the maximum displacement of the purple curve is lower and it is reached in the point where there is the maximum contact force.

5.5.1.2 Second impact point

As for the first impact point, the first step to observe the behaviour of the dashboard is to consider the frame of the head impact every 5 ms up to 20 ms and this is visible in *figures 5.57, 5.58, 5.59, 5.60* and *5.61,* where in each figure is visible a full view of the entire dashboard and a left side section, located in the middle plane of the head impactor.

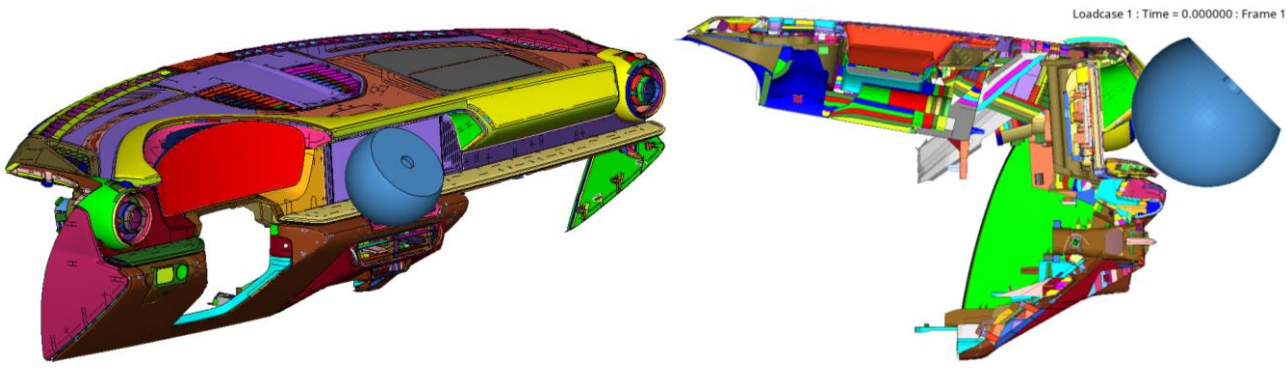

Figure 5.57 – Full view and left side section of the head impact with modified lower shell (time 0 ms)

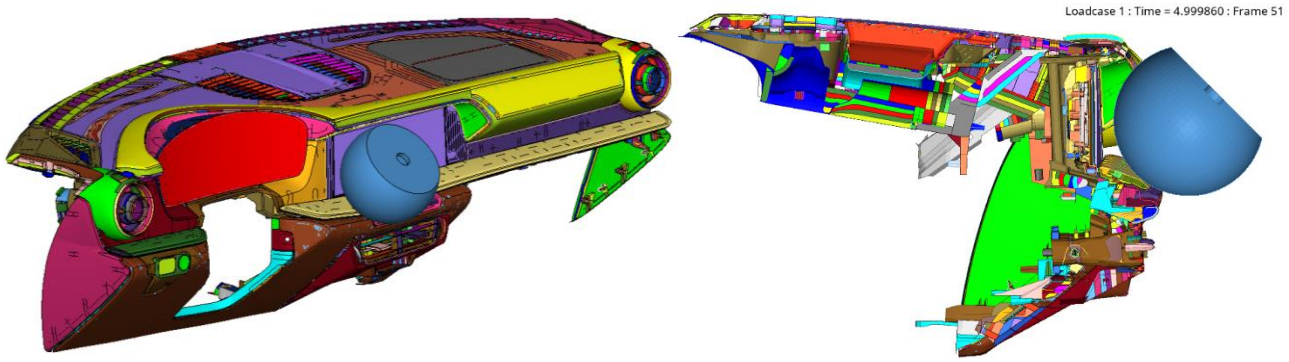

Figure 5.59 – Full view and left side section of the head impact with modified lower shell (time 5 ms)

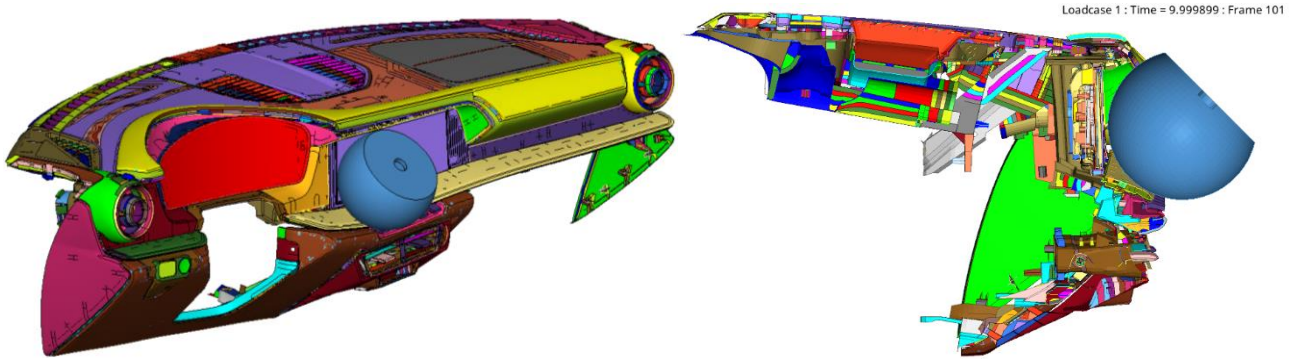

Figure 5.58 – Full view and left side section of the head impact with modified lower shell (time 10 ms)

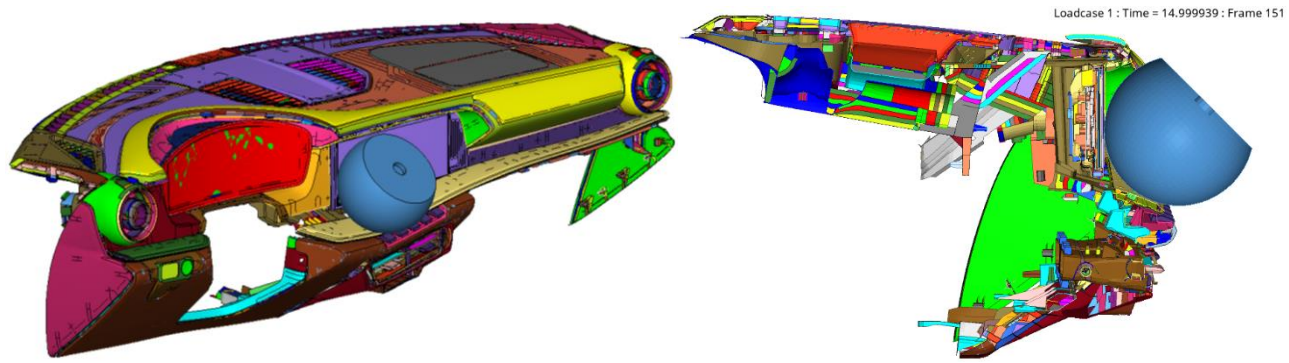

Figure 5.60 – Full view and left side section of the head impact with modified lower shell (time 15 ms)

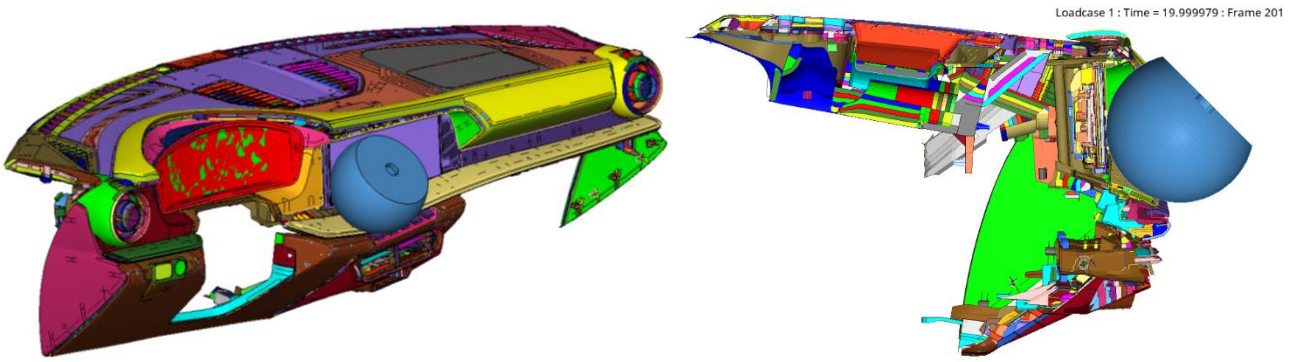

Figure 5.61 – Full view and left side section of the head impact with modified lower shell (time 20 ms)

In *figure 5.62* it is shown a detail of the lower shell of the instrument panel at the end of the simulation. The second impact point with the modified lower shell does not present any element that disappears and fails during the simulation and the occurrence of sharp edges is definitely avoided.

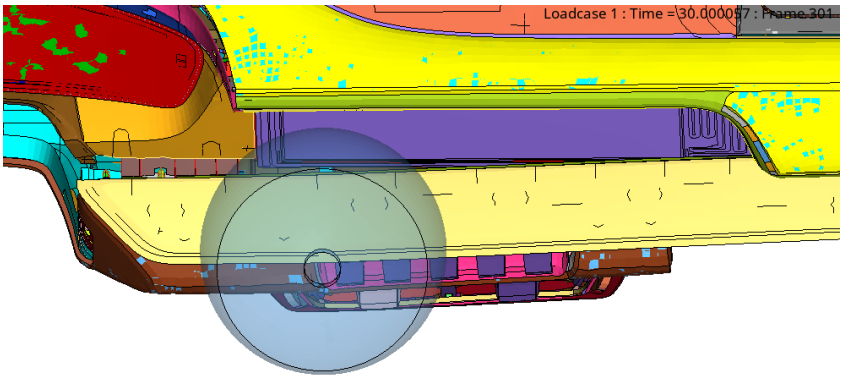

Figure 5.62 – Detail of the lower shell of the instrument panel at the end of the simulation (time 30 ms)

5.5.1.2.1 Energy balance

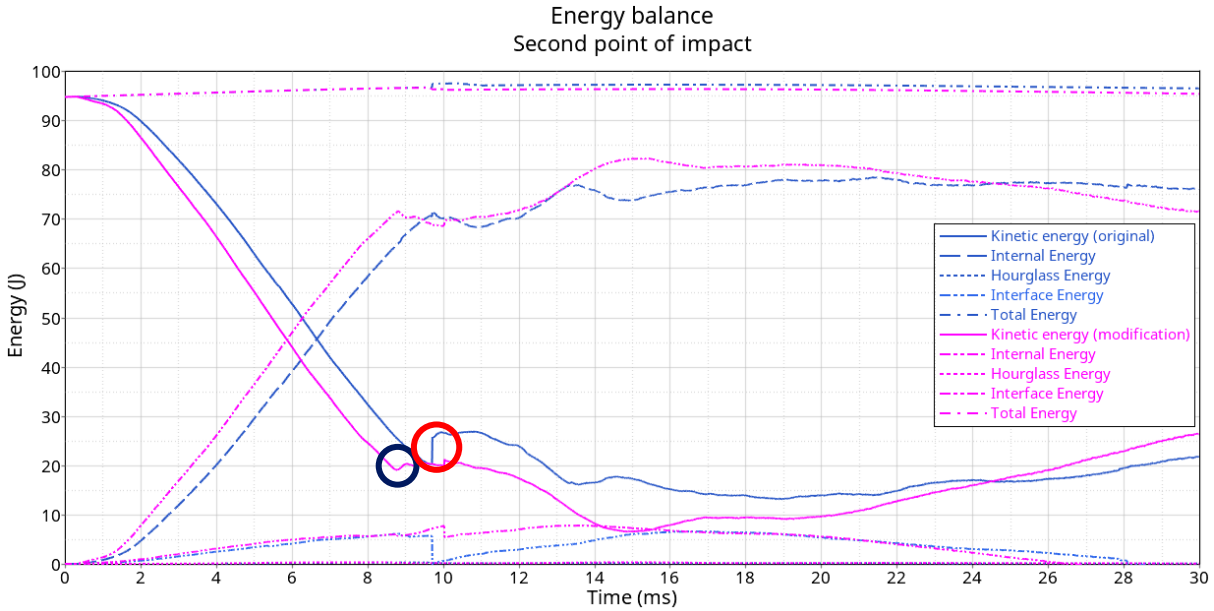

Figure 5.63 – Energy balance comparison

For the second impact point can be done similar observations to the ones about the energy balance comparison for the first impact one. The influence of the change of material is evident in the first part of the simulation, since the lower shell is the first component that is hit by the head form. Since the stiffness of aluminum alloy is higher than the one of composite material and consequently the slope of the purple curve of the kinetic energy in *figure 5.63*, this causes a shift to the left of the point where the internal energy is equal to the kinetic one. The system is able to absorb more rapidly the energy, considering the same deformation, and higher values of internal energy are reached at the end of the impact phase at about 15 ms, with respect to the original case. From the point where the speed of the impactor is null, as visible in the energy balance plot, there is more transfer of energy from the system back to the head form in the dashboard

with the lower shell made of AlSi7Mg0.3 with respect to the initial case, due to higher mechanical properties of the aluminum alloy.

Focusing on the black circle in *figure 5.63*, it is possible to see a very small positive drop in the purple curve of the kinetic energy of the lower shell made of AlSi7Mg0.3. This is caused by the detachment of the threaded connection between two components of the dashboard, as shown in *figure 5.64,* and it is the same threaded connection that fails in the original case, as highlighted in the red circle of *figure 5.63*. In the simulation with the modified lower shell, the failure of the threaded connection occurs before because aluminum alloy is able to absorb higher energy in a smaller time and the drop of kinetic energy is not as abrupt and big as the original case but quite negligible in the energy balance graph. This smaller drop is caused by higher stiffness of the system and the connecting element tears with lower release of energy but, since it is still present, a possible solution is to increase locally the thickness of the reinforcement part driver side.

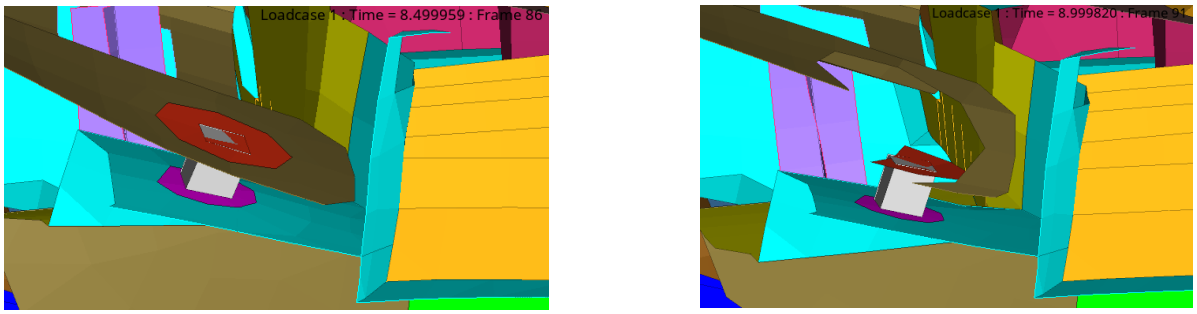

Figure 5.64 – Frame of the threaded connection before (left image) and after (right) the breakage

5.5.1.2.2 Deceleration curve

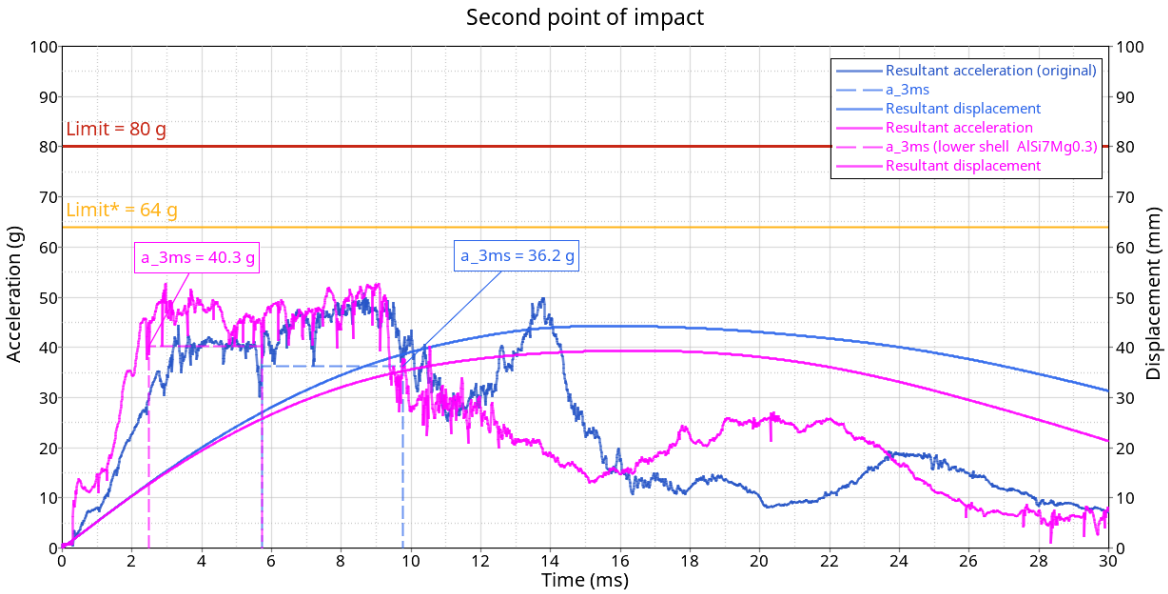

Figure 5.65 – Deceleration curve comparison

Similar considerations, as the first impact point, can be done for the deceleration curve. The a_3ms purple curve in *figure 5.65* is located in a different range of time and reaches higher values with respect to the

original case. This increase of acceleration occurs in the first part of the simulation and this is due to higher Young modulus of the aluminum alloy. Since the influence of the change of material of the first component that gets in contact with the impactor is relevant, it is necessary to monitor the deceleration curve but, even if the values of the acceleration with modified lower shell are higher than the original case, the general requirement of FMVSS 201L regulations (limit = 80 g) and the target requested by the car manufacturer (limit* = 64 g) are fulfilled.

5.5.1.2.3 Contact force between the impactor and the dashboard

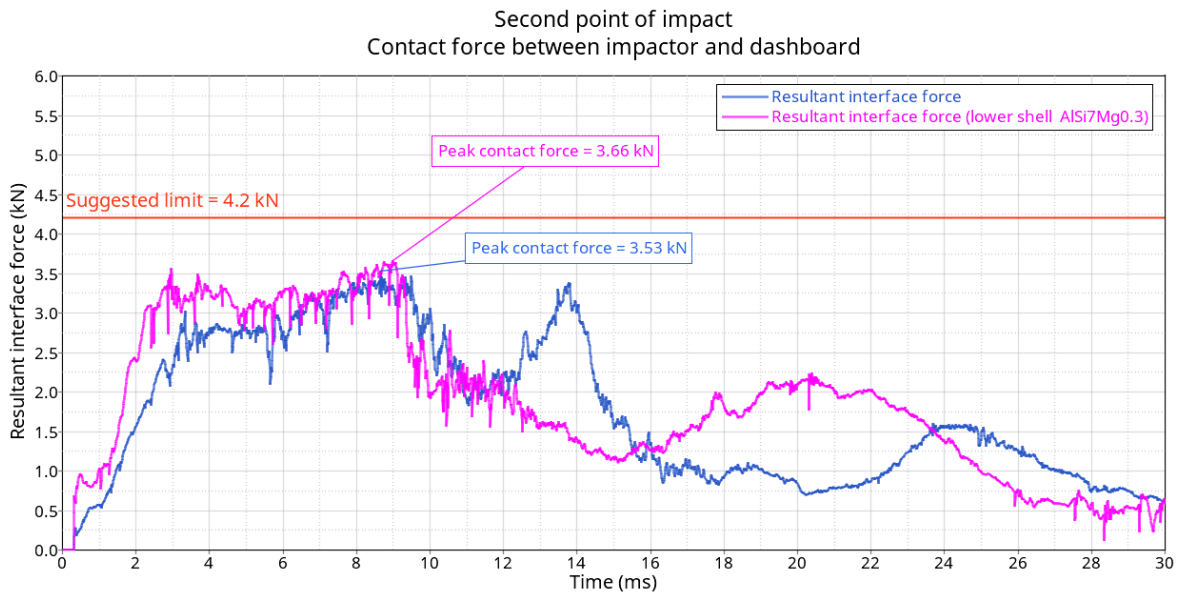

Figure 5.66 – Plot of contact force between the impactor and dashboard over time

The trend of the curves in *figure 5.66* are in accordance with the considerations made for the deceleration curve. There is an increase, due to higher stiffness, of the interface force of the lower shell made of aluminum alloy in the first part of the simulation with respect to the original case but the maximum values of the contact force, even if higher, are below the suggested upper limit.

Focusing on the purple curve of *figure 5.66*, from the maximum values of the interface force at about 9 milliseconds there is a decreasing trend up to the point where the speed of the head impactor is null and then changes direction (15.2 ms). This decrement occurs before the end of the impact phase, and it is due to the detachment of the lower shell that is caused by the breakage of the threaded connection. As visible in the focus of the contact between the head impactor and the lower shell at 9 ms in *figure 5.67*, the deformation caused by the contact is higher with respect to the one in *figure 5.68* at 15.2 ms and this confirms the trend of the purple plot.

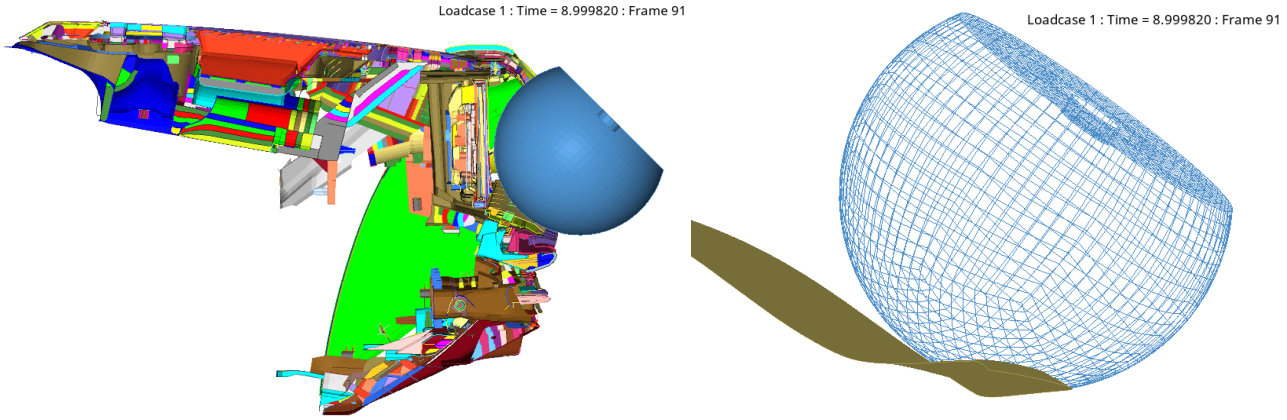

Figure 5.67 –Section of the head impact at time 9 ms (left) and detail of the contact (right)

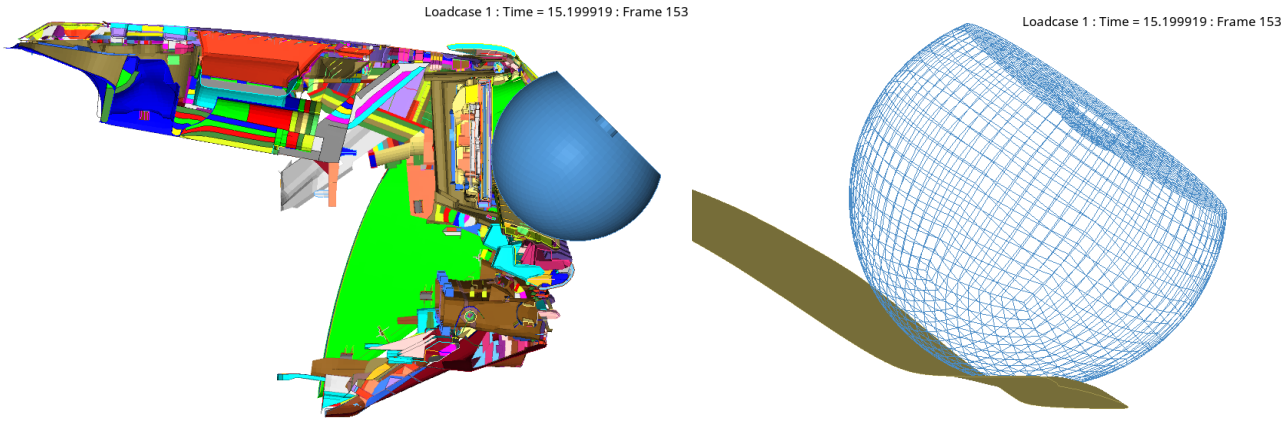

Figure 5.68 –Section of the head impact at time 15.2 ms (left) and detail of the contact (right)

While the trend of the contact force with the modified lower shell is decreasing in the range of time between 9 and 15 milliseconds, in the original case there is a peak in the same period of time and this is highlighted in *figure 5.69*, where it is shown that in the original case there is a higher contact between the monitor and the head impactor while there is just a touch of the impactor with the monitor in the modified case.

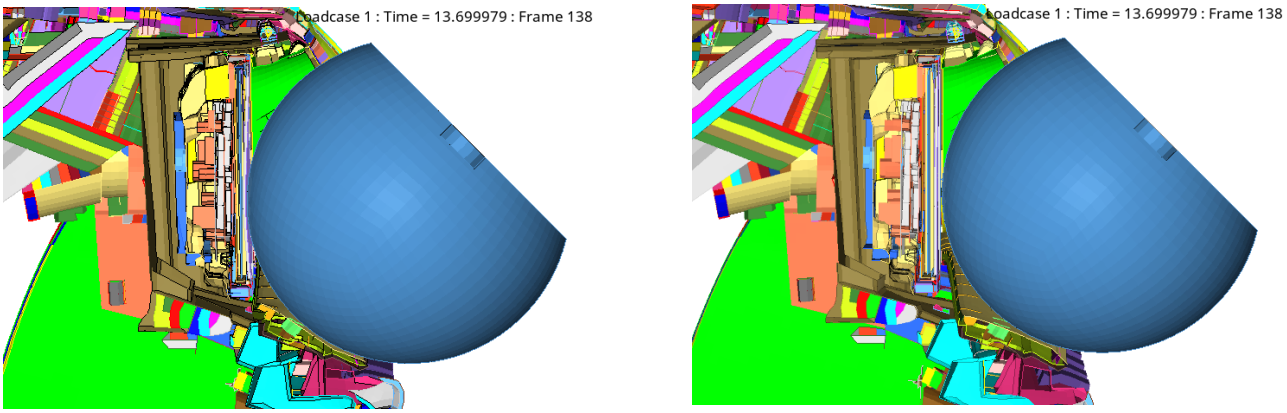

Figure 5.69 – Contact between head form and monitor at time 13.7 ms in the original (left) and modified case (right)

Focusing more on the trend of the purple curve in *figure 5.66*, from 10 ms there is not a linearly decreasing trend but there is an increment of the contact force in the range of time between 15.2 and 20.5 ms with the

presence of a peak. This is due to the fact that the lower shell, detached from the dashboard, tends to return back to its position once the head impactor changes its direction. This consideration is also highlighted in *figure 5.70* and *5.71*, where it is shown the contact between the impactor and the lower shell at time 17.7 and 20.5 ms. With respect to *figure 5.68* at 15.2 ms, the deformation of the lower shell caused by the contact increases up to 20.5 ms.

The range of time where the interface force increases, because in the return motion to its original position the head impactor hits the lower shell, is earlier in the case of lower shell made of AlSi7Mg0.3 (15-20 ms) with respect to the original case (20-25 ms). This is due to the higher stiffness of the modified shell that causes a lower detachment than the original case, as shown in *figure 5.72* with the comparison of the frame of the simulation at 20 ms, since it is able to absorb more energy with higher plastic deformation.

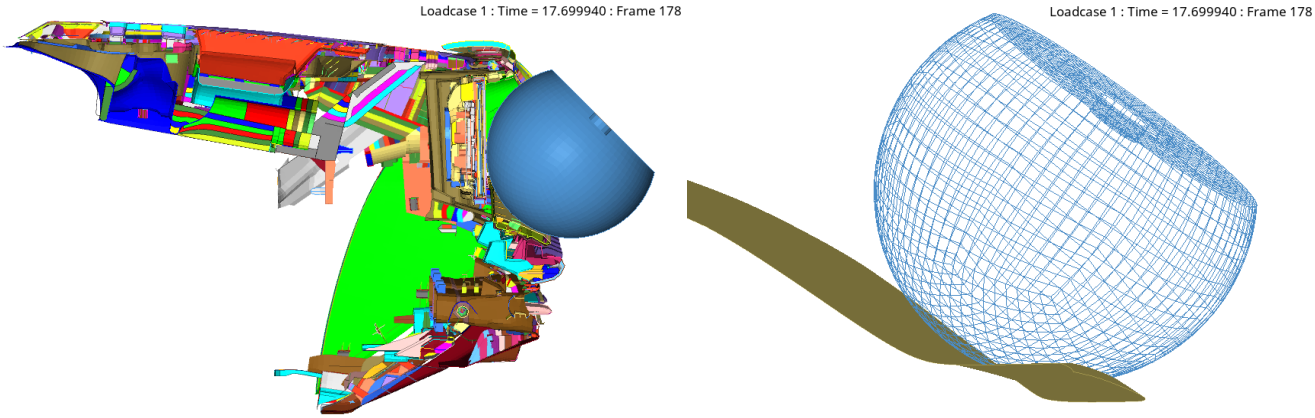

Figure 5.70 –Section of the head impact at time 17.7 ms (left) and detail of the contact (right)

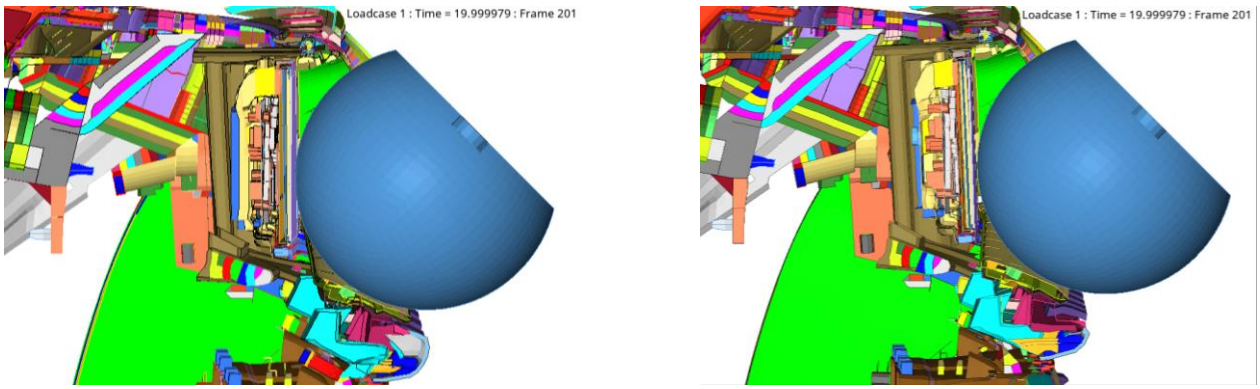

Figure 5.71 – Contact between head form and the lower shell at time 20 ms in the original (left) and modified case

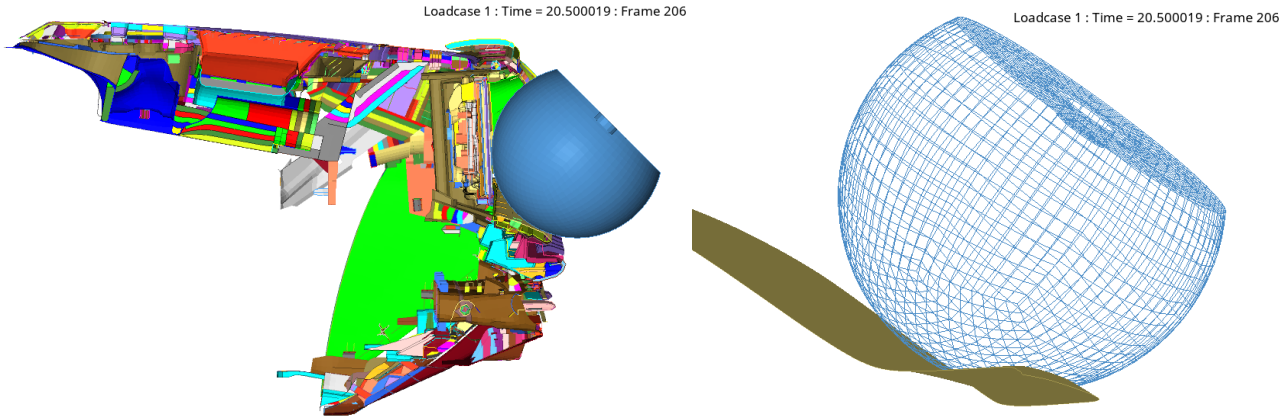

Figure 5.72 –Section of the head impact at time 20.5 ms (left) and detail of the contact (right)

Finally, focusing on the graph in *figure 5.73* that shows the contact force as a function of the displacement, similar considerations can be made in accordance with the ones of the deceleration curve. Since aluminum alloy has higher stiffness than PC/ABS GF20, the maximum displacement that is reached is lower than the original case. From the maximum displacement, the purple curve in *figure 5.73* initially presents an increase of the force due to the contact of the lower shell and the head impactor, that returns back to its initial position after the impact phase; then, as expected, there is a more rapid decreasing trend with respect to the original case, due to the higher capability of the system to transfer back energy to the head impactor.

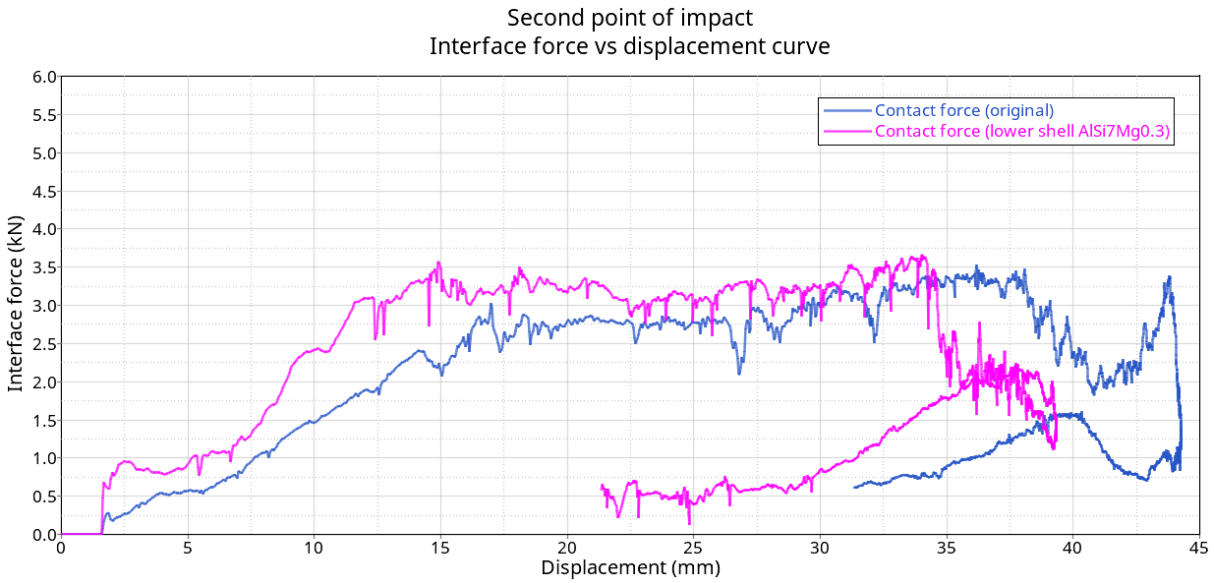

Figure 5.73 – Contact force between the impactor and dashboard – displacement plot

5.5.2 Structural components of the monitor: front frame and rear cover

The material of the different components of the monitor is selected, as before, by the car manufacturer according to a tradeoff between different parameters such as mechanical properties, performance and cost. Focusing on the front frame of the monitor, shown in *figure 5.74*, the car manufacturer has selected an amorphous thermoplastic polymeric material, based on polycarbonate (PC) and acrylonitrile-butadiene-styrene (ABS). This material is a balanced combination of hardness, stiffness and high heat resistance and the peculiar features are high impact resistance over a wide temperature range, low deformation, high dimensional stability and accuracy.

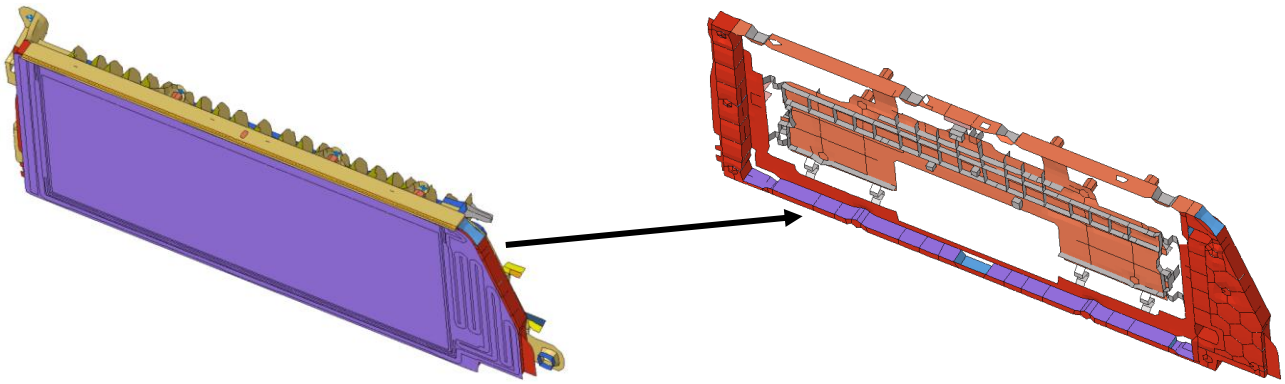

Figure 5.74 – Picture of the monitor of the dashboard with focus on the front frame (right)

As all the plastic materials, due to their viscoelastic behavior, the mechanical properties change not only with temperature, but also with the strain rate. Generally, at high deformation rates, the behavior of the material is mainly elastic and brittle; at low strain rate the elastic region is not present and viscous deformations are prevalent and finally at intermediate deformation speeds the material shows a ductile behavior.

Focusing on the stress-strain curve, it is affected by the strain rate and higher is the strain rate speed, higher is the stiffness of the material and the stress that can be reached, considering the same deformation, as it is possible to see in *figure 5.75*.

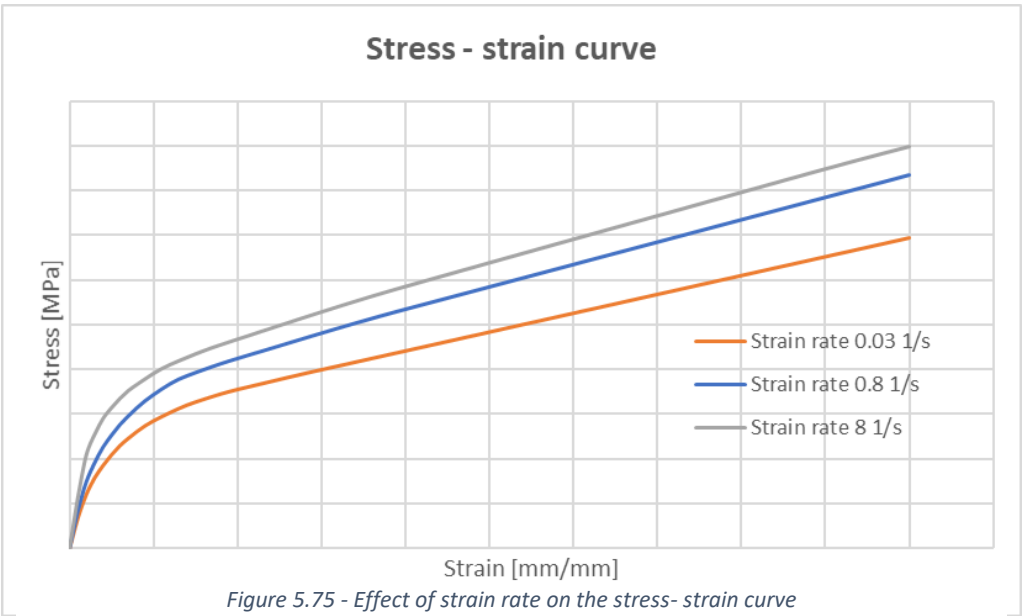

Figure 5.75 - Effect of strain rate on the stress- strain curve

This material is modeled in the software as elasto - plastic with a failure criterion based on the maximum plastic deformation and it is defined, for each strain rate, a load curve giving the effective stress as a function of the effective plastic strain for that rate.

In order to understand the influence on the behavior of the dashboard caused by the change of the material of the front frame of the monitor, the modification still considers a plastic material, that is polypropylene (PP). It is a thermoplastic polymer and it is the most used in the automotive field. PP is mixed with 20 % of talc in order to increase the elastic modulus but it is necessary to choose the right percentage of talc in order not to compromise the dimensional stability at high temperatures. PP has high mechanical strength, dimensional stability, high impact resistance, it is cheap and it has low relative density, that is one of the lightest polymers. The values of the main mechanical properties of the two materials are reported in the *table 5.2.*

Material	Density [kg/dm^3]	Young modulus [GPa]	Poisson ratio [-]	Yield strength [MPa]
PC+ABS (original)	1.13	2.6	0.37	54
PP TD20 (modification)	1.07	2.74	0.4	26

Table 5.2 – Mechanical properties of the original and modified material of the front frame

The elastic and mechanical properties of the PC+ABS and PP TD20 are very similar but the yield strength of PC+ABS is twice higher than PP TD20 and the small drawback is that the weight of the front frame of the monitor in PC+ABS is 5.7 % higher than the one made of PP TD20.

Focusing instead on the rear cover of the monitor, shown in *figure 5.76*, the car manufacturer has selected the magnesium alloy AZ91D, where the main alloying elements are aluminum, zinc and manganese. The main reasons of the choice of magnesium for structural components are the highest weight- strength ratio among all the common metals, good dimensional stability, excellent damping properties, greater impact load capacity than aluminum alloy and, with the use of appropriate alloying elements, it is possible to achieve high strength and elastic modulus. This material is modeled in the software as elasto - plastic with a failure criterion based on the maximum plastic deformation.

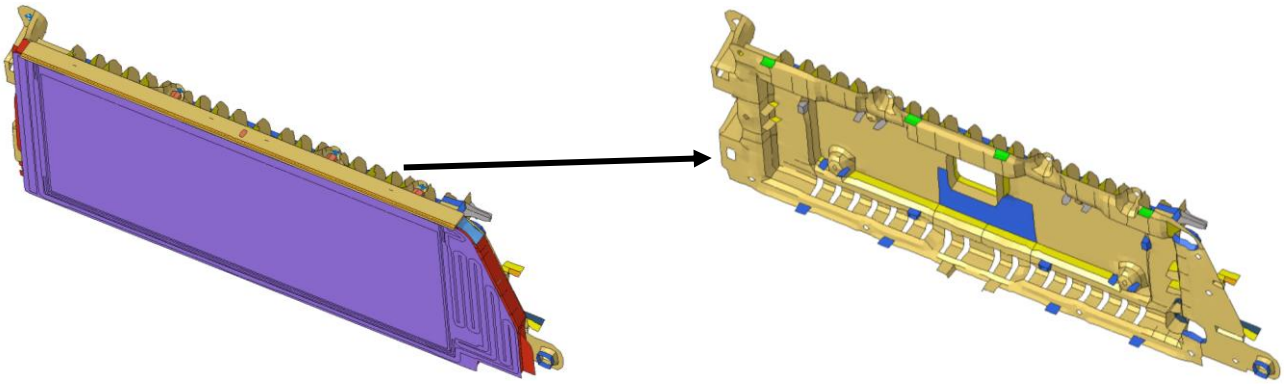

Figure 5.76 – Monitor of the dashboard with focus on the rear cover (right)

A change of the material of the rear cover is analyzed, considering the aluminum alloy AlSi7Mg0.3, where the main alloying elements are magnesium, silicon and manganese. It is characterized by excellent mechanical properties and corrosion resistance, very good weldability and workability, cheapness and generally Al-Si alloys are very largely used in the automotive field. The values of the main mechanical properties of the two materials are reported in the *table 5.3*.

Material	Density [kg/dm^3]	Young modulus [GPa]	Poisson ratio [-]	Yield strength [MPa]
AZ91D Mg alloy (original)	1.81	45	0.35	160
AlSi7Mg0.3 (modification)	2.47	70	0.33	190

Table 5.3 – Mechanical properties of the original and modified material of the rear cover

The elastic modulus and the yield strength of the aluminium alloy are higher than the ones of the magnesium alloy but, on the contrary, due to its higher density, the weight of the rear cover of the monitor in Al alloy is 36.5 % higher than the one made of Mg alloy.

5.5.2.1 First impact point

The first step to observe the behaviour of the dashboard is to consider the frame of the head impact simulation every 5 ms up to 20 ms. In *figure 5.77, 5.78, 5.79, 5.80* and *5.81* it is shown the simulation with the modified front frame while in *figure 5.82, 5.83, 5.84, 5.85* and *5.86* the one with the modified rear cover. In each figure is visible a full view of the entire dashboard and a left side section, located in the middle plane of the head impactor.

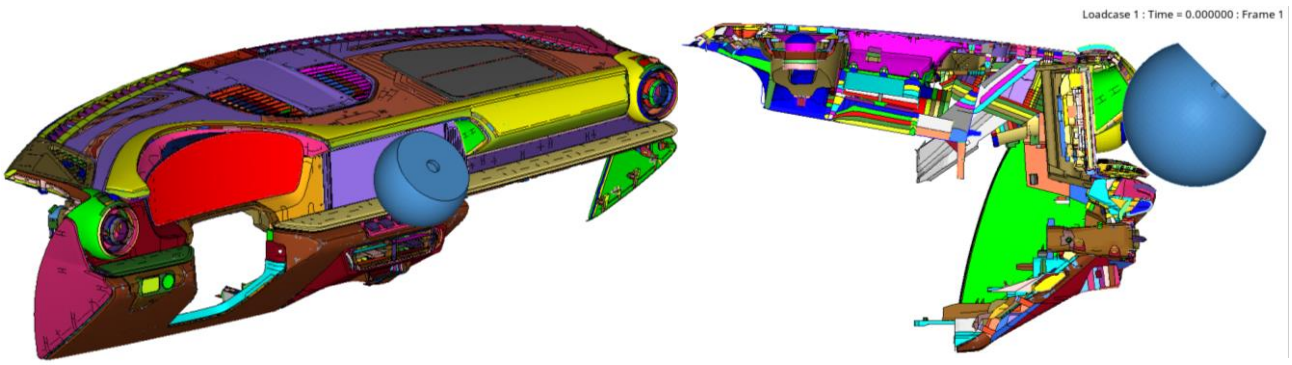

Figure 5.77 – Full view and left side section of the head impact with modified front frame (time 0 ms)

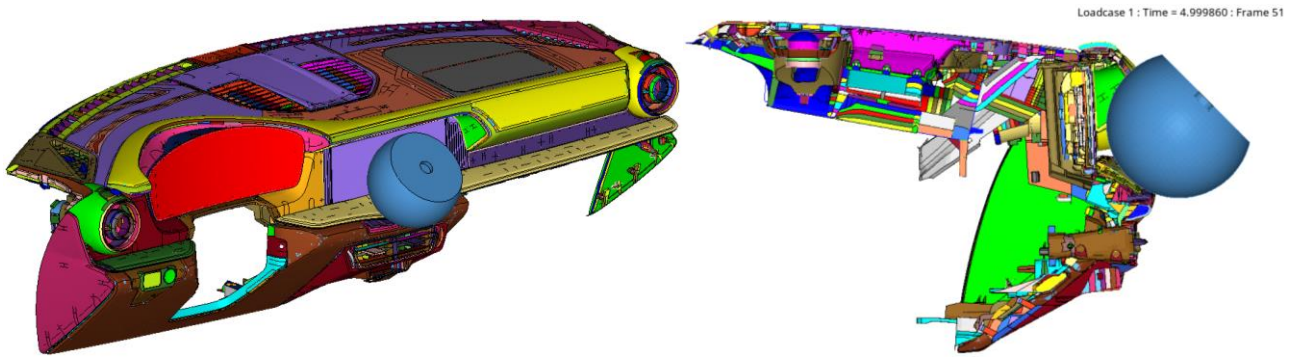

Figure 5.78 – Full view and left side section of the head impact with modified front frame (time 5 ms)

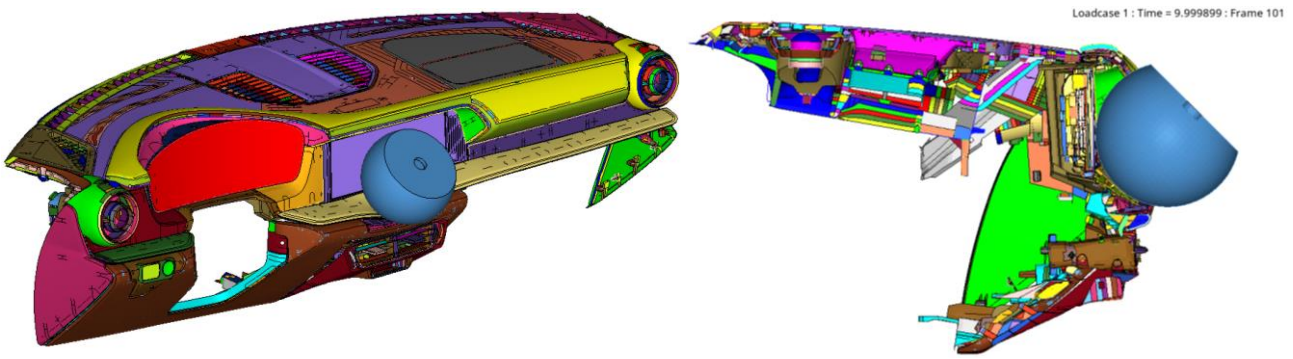

Figure 5.79 – Full view and left side section of the head impact with modified front frame (time 10 ms)

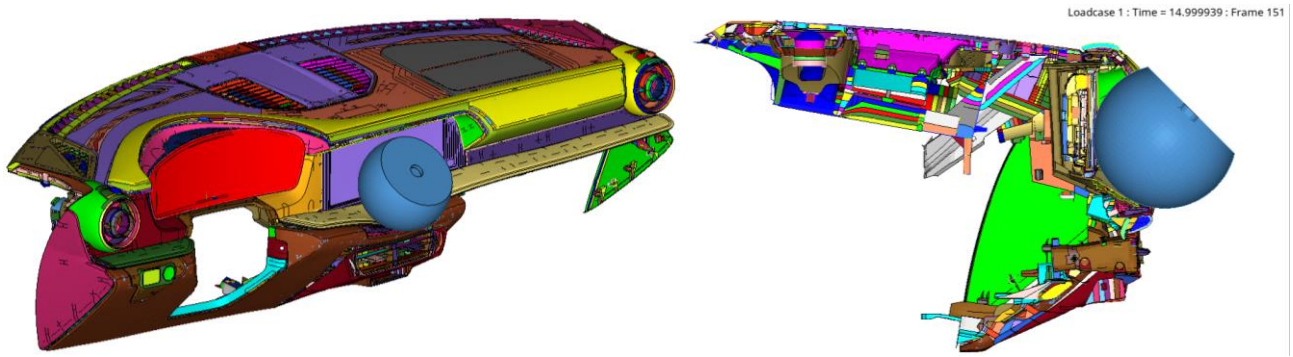

Figure 5.80 – Full view and left side section of the head impact with modified front frame (time 15 ms)

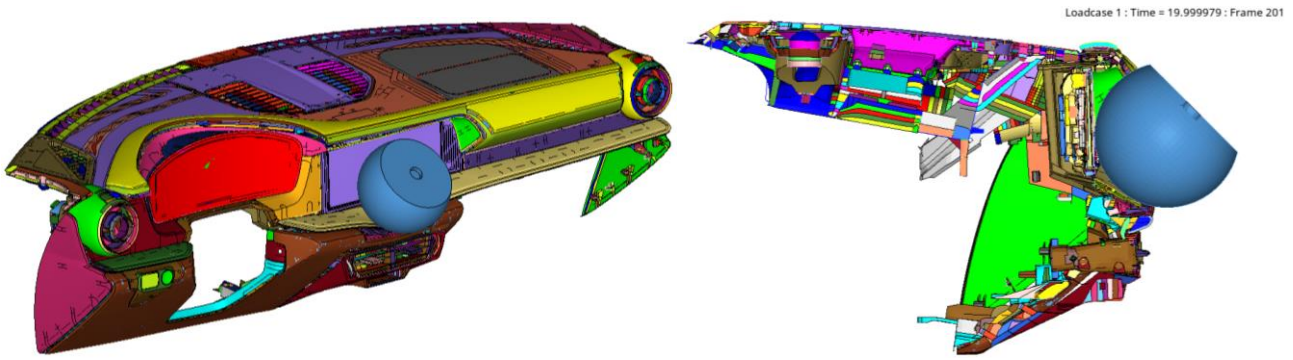

Figure 5.81 – Full view and left side section of the head impact with modified front frame (time 20 ms)

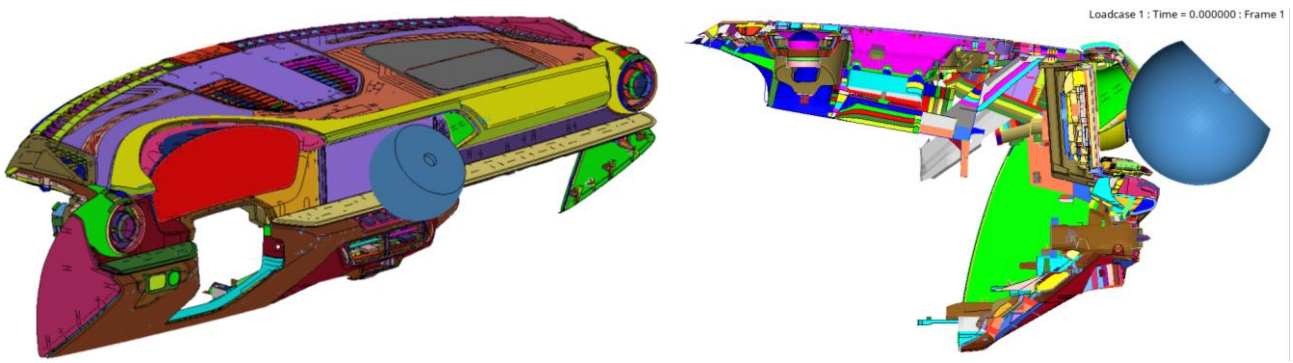

Figure 5.82 - Full view and left side section of the head impact with modified rear cover (time 0 ms)

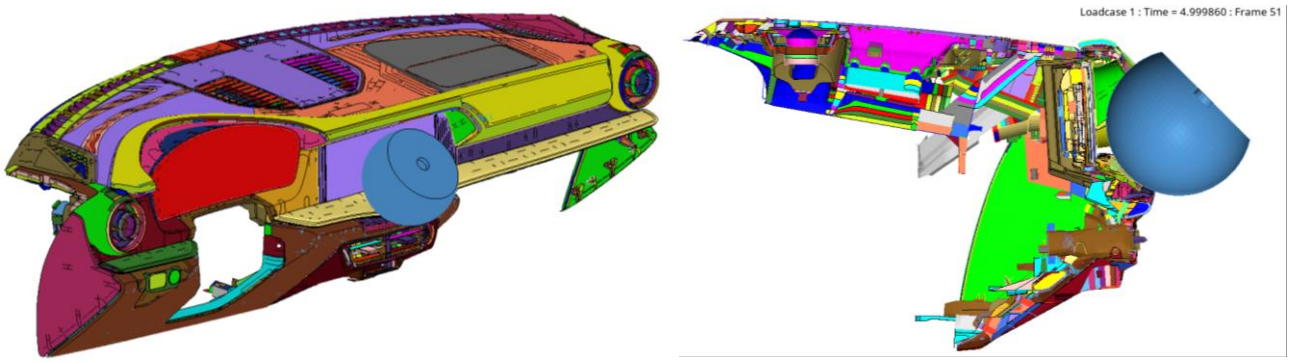

Figure 5.84 - Full view and left side section of the head impact with modified rear cover (time 5 ms)

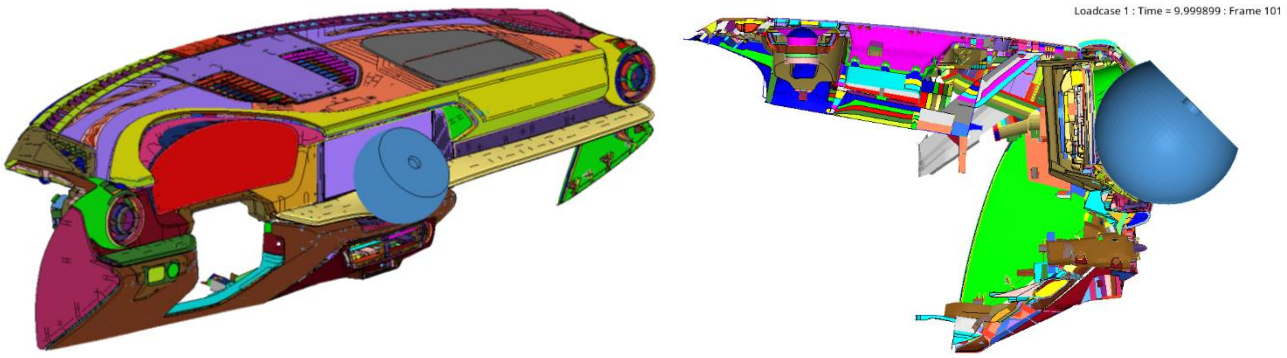

Figure 5.83 - Full view and left side section of the head impact with modified rear cover (time 10 ms)

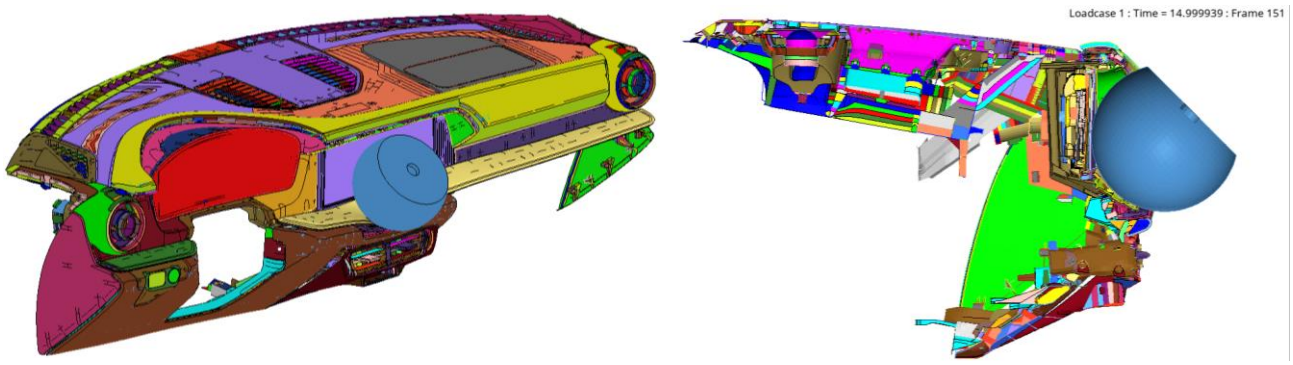

Figure 5.85 - Full view and left side section of the head impact with modified rear cover (time 15 ms)

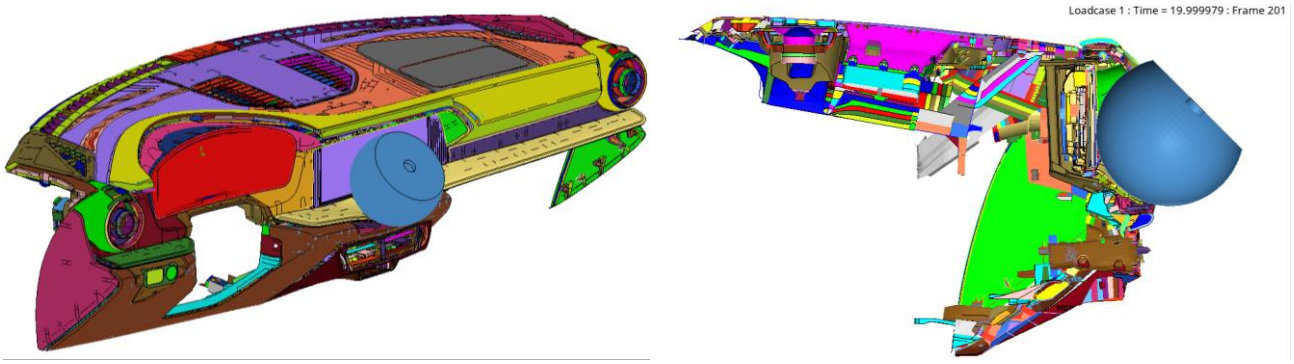

Figure 5.86 - Full view and left side section of the head impact with modified rear cover (time 20 ms)

Finally, in *figures 5.87,5.88* and *5.89* it is shown a focus on the front frame of the monitor (yellow component) while in *figures 5.90, 5.91* and *5.92* it is shown a focus on the rear cover (green component).

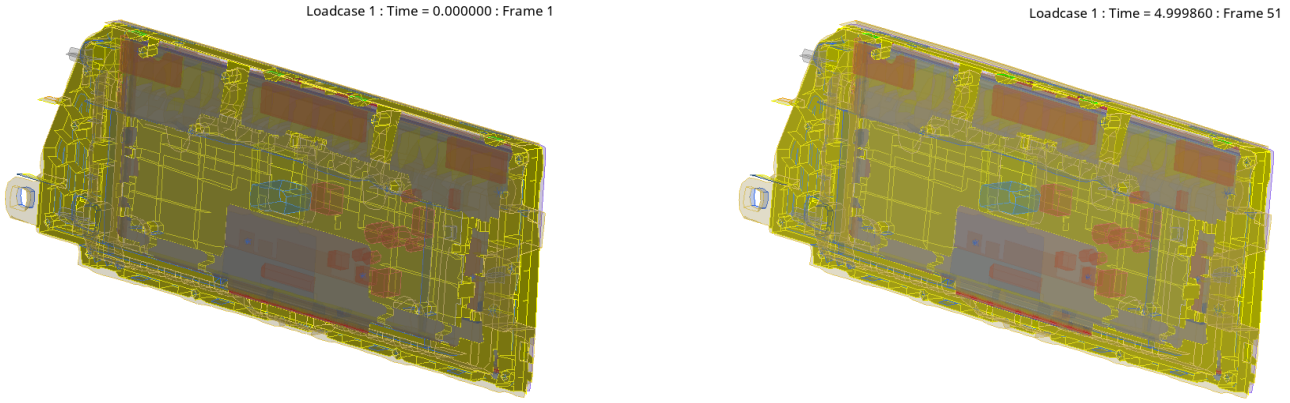

Figure 5.87 – Transparent bottom view of the monitor with only front frame visible in yellow at time 0 and 5 ms

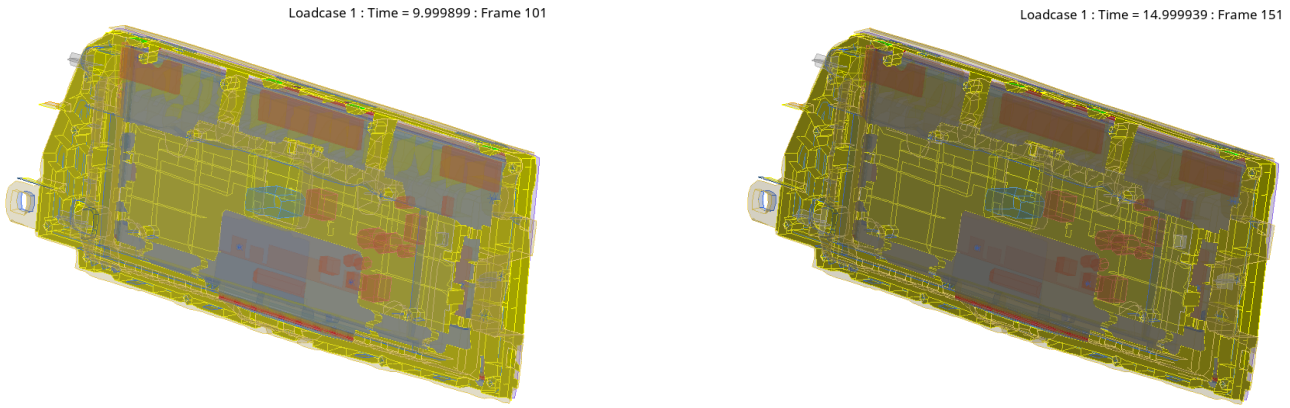

Figure 5.88 – Transparent bottom view of the monitor with only front frame visible in yellow at time 10 and 15 ms

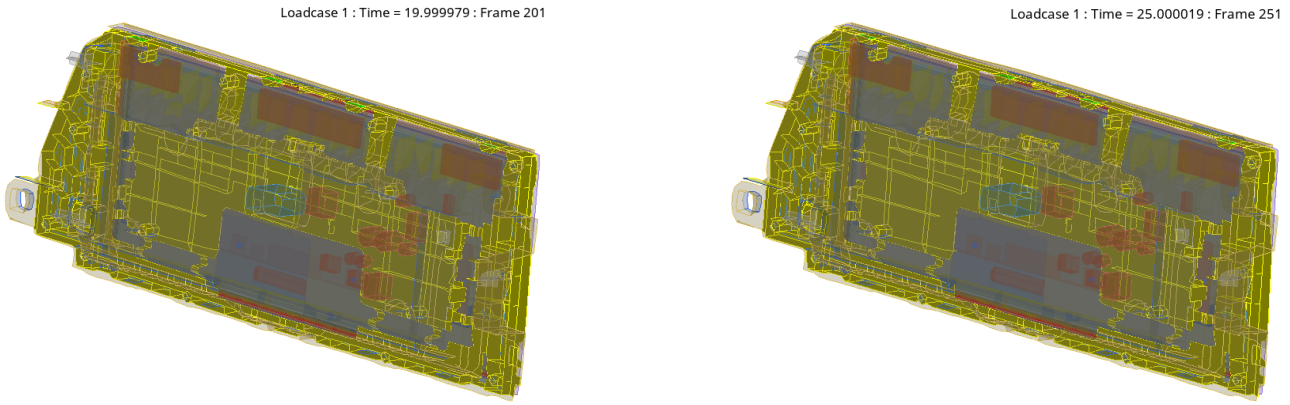

Figure 5.89 – Transparent bottom view of the monitor with only front frame visible in yellow at time 20 and 25 ms

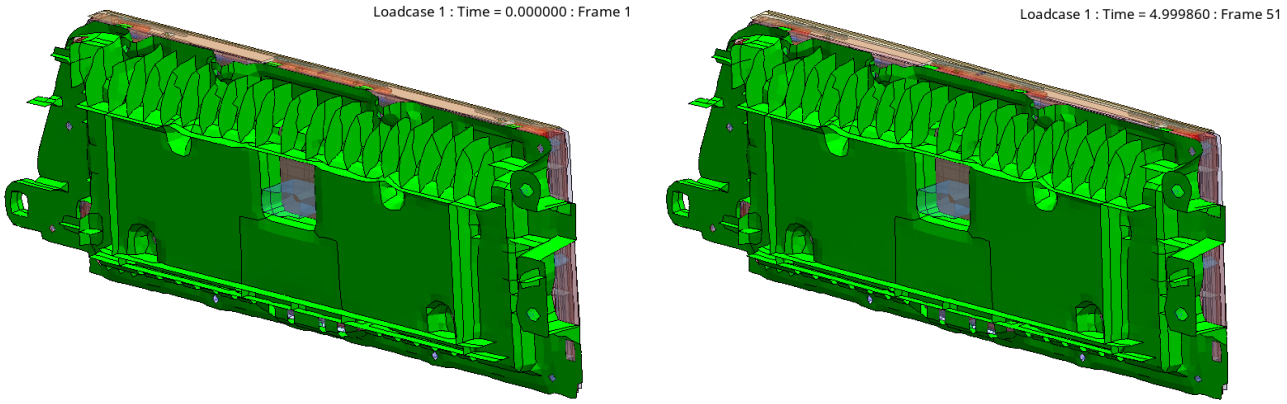

Figure 5.91 – Transparent bottom view of the monitor with only rear cover visible in green at time 0 and 5 ms

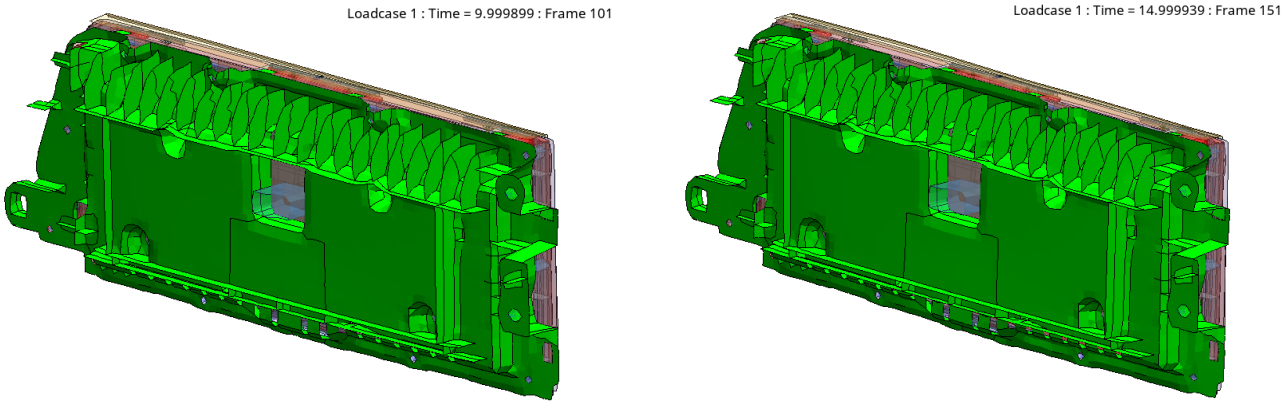

Figure 5.90 – Transparent bottom view of the monitor with only rear cover visible in green at time 10 and 15 ms

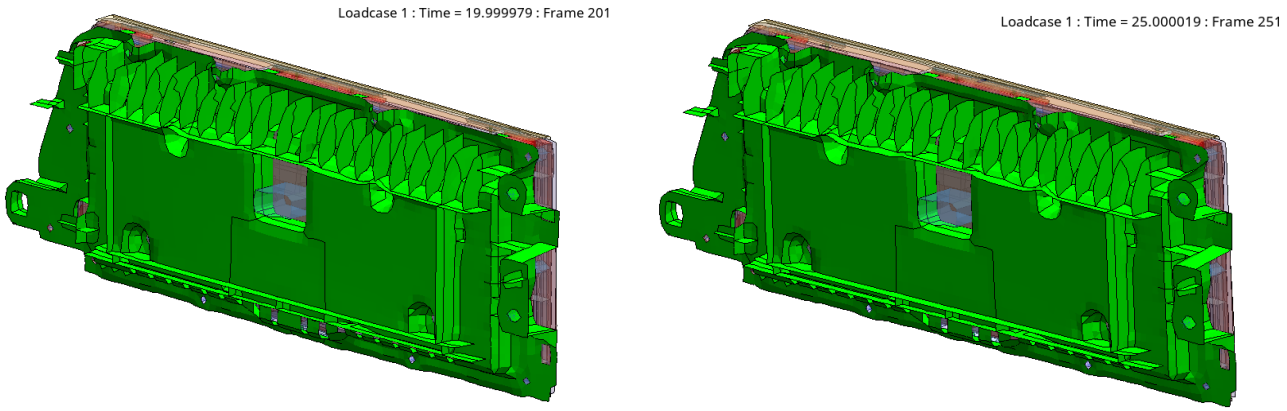

Figure 5.92 – Transparent bottom view of the monitor with only rear cover visible in green at time 20 and 25 ms

5.5.2.1.1 Energy balance

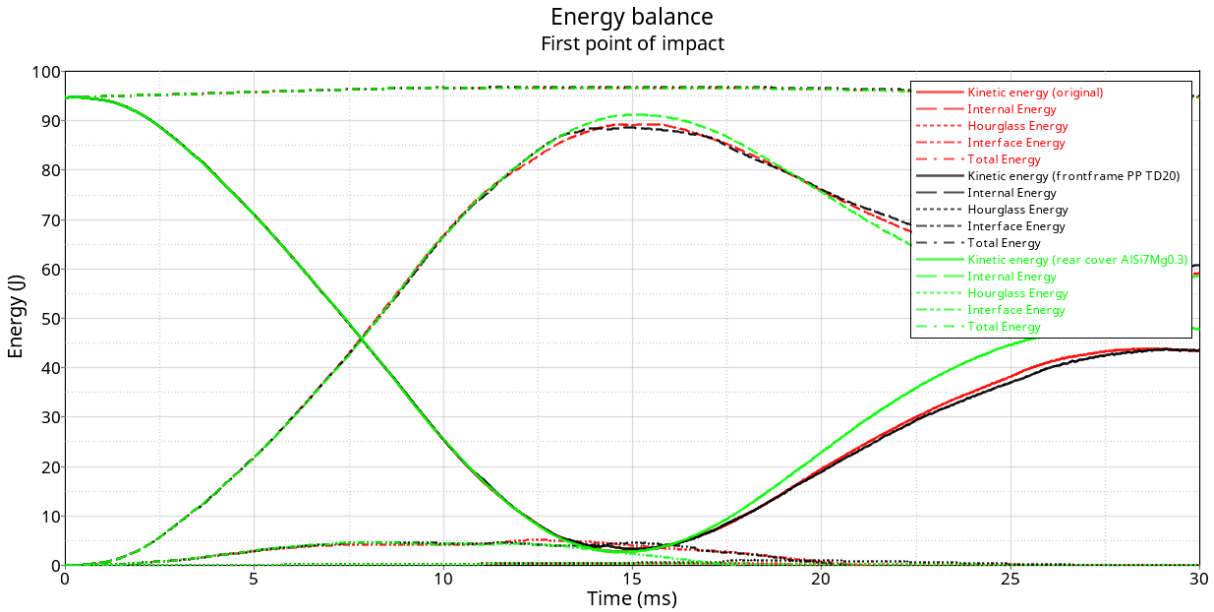

Figure 5.93 – Energy balance comparison

Looking at *figure 5.93*, it is possible to observe that the black curves, where the dashboard presents the modified front frame of the monitor made of PP TD20, are almost superimposed and so the change of the material of the front frame of the monitor is negligible from the point of view of the energy balance. This is due to the fact that the mechanical properties of the original front frame made of PC+ABS and the ones of the front frame made of PP TD20 are very similar and in addition, this is not the first component to get in contact with the head impactor but, since it is located in the bottom part of the monitor, it affects the general behavior of the entire dashboard. There is not the shift of the point where the internal energy is equal to the kinetic one and this shift is not present also in the change of the material of the rear cover from magnesium alloy to aluminum one and so the effect of the change of material can be considered negligible in this case.

Even if the stiffness of the rear cover made of aluminum alloy is higher than the one made of magnesium, the slope of the green curve of the internal energy is almost superimposed to the original one. The only visible effect on the plot is that the dashboard with the modified rear cover is able to absorb more energy in the impact phase and after the impact, when the head impactor returns back to its initial position, it is able to release back to the head form higher energy and this is in accordance with higher stiffness of aluminum alloy.

5.5.2.1.2 Deceleration curve

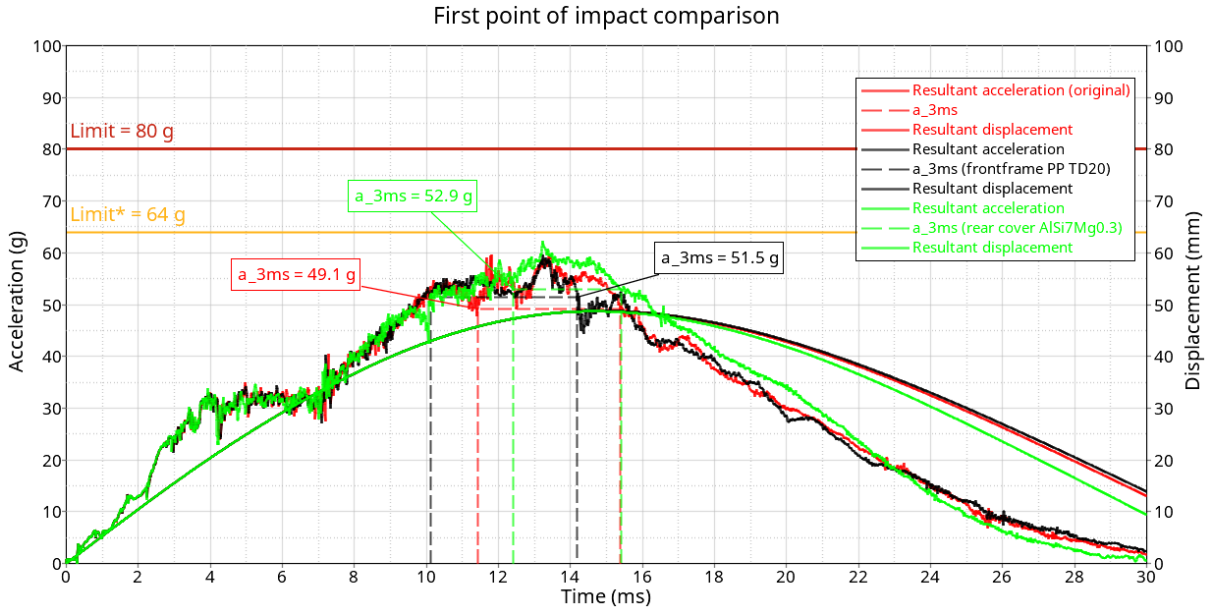

Figure 5.94 – Deceleration curve comparison

Looking at the plot of the resultant acceleration in *figure 5.94*, the general requirement of FMVSS 201L regulations (limit = 80 g) and the target requested by the car manufacturer (limit* = 64 g) are fulfilled. Focusing on the integral of 3 milliseconds (a_3ms), it is more visible the effect of the material of the structural elements of the monitor. In fact, the value of a_3ms curve with the modified front frame is higher than the original case, due to the slightly higher stiffness of PP TD20 with respect to PC+ABS and a similar consideration can be done with the modified rear cover, where the effect of higher stiffness of Al alloy with respect to Mg alloy is more evident and the highest value of the curve is reached.

5.5.2.1.3 Contact force between the impactor and the dashboard

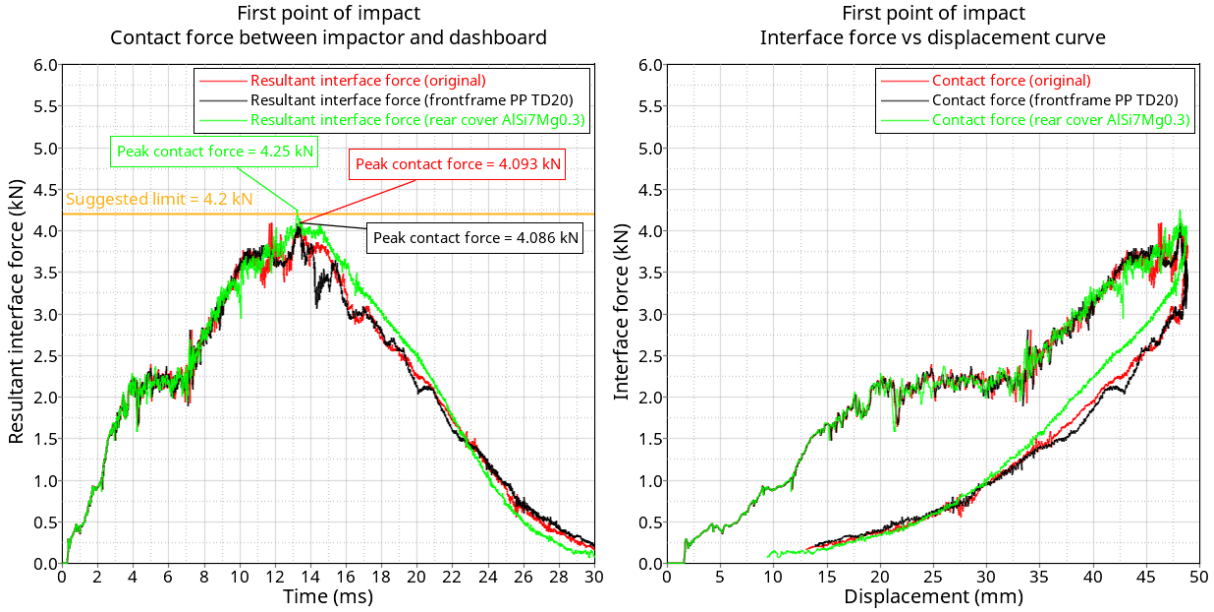

Figure 5.95 – Comparison between curves of contact force between the impactor and dashboard

The graphs in *figure 5.95* are in accordance with the considerations made for the deceleration curve. On the plot that shows the contact force over the simulation, it is possible to observe that the trend of the black curve with the modified front frame is almost superimposed to the original one and the peak contact force is slightly higher than the original one, but the difference can be considered negligible. In this case, the requirement of the suggested upper limit of the contact force is satisfied while focusing on the green curve, it is possible to see that in the dashboard with the modified rear cover there are some points that are above the suggested limit, and this is due to higher stiffness of the aluminum alloy. As previously described, this condition is still acceptable in terms of virtual validation, but it is necessary to check if possible problems may arise when physical tests are carried out.

Focusing instead on the plot that shows the contact forces as a function of the displacement, the green curve with the modified rear cover made of Al alloy, as expected, shows a more elastic behavior because, from the maximum displacement, the interface force decreases more rapidly with respect to the original case. This is caused by a higher release of energy from the dashboard to the head form after the impact phase and consequently less presence of plastic permanent deformations.

5.5.2.2 Second impact point

The first step to observe the behaviour of the dashboard is to consider the frame of the head impact simulation every 5 ms up to 20 ms. In *figures 5.96, 5.97, 5.98, 5.99* and *5.100* it is shown the simulation of the second impact point with the modified front frame while in *figures 5.101, 5.102, 5.103, 5.104* and *5.105* the one with the modified rear cover. In each figure is visible a full view of the entire dashboard and a left side section, located in the middle plane of the head impactor.

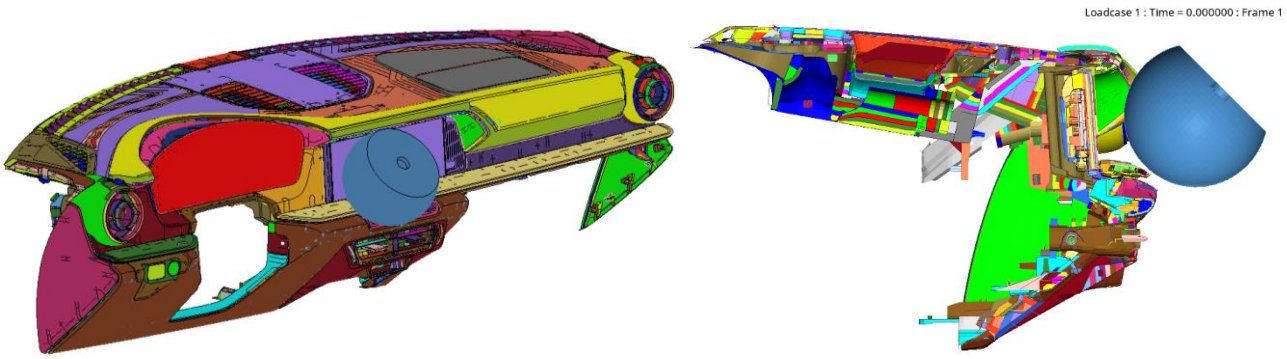

Figure 5.96 – Full view and left side section of the head impact with modified front frame (time 0 ms)

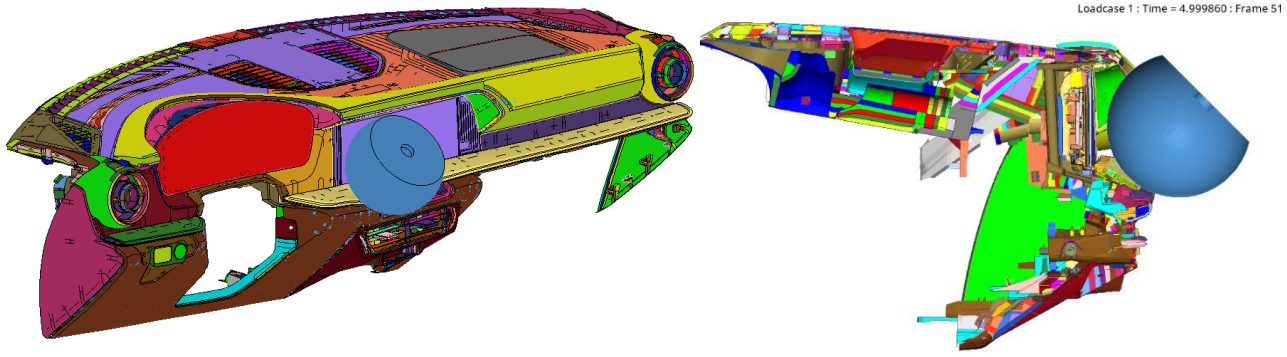

Figure 5.97 – Full view and left side section of the head impact with modified front frame (time 5 ms)

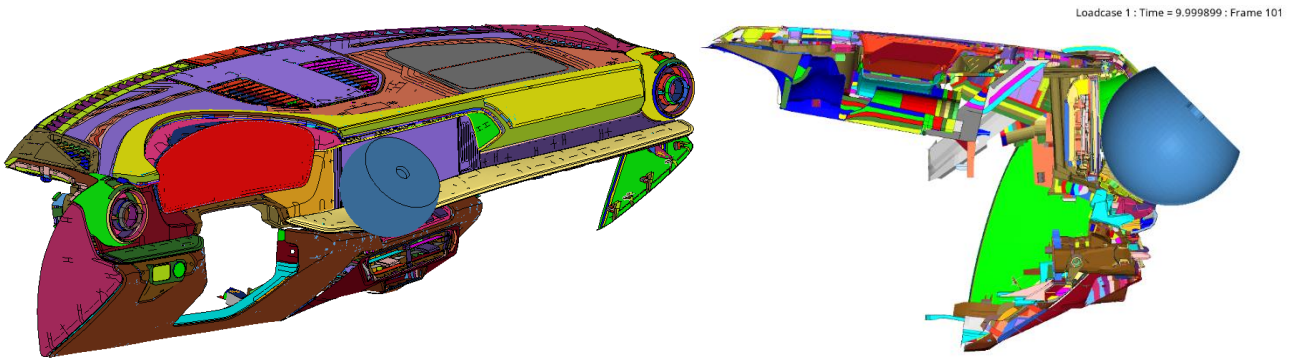

Figure 5.99 – Full view and left side section of the head impact with modified front frame (time 10 ms)

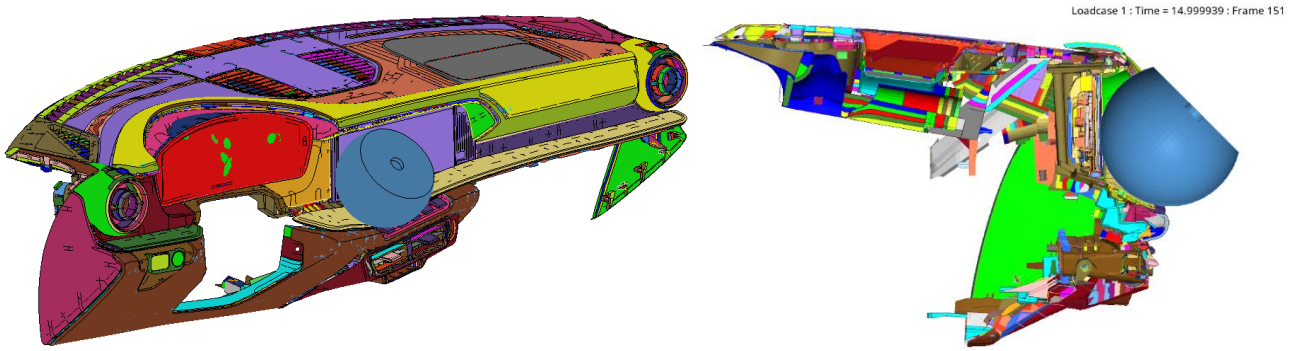

Figure 5.98 – Full view and left side section of the head impact with modified front frame (time 15 ms)

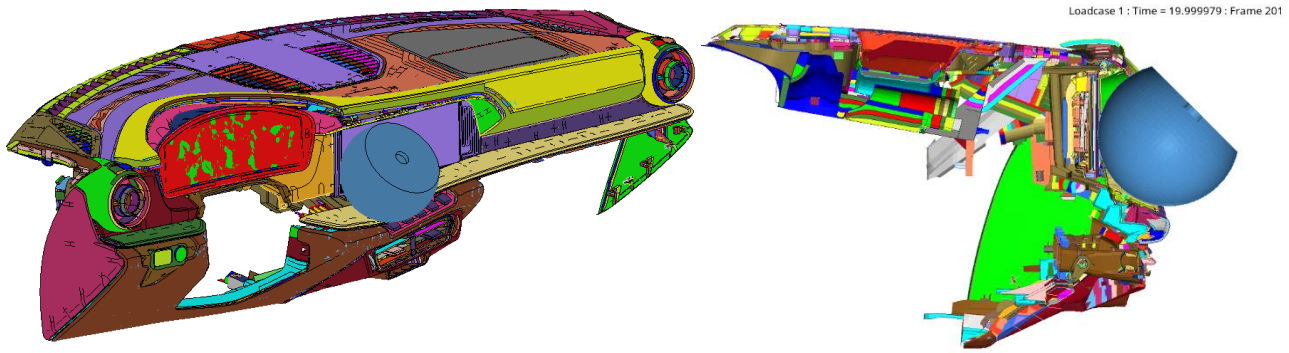

Figure 5.100 – Full view and left side section of the head impact with modified front frame (time 20 ms)

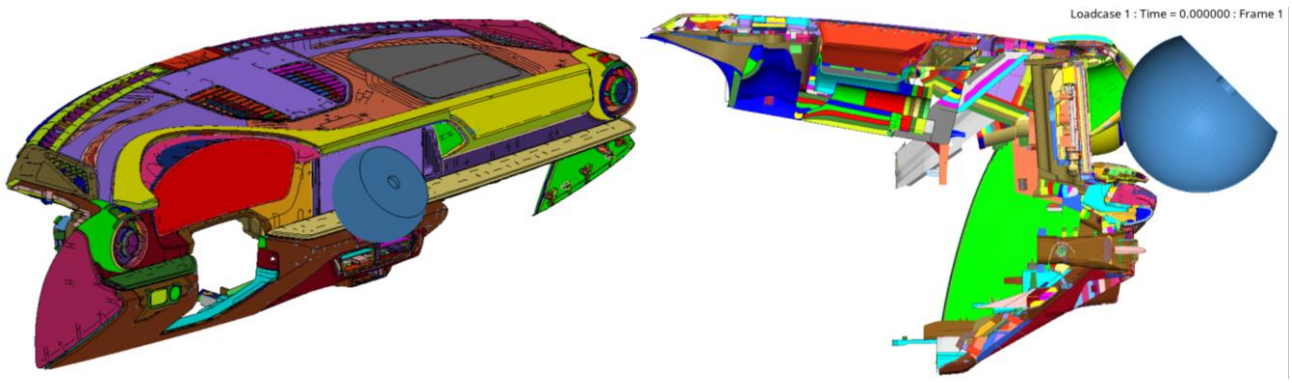

Figure 5.101 – Full view and left side section of the head impact with modified rear cover (time 0 ms)

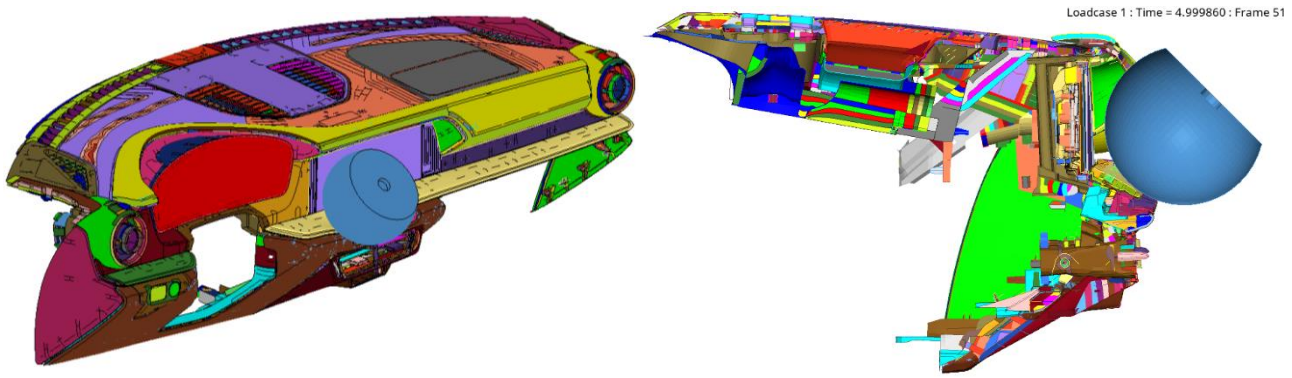

Figure 5.102 – Full view and left side section of the head impact with modified rear cover (time 5 ms)

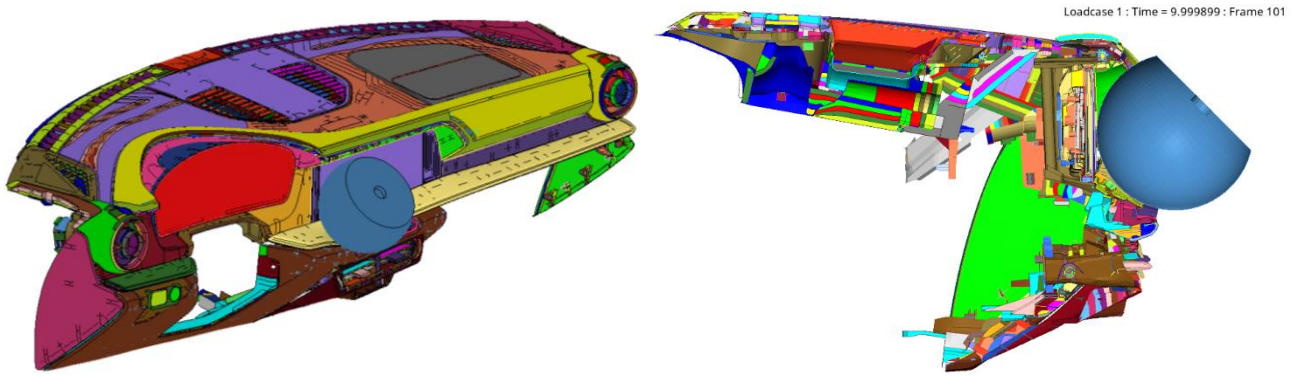

Figure 5.103 – Full view and left side section of the head impact with modified rear cover (time 10 ms)

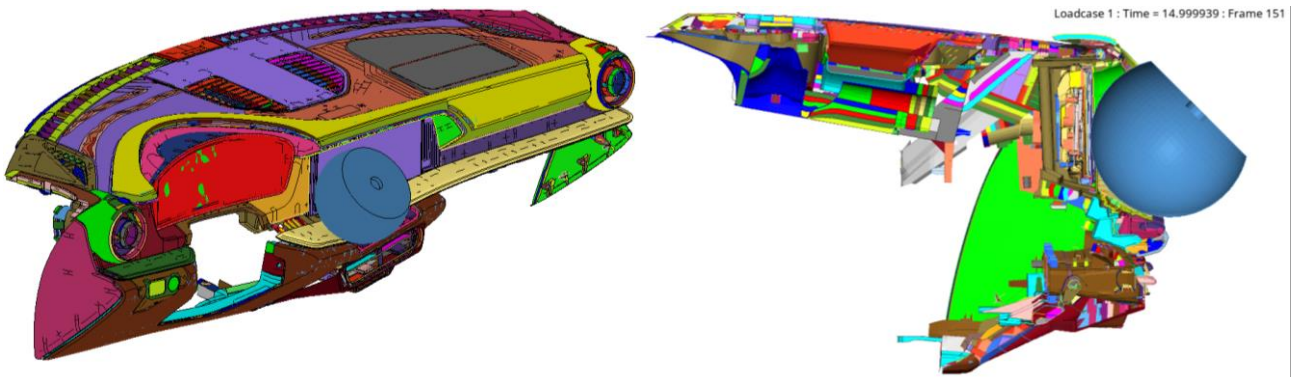

Figure 5.104 – Full view and left side section of the head impact with modified rear cover (time 15 ms)

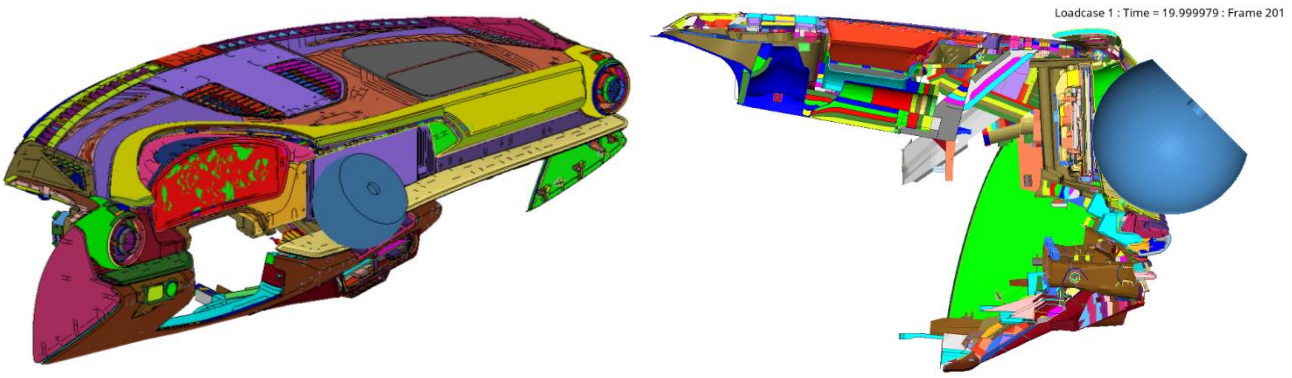

Figure 5.105 – Full view and left side section of the head impact with modified rear cover (time 20 ms)

Finally, in *figures 5.106, 5.107* and *5.108* it is shown a focus on the front frame of the monitor (yellow component) while in *figures 5.109, 5.110* and *5.111* it is shown a focus on the rear cover (green component).

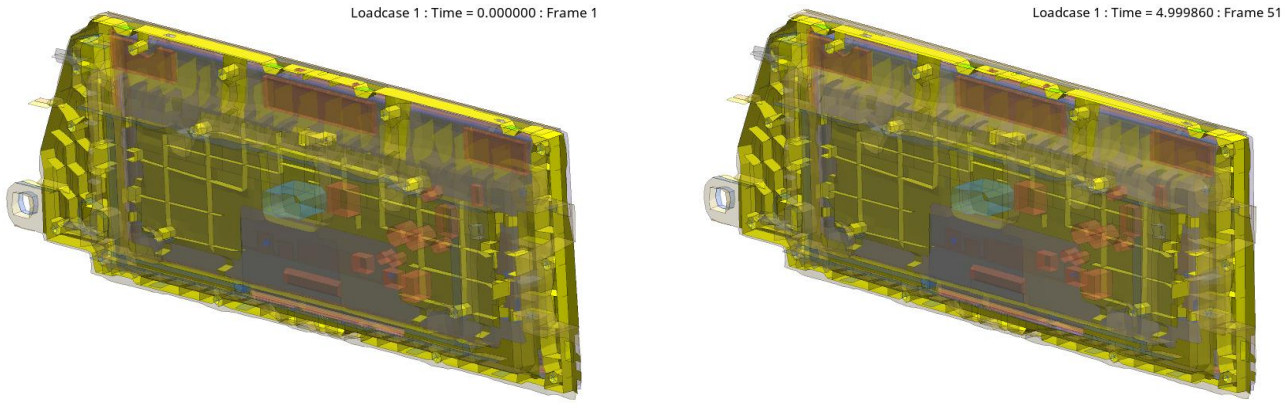

Figure 5.106 – Transparent bottom view of the monitor with only front frame visible in green at time 0 and 5 ms

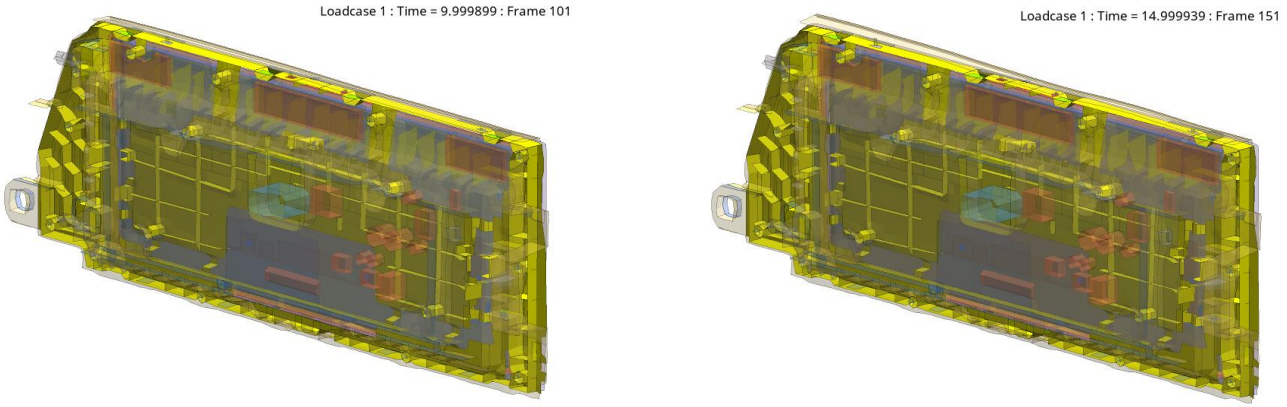

Figure 5.107 – Transparent bottom view of the monitor with only front frame visible in green at time 10 and 15 ms

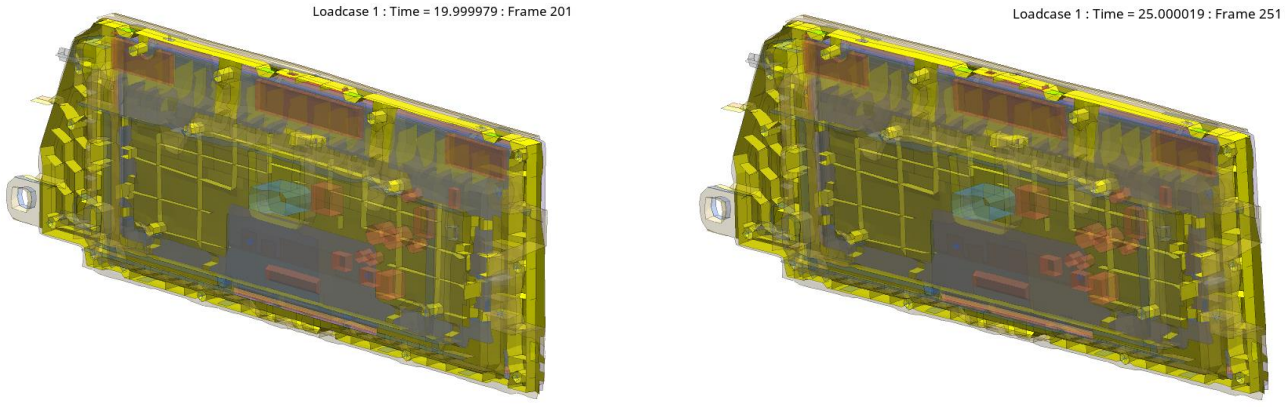

Figure 5.108 – Transparent bottom view of the monitor with only front frame visible in green at time 20 and 25 ms

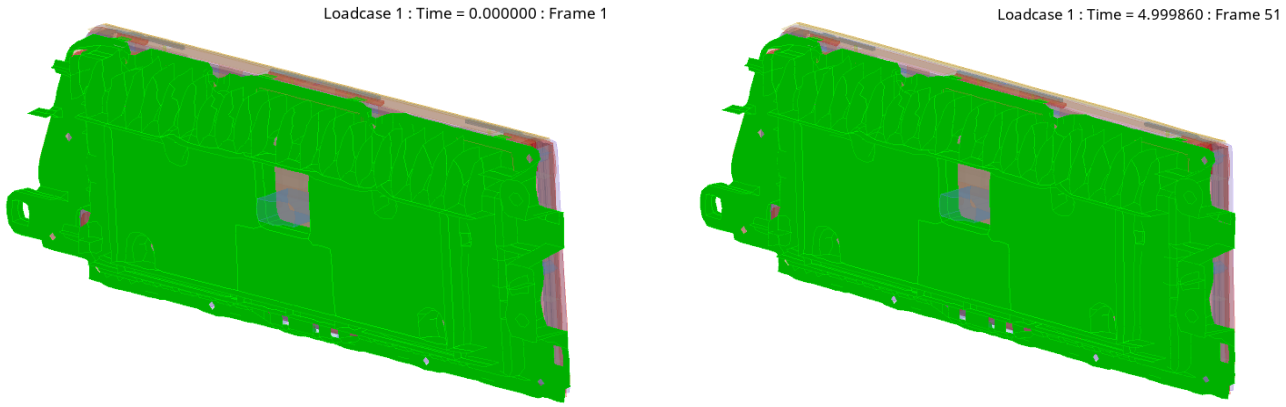

Figure 5.109 – Transparent bottom view of the monitor with only rear cover visible in green at time 0 and 5 ms

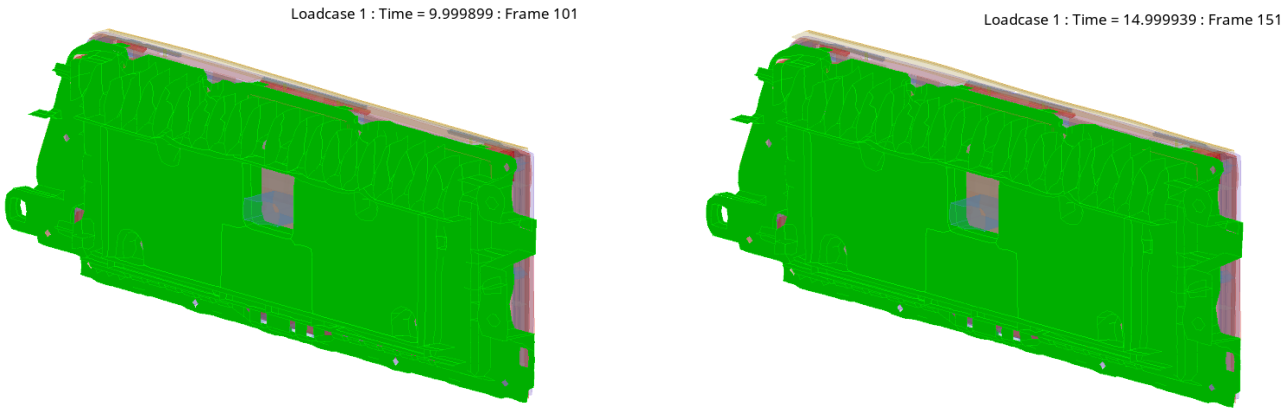

Figure 5.110 – Transparent bottom view of the monitor with only rear cover visible in green at time 10 and 15 ms

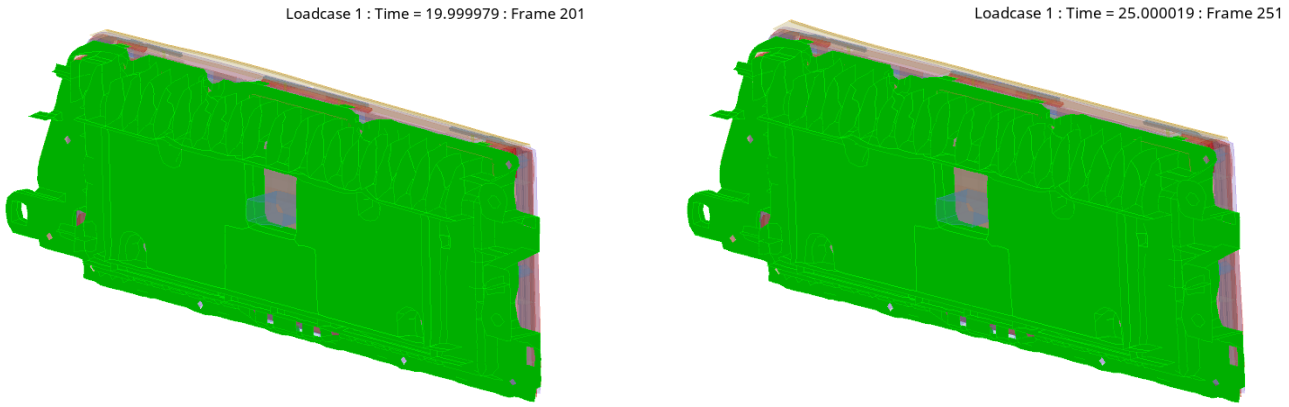

Figure 5.111 – Transparent bottom view of the monitor with only rear cover visible in green at time 20 and 25 ms

5.5.2.2.1 Energy balance

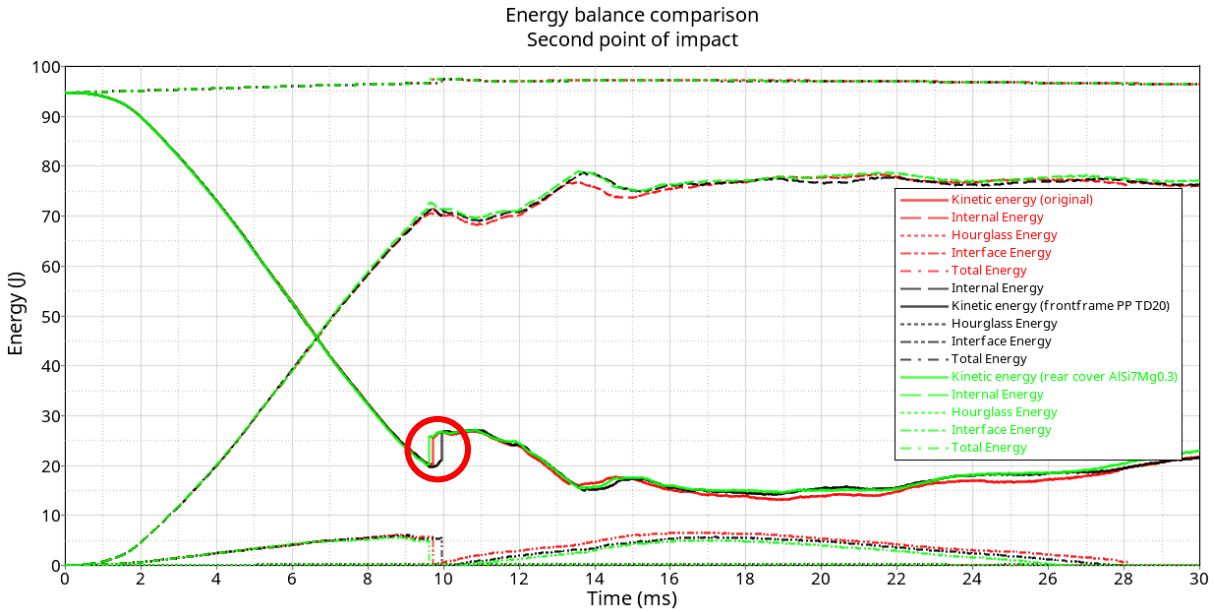

Figure 5.112 – Energy balance comparison

Looking at *figure 5.112*, it is possible to observe that the black and green modified curves are almost superimposed to the original case and so the change of the material respectively of the front frame and the rear cover of the monitor is negligible from the point of view of the energy balance. There is no shift, as expected and described before for the first point of impact with the change of material of the structural components of the monitor, of the point where the internal energy is equal to the kinetic one. The only small difference is highlighted in the red circle in the graph and is related to the breakage of the same threaded connection described in the original second point of impact. The breakage occurs slightly later in the case of the modified front frame made of PP TD20 with respect to the original case, as it is also shown in *figure 5.113*, where at 9.8 ms there is not still breakage in the case of the modified front frame.

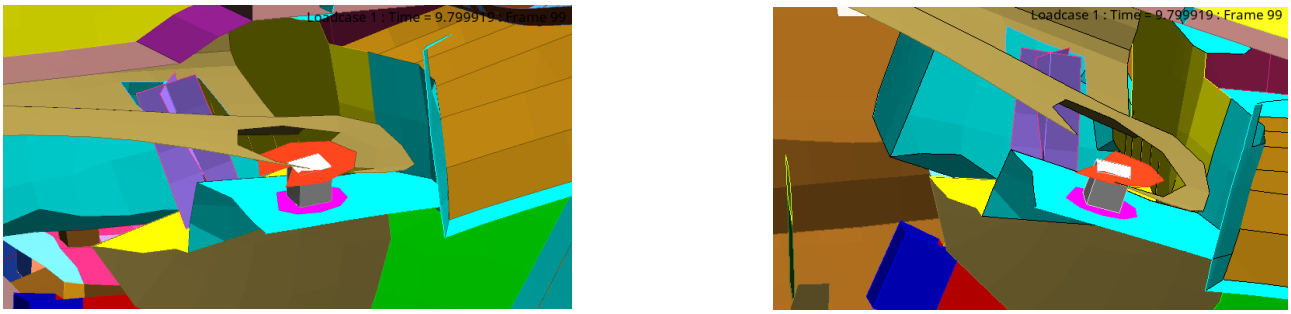

Figure 5.113 – Frame of the threaded connection at 9.8 ms in the case of modified front frame (left) and original one (right)

The second point of impact is located in the left end side of the monitor and since the structure of the front frame is prevalently on its end sides, the influence of the change of the material is more relevant. In this case, therefore, the delay of the breakage is caused by slightly higher stiffness of the front frame made of PP TD20.

5.5.2.2.2 Deceleration curve

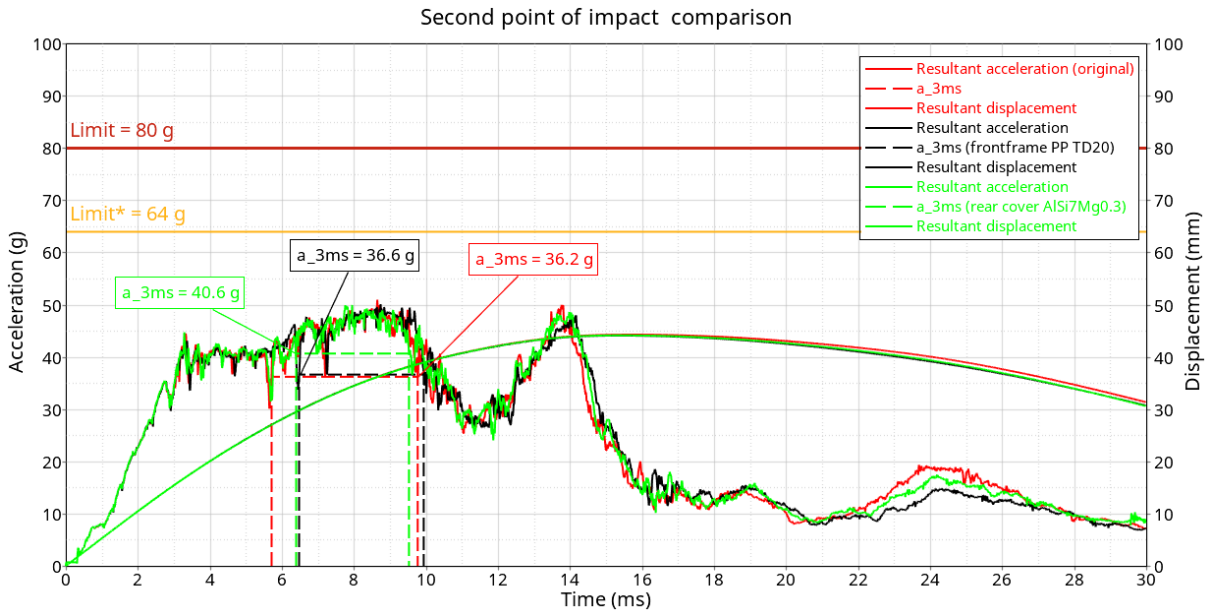

Figure 5.114 – Deceleration curve comparison

Looking at the plot of the resultant acceleration in *figure 5.114*, the general requirement of FMVSS 201L regulations (limit = 80 g) and also the target requested by the car manufacturer (limit* = 64 g) are fulfilled. Focusing on the integral of 3 milliseconds, the value of a_3ms curve with the modified front frame is, as expected, higher than the original case and similarly with the modified rear cover, where the highest value of the curve is reached due to the higher stiffness of the aluminum alloy.

5.5.2.2.3 Contact force between the impactor and the dashboard

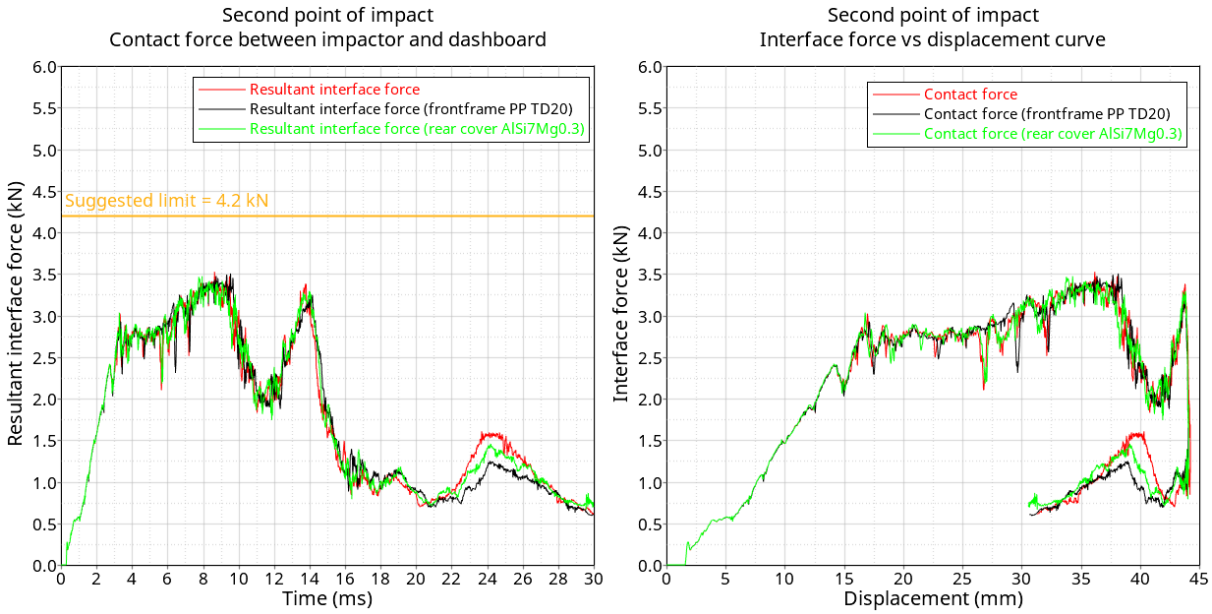

Figure 5.115 – Comparison between curves of contact force between the impactor and dashboard

Even in the graphs of the contact force in *figure 5.115* it is possible to see that the curves are almost superimposed and so the influence of the change of the material of the structural components of the monitor is negligible from the point of view of head impact. The presence of two peaks in the plot of the contact force over the entire duration of the simulation, also with the modifications, is caused by the same phenomena that were described before in the original case of the second point of impact.

5.6 COMPARISON BETWEEN DIFFERENT SPEEDS OF THE HEAD IMPACTOR

This comparison is performed in order to underline how the tests are performed and it is considered the first point of impact as representative of the behavior of the system. The Impact tests are engineered in order to pass them and so if the boundary conditions are changed, the system is not oversized. The system is sufficiently sized to work with the requirements imposed but if the speed of the head impactor increases, then the behavior of the dashboard is no more acceptable.

The choice of a speed of 24.1 km/h of the head impactor is what European regulation suggests if there is not the presence of the airbags. In this case the speed of the impactor to be considered is 19 km/h because this is the requirement of FMVSS 201L regulation in the presence of the dual airbags.

As done for all the previous cases, the first step to observe the behaviour of the dashboard is to consider the frame of the head impact simulation every 5 ms up to 20 ms. In the *figures 5.116,5.117, 5.118, 5.119* and *5.120* it is shown a comparison of the full view of the dashboard of the different frames of the simulation between the case of the speed of the head impactor equal to 19 km/h and the one with speed equal to 24.1 km/h. In the *figures 5.121, 5.122, 5.123, 5.124* and *5.125* this comparison is performed on the left side section of the dashboard, where the section is placed in the middle plane of the head form.

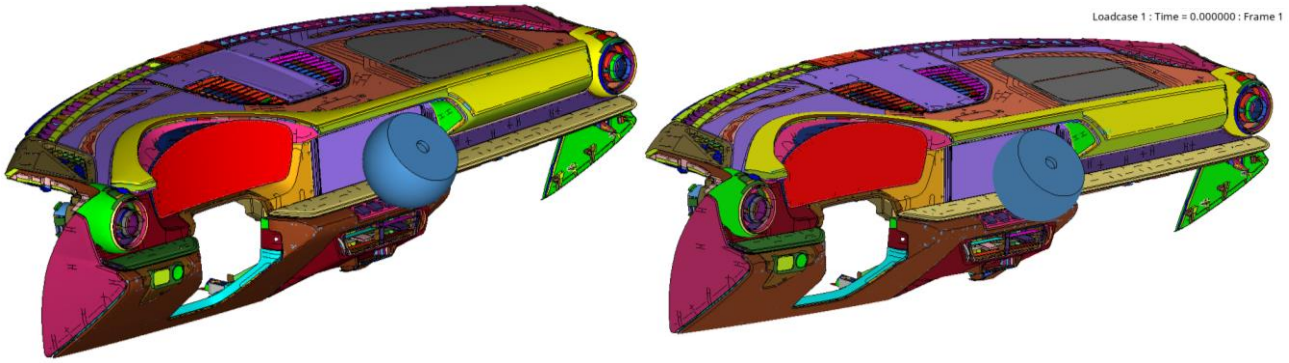

Figure 5.116– Full view of the impact simulation with speed of impactor of 19 (left) and 24.1 km/h (right) (time 0 ms)

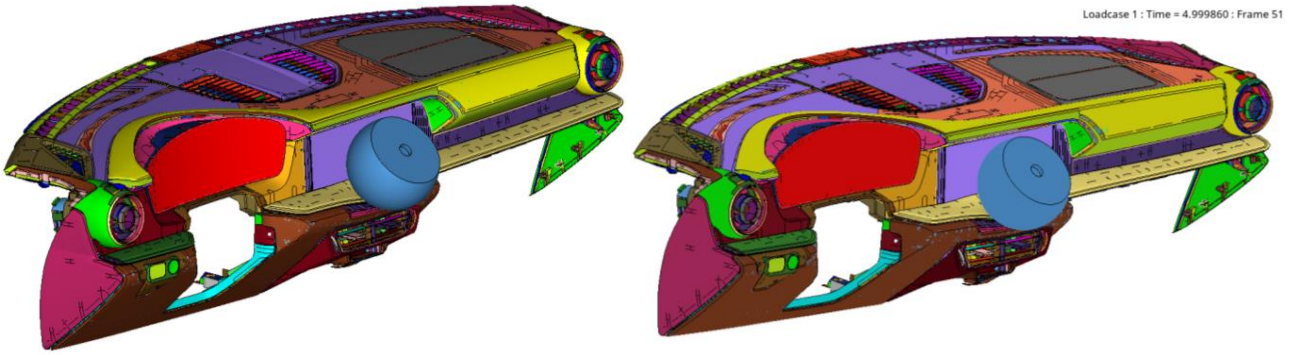

Figure 5.117 – Full view of the impact simulation with speed of impactor of 19 (left) and 24.1 km/h (right) (time 5 ms)

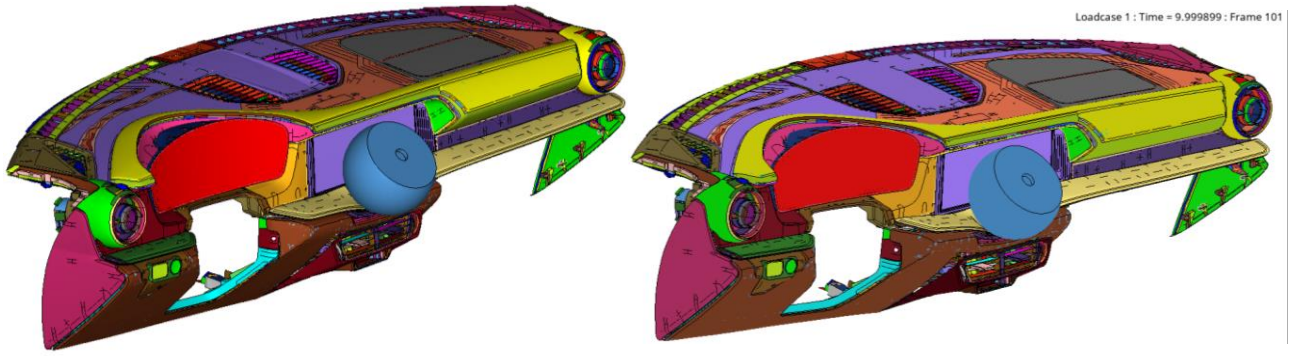

Figure 5.118 – Full view of the impact simulation with speed of impactor of 19 (left) and 24.1 km/h (right) (time 10 ms)

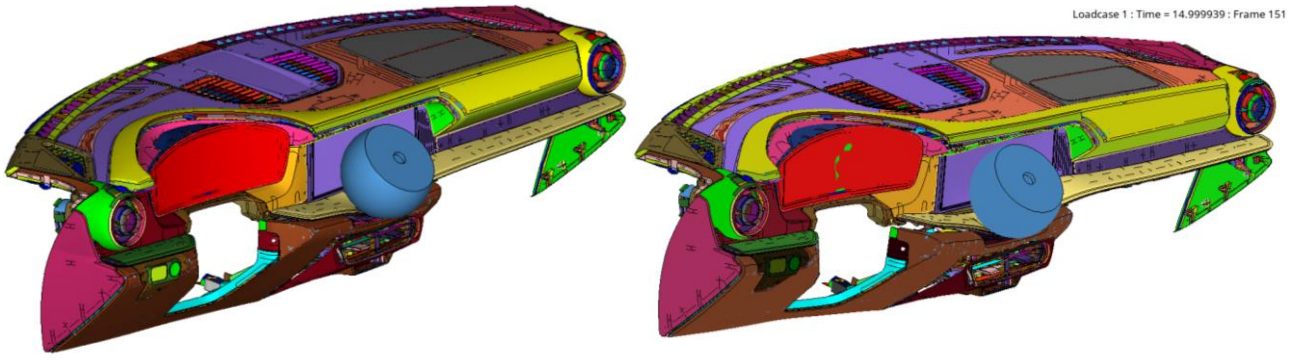

Figure 5.119 – Full view of the impact simulation with speed of impactor of 19 (left) and 24.1 km/h (right) (time 15 ms)

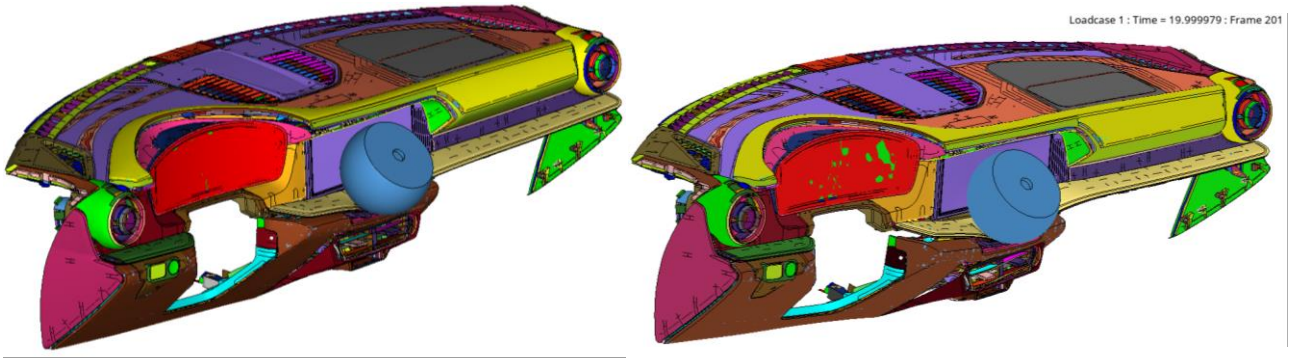

Figure 5.120 – Full view of the impact simulation with speed of impactor of 19 (left) and 24.1 km/h (right) (time 20 ms)

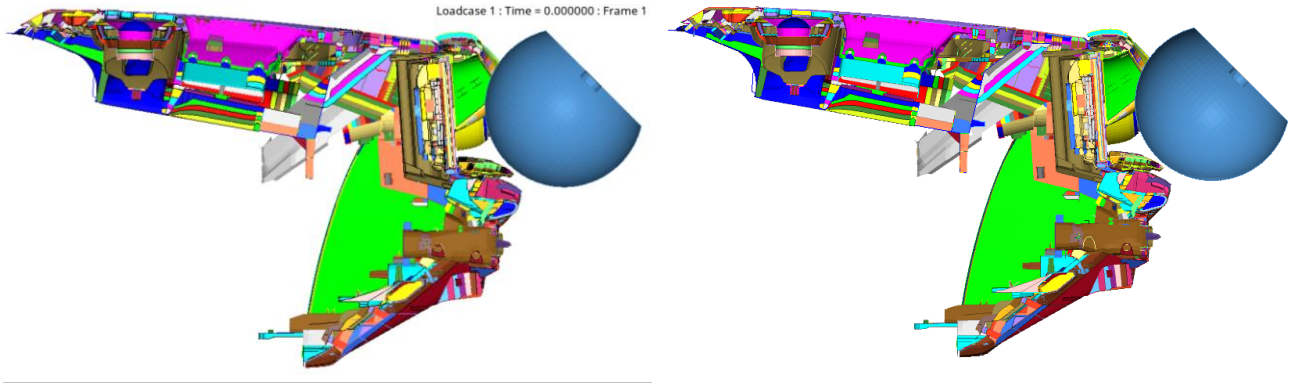

Figure 5.121 – Left side section of the impact simulation with speed of impactor of 19 (left) and 24.1 km/h (right) (time 0 ms)

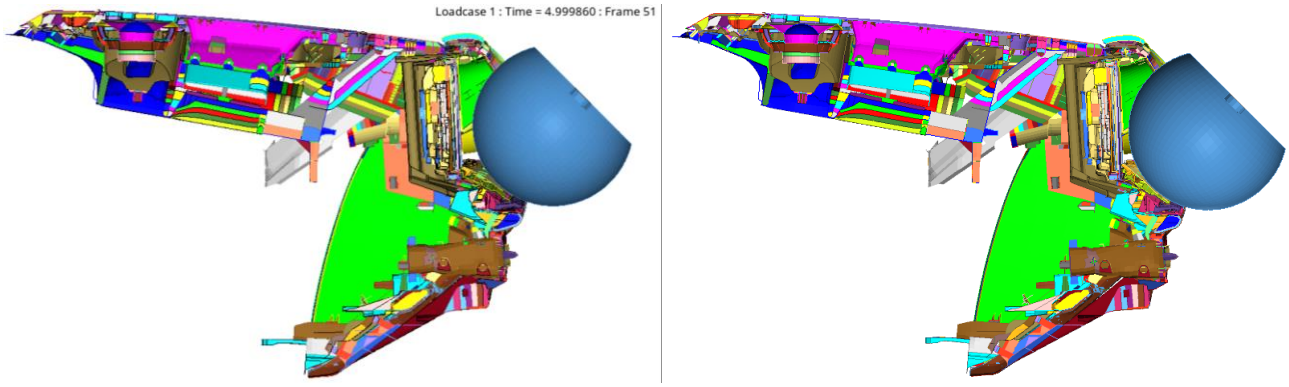

Figure 5.122 – Left side section of the impact simulation with speed of impactor of 19 (left) and 24.1 km/h (right) (time 5 ms)

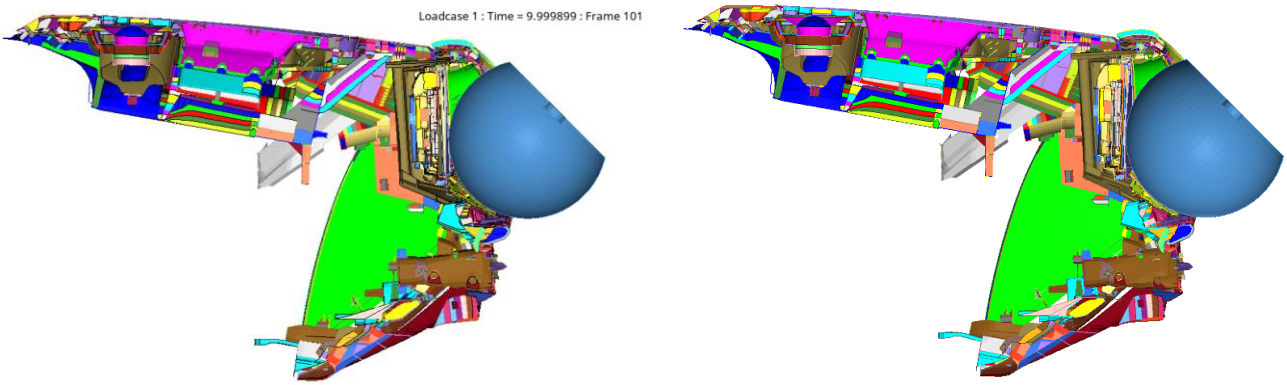

Figure 5.123 – Left side section of the impact simulation with speed of impactor of 19 (left) and 24.1 km/h (right) (time 10 ms)

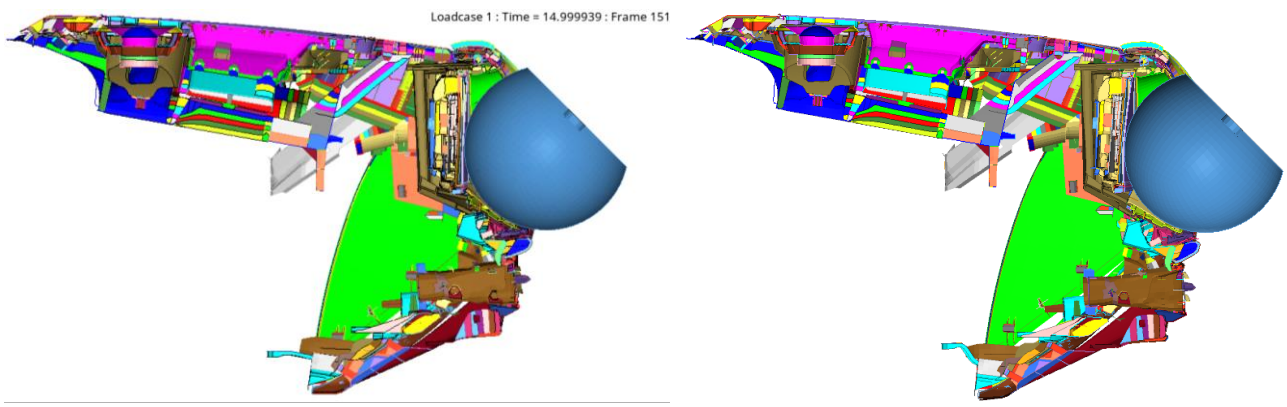

Figure 5.124 – Left side section of the impact simulation with speed of impactor of 19 (left) and 24.1 km/h (right) (time 15 ms)

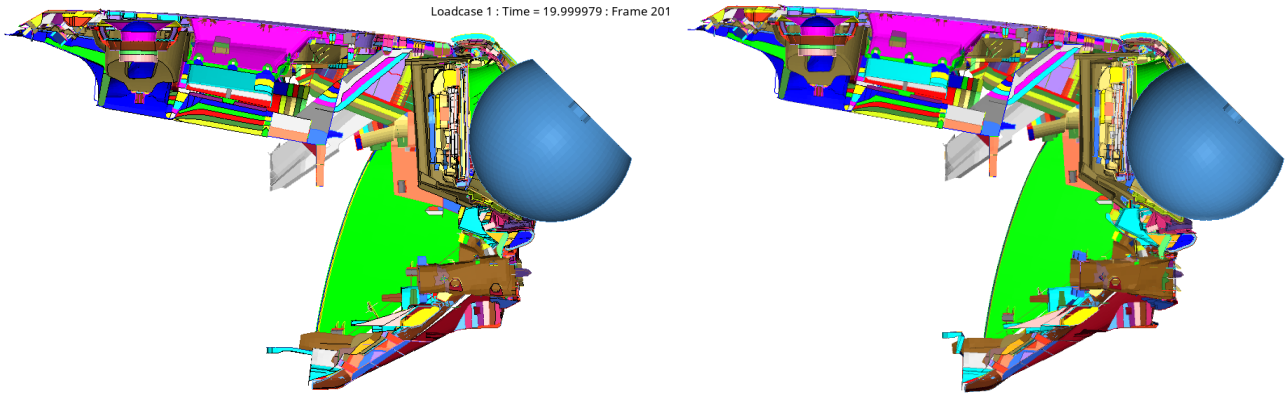

Figure 5.125 – Left side section of the impact simulation with speed of impactor of 19 (left) and 24.1 km/h (right) (time 20 ms)

5.6.1 Energy balance

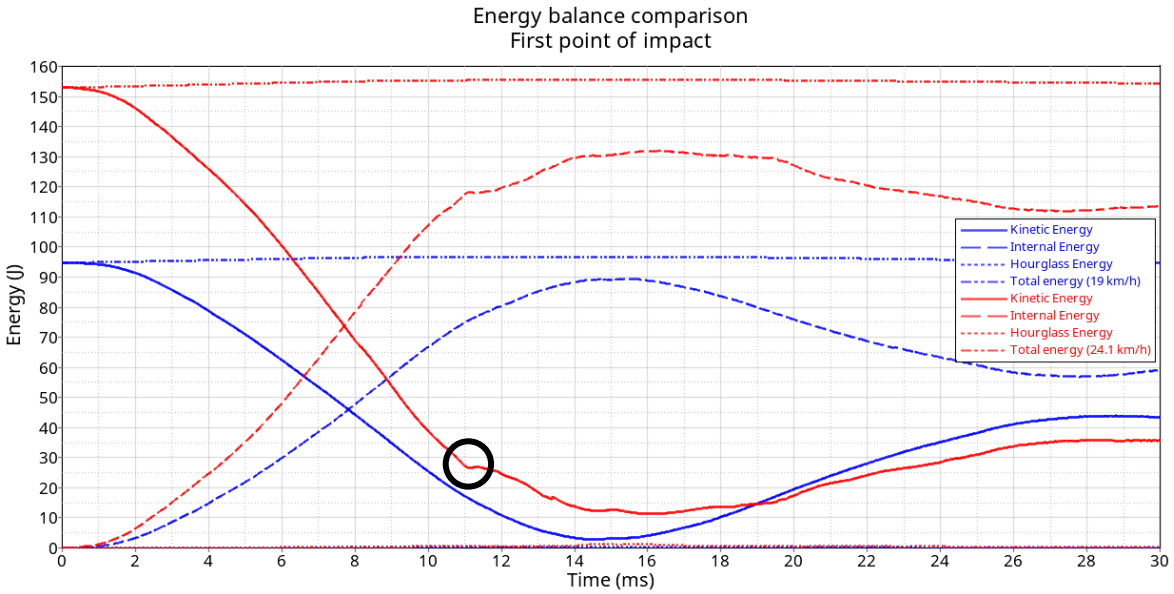

Figure 5.126 – Energy balance comparison

Looking at *figure 5.126,* the first observation is the different total energy of the system at the beginning of the simulation (t=0 ms). It is equal to the initial kinetic energy of the head form and is related to its mass and its initial velocity; so higher the speed of the impactor, higher the kinetic energy and this is visible in the plot of *figure 5.126*. There is no shift of the point where the kinetic energy is equal to the internal one, as expected because the dashboard is the same and the only condition that changes is the speed of the impactor. Focusing on the plot of the resultant velocity in *figure 5.127,* from t = 0 ms the speed decreases in the impact phase as well as progressively the head impactor gets in contact with the dashboard and the kinetic energy of the head impactor is transformed into internal energy of the system. In the point where the speed of the impactor is null, there is the change of the direction of the motion and this is reached later for the case of 24.1 km/h, due to higher initial velocity.

The behavior of the dashboard with the head impactor at 19 km/h is more elastic with respect to 24.1 km/h, meaning that the system has the time to release back energy in the form of kinetic energy from the

dashboard to the head impactor after the impact phase and consequently there are less permanent residual plastic deformations. This is also highlighted in the higher kinetic energy of the blue curve in *figure 5.126* at the end of the simulation with respect to the case where the speed of the head form is 24.1 km/h, that is caused by a more rapid decrease of the internal energy and better transfer of energy after the impact phase.

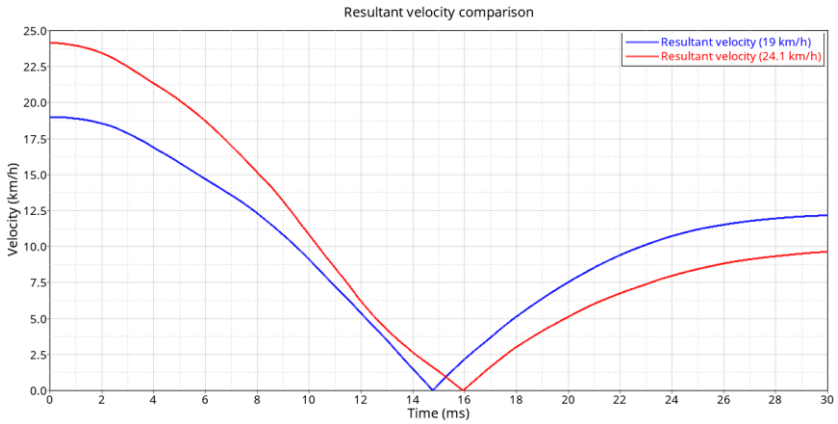

Figure 5.127 – Resultant velocity comparison

Focusing instead on the black circle in *figure 5.126,* it is highlighted a small discontinuity in the red curve (24.1 km/h) of the kinetic energy at 11.2 ms and this is caused by the same threaded connection that fails in the second point of impact with speed of the head impactor of 19 km/h. The higher speed of the head impactor causes more permanent plastic deformations and higher probability of breakage of threaded connections. In *figure 5.128* is visible the comparison of the threaded connection at 11.2 s in the case of 19 and 24.1 km/h speed of the head impactor. In the case of 19 km/h the breakage of the threaded connection is avoided while in the case of 24.1 km/h the failure of the threaded connection is present.

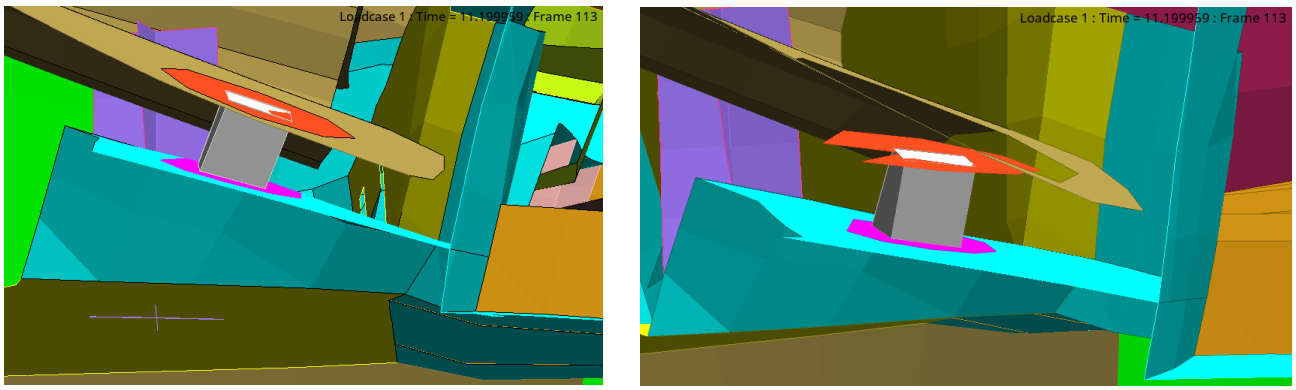

Figure 5.128 – Frame of the threaded connection at 11.2 ms in the case of 19 (left) and 24.1 km/h (right) speed of head impactor

5.6.2 Deceleration curve

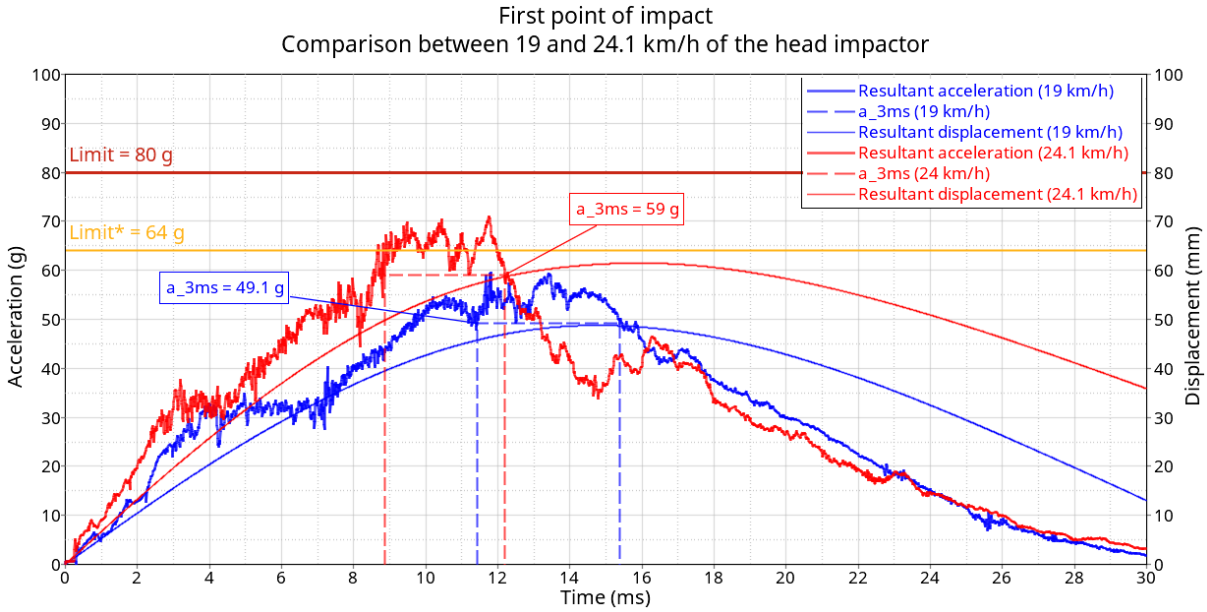

Figure 5.129 – Deceleration curve comparison

According to FMVSS 201L, the deceleration shall not exceed 80 g continuously for more than 3 ms (a_3ms curve). Higher initial speed of the head impactor implies higher values of the acceleration, as it is possible to see in *figure 5.129* but the general requirement of FMVSS 201L regulation and the target of the car manufacturer (limit* = 64 g) are fulfilled in both the cases.

5.6.3 Contact force between the impactor and the dashboard

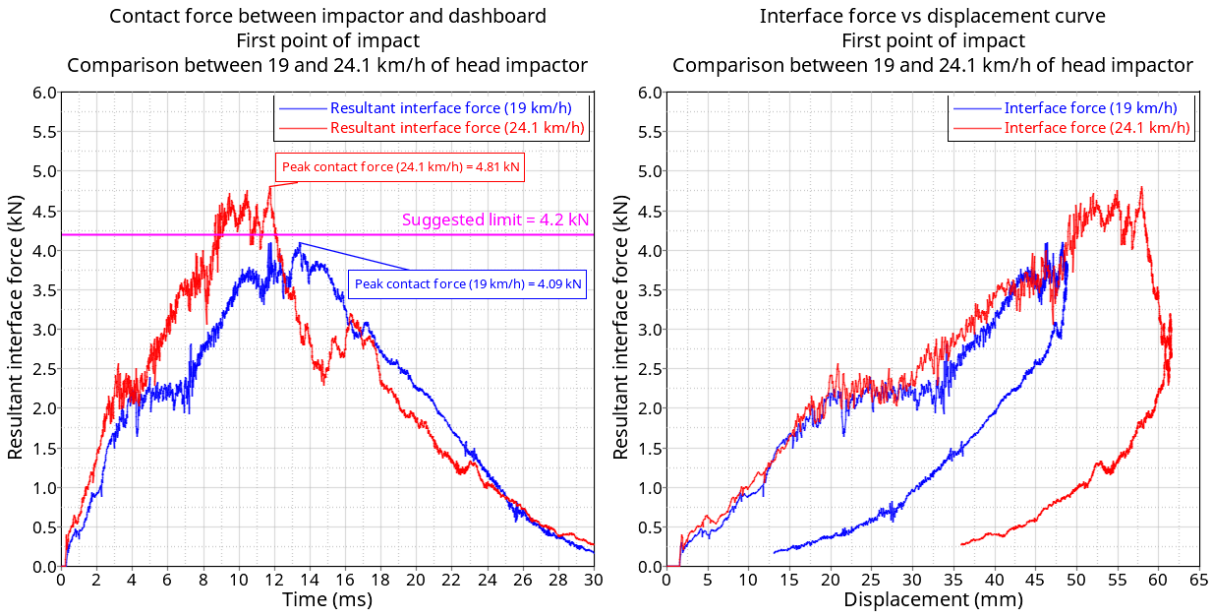

Figure 5.130 – Contact force between the impactor and dashboard curves

On the left graph in *figure 5.130*, showing the contact force that is transferred over the duration of the simulation between the head impactor and the dashboard, the suggested requirement of the car manufacturer of not exceeding 4.2 kN is not fulfilled in case of the speed of head impactor of 24.1 km/h. Since the suggested limit is exceeded in case of 24.1 km/h, this condition is a warning for the car manufacturer, that has to check with physical tests if possible problems may arise in the dashboard or if, even if the values of the contact force are higher than the upper limit, this condition is still acceptable. With respect to the case where the speed of the head impactor is 19 km/h, with 24.1 km/h the contact force does not increase up to the maximum value and then decreases up to almost null value but there is the presence of a peak at about 16 milliseconds, where, after an initial decreasing trend, the contact force increases again.

The negative drop of the red curve in *figure 5.130*, between 11.7 and 14.8 ms, is caused by the detachment of the lower shell of the instrument panel. So, at the beginning of the detachment, the contact between the dashboard and the head impactor decreases up to 14.8 ms. From this point, the contact force increases initially up to the peak at 16.3 ms and this is caused by the tendency of the lower shell of the instrument panel to return to its initial position. The contact between the dashboard and the head impactor increases and consequently the contact force. In *figure 5.131*, starting from the left to the right, it is shown only the contact between the lower shell (gold component) and the head form (blue component) at time 11.7 ms, 14. 8 and 16.3 ms. The deformation of the lower shell caused by the contact of the head form is higher, as expected, at 11.7 ms with respect to 14. 8 ms and similarly it is higher at 16.3 ms with respect to 14.8 ms and this confirms the considerations made and the trend of the red curve of the contact force in *figure 5.130.*

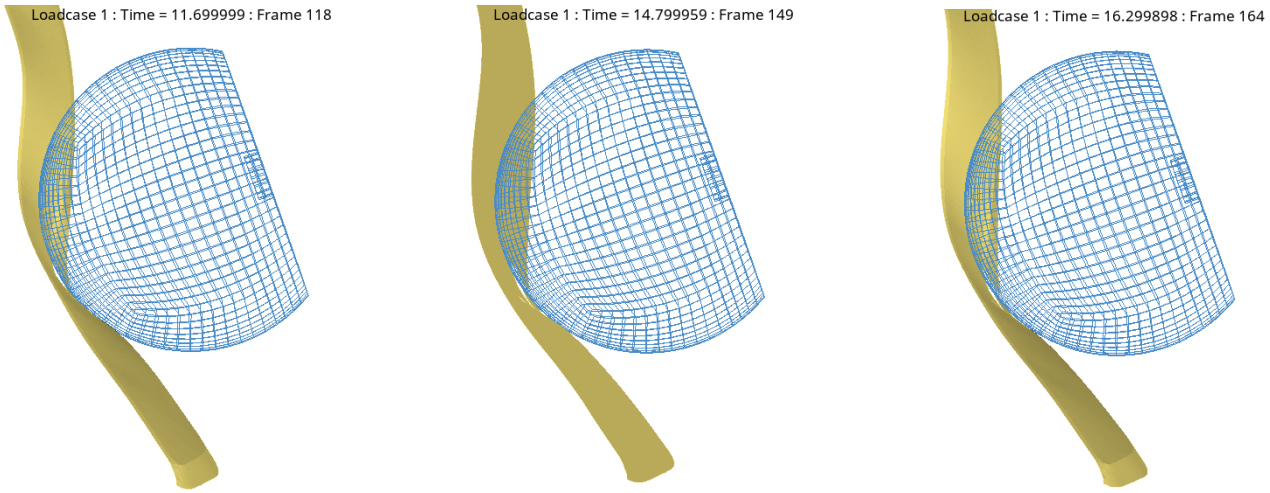

Figure 5.131 – Contact between the head form and lower shell at time 11.7, 14.8 and 16.3 ms

On the right graph of *figure 5.131* it is possible to observe that the maximum displacement that is reached in case of 24.1 km/h is higher than 19 km/h and this is due to higher initial velocity of the head impactor and consequently higher kinetic energy at the beginning. While in case of 19 km/h the maximum displacement is reached in correspondence of peak contact force and from that point there is a rapid decreasing trend of the

force, in case of 24.1 km/h, the displacement increases again after the point where the peak contact force is achieved, and this is caused by the detachment of the lower shell. In this latter case, the decreasing trend of the contact force is less rapid, and this is because there are more plastic permanent deformations at the end and the system has no sufficient time to transfer energy back to the head form after the impact phase.

5.6.4 Observation

In *figure 5.132* it is shown a comparison of the detail of the lower shell of the instrument panel at the end of the simulation in the case of the speed of the head impactor of 19 and 24.1 km/h.

Focusing on the case of 24.1 km/h, it is possible to observe that there are more elements of the lower shell that fail and disappear because the failure criteria of the material is based on maximum plastic deformation and the maximum value is reached. There is, consequently, higher probability of presence of sharp edges and this must be avoided when physical tests are carried out. In addition, as visible on the monitor, there is the explosion of some fragments in the protective cover glass, and this is not acceptable in terms of virtual validation.

This comparison confirms that the dashboard is designed just to pass impact tests, without oversizing it.

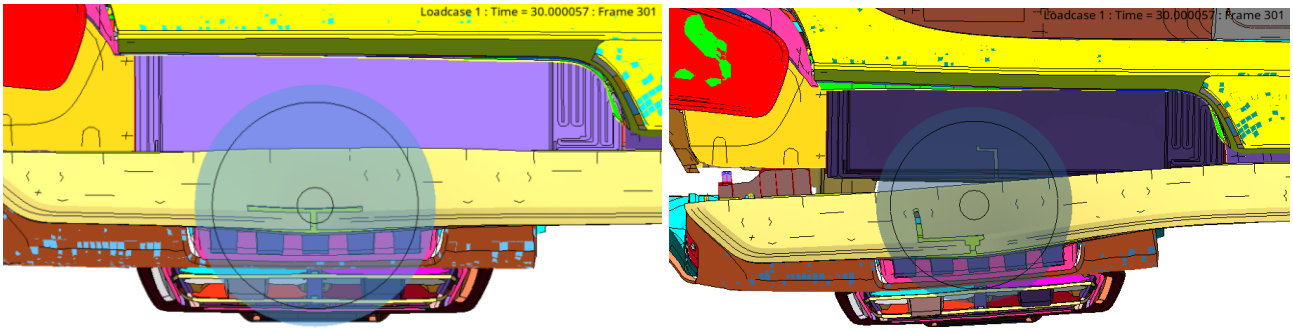

Figure 5.132 – Detail of lower shell at the end of the simulation with speed of 19 (left) and 24.1 km/h (right) of the head impactor

6 CONCLUSIONS

The main purpose of this thesis was the virtual validation of the head impact on the dashboard of the vehicle, focusing on the interaction between the head impactor and the monitor of the dashboard. To achieve this goal, the first part of the work was based on the setup and some preliminary structural analyses on the monitor of the dashboard, that is one of the main components that gets in contact with the head form. After these preliminary tests, head impact simulations have been performed in two impact points, selected by the car manufacturer as the most representative, and analyzed to consider possible issues and improvements. Finally, it is considered a change of the material of the components in contact with the impactor during the simulation, to understand how these modifications change the general response of the dashboard.

From the preliminary structural analyses performed on the monitor of the dashboard, it has been possible to observe that:

- the modal analysis in free- free condition has confirmed that all the different components of the monitor are correctly connected and consequently only six rigid modes are present.
- The natural frequencies of the monitor are higher than the value of acceptable limit (35 Hz), that is the typical frequency of the engine and gearbox coupling. They are consequently out of dangerous range for perceived quality and far from characteristic frequencies to have resonance.

Focusing instead on the head impact simulations, it has been possible to observe that:

- the general requirement of FMVSS 201L regulations (limit = 80g) and the target of the car manufacturer (limit* = 64g) is achieved for both the impact points.
- The contact force between the head impactor and the dashboard does not exceed 4.2 kN, that is the upper limit suggested by the car manufacturer.
- The splintering effect is avoided in both cases, since there are not fragments of glass that explode in the dashboard and there is not the presence of under flush and over flush, meaning that there not lack of tangency between the surfaces of the components in contact in the dashboard.
- Focusing only on the second point of impact, there is the detachment of the lower shell of the instrument panel, due to the breakage of threaded connection, and this phenomenon is a warning that has to be checked with physical tests. The best solution to avoid this breakage is to increase locally the thickness of the reinforcement part driver side. This can be a possible proposal for the car manufacturer if this issue is present also on the real component, but it must be feasible in terms of manufacturing process to produce it.
- The lower shell of the instrument panel presents some elements that fail and disappear, with a higher number of elements in the first impact point with respect to the second, due to the achievement of

the maximum plastic deformation. This phenomenon is a warning for the car manufacturer that must check with physical tests if sharp edges are present below that shell and, if they are present in the real component, it is necessary to change the type of material, as considered in this thesis. This improvement, due to the higher stiffness of the aluminum alloy, allows to avoid the formation of sharp edges but as a drawback an increase of the weight of the dashboard. So, this can be a possible solution but, as a consequence of the change of the material, there is the failure, for both impact points, of the same threaded connection that fails in the second impact point.

- Considering the change of the material of the structural components of the monitor (front frame and rear cover), the effect on the general response of the dashboard in terms of head impact can be considered negligible, because they are components that are not directly in contact with the head form and its influence is not relevant as the one caused by the change of the material of the lower shell, that is the first component to directly get in contact with the head form.
- The comparison of the head impact simulation at different speeds of the head impactor has highlighted that the models of the dashboard are designed in order just to pass the test and so the system is not oversized. In fact, with higher velocity of the impactor, the virtual validation is not fulfilled because there is the explosion of some fragments in the glass panel.

In conclusion, the best solution that is suggested for the virtual validation of the head impact on the dashboard of the vehicle is different from the original one, given by the car manufacturer. In particular it is considered a change of the material of the lower shell of the instrument panel and an increase of the thickness of the reinforcement part driver side. On the contrary, this causes an increase of 2 % of the weight of the entire dashboard.

7 BIBLIOGRAPHY

[1] U.S. Department of Transportation National Highway Traffic Safety Administration: Laboratory test procedure for FMVSS 201 Occupant Protection in Interior Impact

"Automotive Safety Handbook" 2nd Edition, Ulrich Seiffert and Lothar Wech

"Integrated Automotive Safety Handbook", Ulrich Seiffert and Mark Gonter

"Shigley's Mechanical Engineering Design" 11th edition, Richard G. Budynas and J.Keith Nisbett

Automotive vehicle safety", George A.Peters and Barbara J.Peters

"The Finite Element Method in engineering" 6th edition, Singiresu S.Rao